

# Optimal Groundwater Remediation



## Advanced Chemical Engineering Design

Dr. Miguel Bagajewicz  
University of Oklahoma  
March 14, 2008  
Taren Blue, Laura Place

## Executive Summary

This report is an exercise in the use of computational fluid dynamics and mathematical modeling to analyze the remediation process of groundwater. The purpose of this model is to minimize contaminants in an aquifer while minimizing cost. The mathematical model involves differing well configurations, pumping rates, and the use of fluid flow characteristics to evaluate the concentration profiles in the aquifer. This model builds on previous two dimensional models by adding simulations in Fluent flow simulation software in order to create a three dimensional model, and by investigating dynamic optimization through changing well configuration with time.

The geometry of a 2000 m<sup>3</sup> aquifer was drawn into Gambit, Fluent's geometry software. This was imported into Fluent and boundary conditions were named for inlets and outlets of the aquifer. Fluid flow simulations were run. The velocities were analyzed at different points throughout the aquifer. Using the velocities in the contamination volume, a mathematical model was developed for the calculation of the contaminant concentration at points throughout the aquifer with time. The remediation time for each geometry and pumping rate was determined based on when the concentration of contamination within the aquifer dropped below the desired level.

Well configuration was found to have a very large effect on flow patterns within the contamination plume. Seven well configurations were used in the analysis of flow profiles. Seven flow rates were used in each of the well scenarios. Remediation time was seen to be highly dependent upon flow rate. In some portions of the plume where the velocity of the water was at a maximum, the concentration profile was seen to behave as a step function. Cost analysis was performed for each of the evaluated scenarios. The cost was based on fixed initial and continuous costs, and variable operating costs. The biggest factors affecting cost were then the number of wells and overall remediation time.

After this initial study was performed a refined fluid flow model was created. A more realistic geometry of an 8,000 m<sup>3</sup> aquifer was created in Gambit and, again, imported into Fluent where inlet and outlet boundary conditions were defined. Simulations were run and the velocity data was imported into excel for analysis. Three different initial contamination plumes were explored in this study. In order to more effectively clean the differing plumes, unique pumping schemes were designed and varied with time. The total flow rate into and out of the aquifer was held constant throughout the entire remediation process. Each simulation was examined individually and as part of the dynamic model. Then, final concentrations were compared to investigate the most efficient pumping scheme. It was found that pumping scheme optimization is highly dependent upon the initial contamination profile. It was also found that this method can effectively model a dynamic pumping optimization scheme and can produce concentrations lower than those achievable with constant pumping configuration.

## Table of Contents

Introduction .....	4
Options for Lowering Contaminant Concentrations.....	7
Industrial Practices and Current Research.....	10
Optimization .....	11
Uncertainties and Problems with Remediation .....	11
Previously Developed Models.....	12
Fluid Flow Analysis .....	14
Initial Fluid Flow Approach .....	14
Gambit.....	14
Fluent .....	<b>Error! Bookmark not defined.</b>
Initial Fluid Flow Simulations .....	21
Concentration Profiles .....	26
Results and Discussion .....	30
Economics .....	45
Secondary Fluid Flow Approach.....	48
Gambit.....	49
Initial Plume Profiles .....	50
Pumping Strategies .....	51
Secondary Fluid Flow Simulations .....	53
Fluent .....	<b>Error! Bookmark not defined.</b>
Construction of Concentration Profiles from Fluent Data .....	62
Results and Discussion .....	63
Further Studies and Future Work .....	67
Conclusions .....	68
Works Cited.....	69

## Introduction

Groundwater remediation involves the removal of contaminants from a water supply. Groundwater contamination can generally be a result of agricultural or industrial processes (Hanford Site). Major sources of contamination can be storage tanks, septic systems, landfills, hazardous waste sites, and road salts and other chemicals (The Groundwater Foundation). Contaminants can include organic and inorganic compounds, microorganisms, disinfection byproducts, disinfectants, and radionuclides. Groundwater can also be contaminated with volatile organic compounds, or VOCs. According to the National Water-Quality Assessment Program, in the United States, trihalomethanes and solvents were the most frequently detected VOC groups.

In the United States, the contamination by some chemicals can be specific to certain regions of the nation. For example, arsenic can be seen to be concentrated in areas in and around large cities.

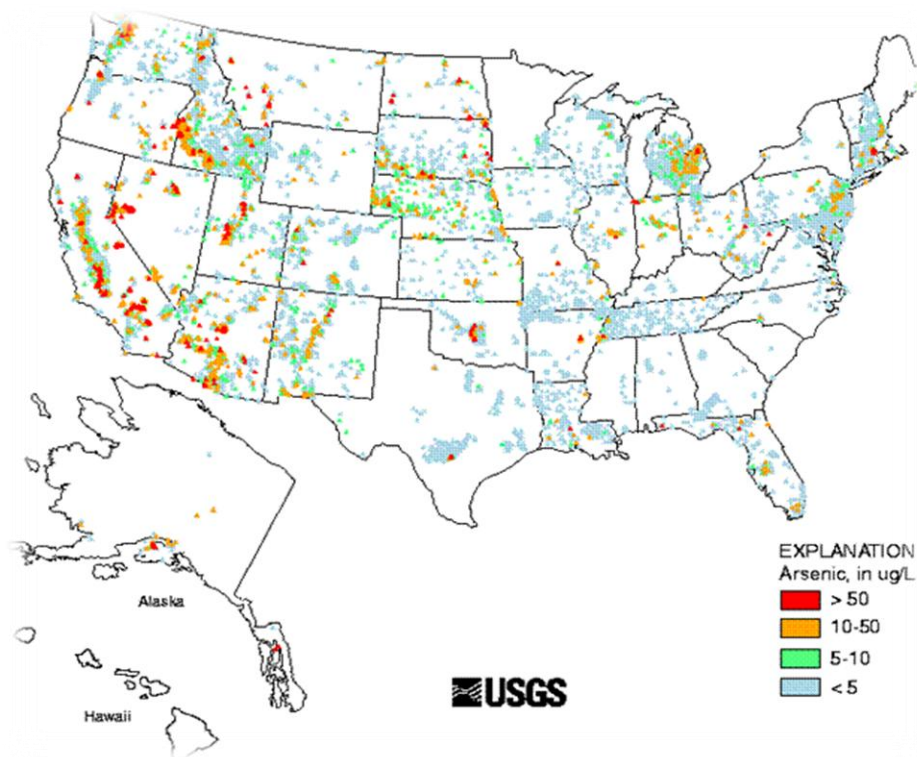


Figure 1: Arsenic Contamination in the United States

Other than the United States, arsenic contamination is a large problem in countries including Mexico, England, Chili, Argentina, Poland, Mongolia, Japan, Taiwan, Nepal, Bangladesh, and Vietnam. Nitrates in the United States are observed to be concentrated in areas that have large farming areas. This can be seen in figure 2.

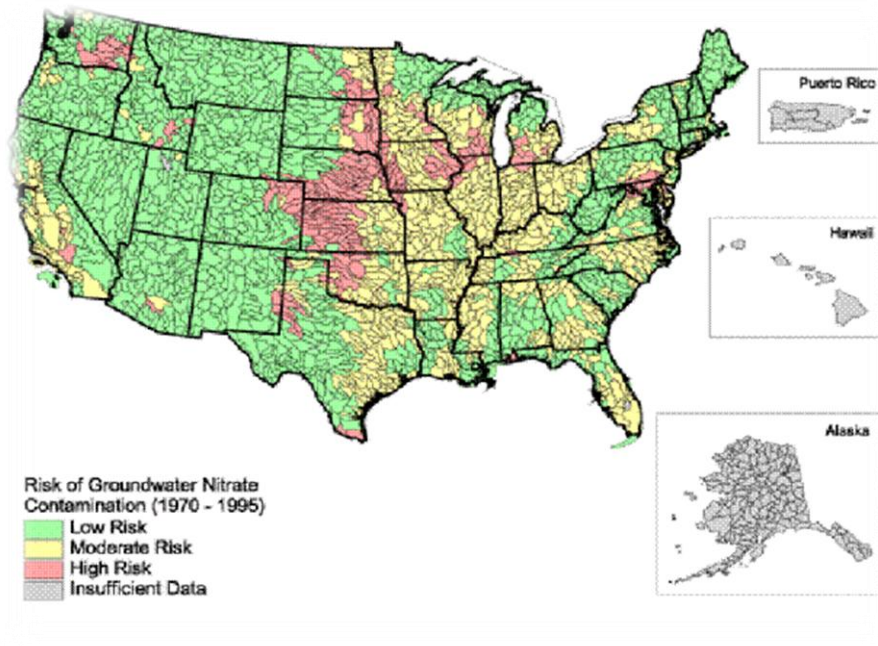


Figure 2: Nitrate Contamination in the United States

This is due to the widespread use of fertilizers in agricultural practices. Other areas where nitrates are a problem are Latin America, west, south and east Asia, north Africa, and other developing countries. Heavy metals and minerals, the problems associated with “hard” water, are seen to be mostly concentrated in the Midwest and eastern United States, as seen in figure 3.

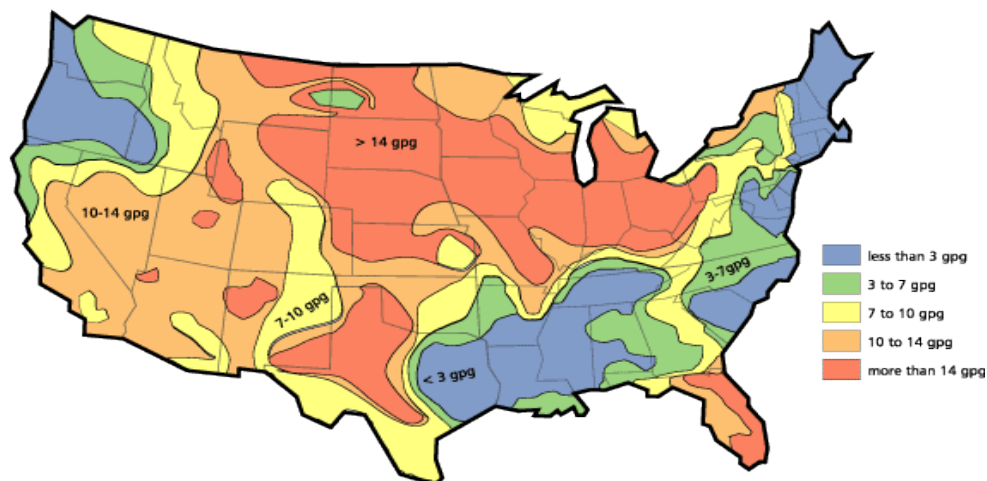


Figure 3: Hard Water in the United States

VOCs (volatile organic compounds) are a common problem in many areas because they come from many paints, varnishes, solvents and cleaners. The problem areas exist in large cities because these

particular chemicals come from industrial processes. The profile for VOC contamination in the United States is shown in figure 4.

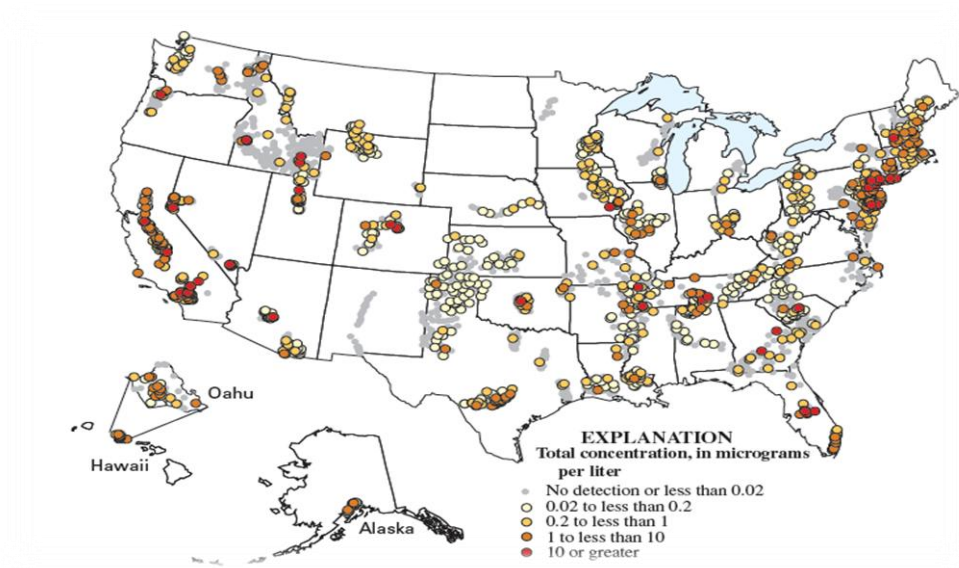


Figure 4: VOC Contamination in the United States

The major driving force behind the need for groundwater remediation is the adverse effects contaminants have on the public. The following table outlines some of the common groundwater contaminants and their adverse affects on health.

Compound	Potential Health Affects	Sources of Contamination	
Benzene	Known Carcinogen	Discharge from factories, leaching from gas storage tanks and landfills	†,† †
Vinyl Chloride	Known Carcinogen	Leaching from PVC pipes, discharge from plastic factories	†,† †
Arsenic	Skin damage or problems with circulatory systems, and may have increased risk of getting cancer	Erosion of natural deposits, runoff from orchards, runoff from glass & electronics production wastes	††
Copper	Gastrointestinal distress, liver or kidney damage, and more	Corrosion of pipes and household plumbing systems, erosion of natural deposits	††
Lead	Delays in physical and mental development in children, possible deficits in attention span and learning disabilities. Adults can experience kidney problems or high blood pressure	Corrosion of pipes and household plumbing systems, erosion of natural deposits	††
Mercury	Kidney damage	Erosion of natural deposits, discharge from refineries and factories, runoff from landfills and crop lands.	††
Trihalomethanes	Liver, kidney or central nervous system problems, increased risk of cancer	Byproduct of drinking water disinfection	††, †††
Nitrate	In infants, could cause illness or death; characterized by shortness of breath or blue-baby syndrome.	Runoff from fertilizer, leaching from septic tanks, sewage, and erosion of natural deposits.	††

**Table 1: Contaminants and Health Effects**

Because of their clear adverse effects on the community, these types of contaminants need to be removed from polluted sites.

## Options for Lowering Contaminant Concentrations

Two very general options exist for lowering the concentration level of undesirable compounds found in groundwater. They are dilution and treatment. In previous years, dilution was used to lower contamination concentration because it is much less expensive than treatment of the contamination. The problem with dilution is that it does not solve the problem but merely pushes the contamination volume, or the plume, away from the original contamination site. Many of the current conventional methods for treatment involve a pump-treat-inject (PTI) method. This consists of pumping water from an aquifer, treating the water for contamination, and re-injecting clean water back into the aquifer. A general PTI schematic is shown in Figure 5.

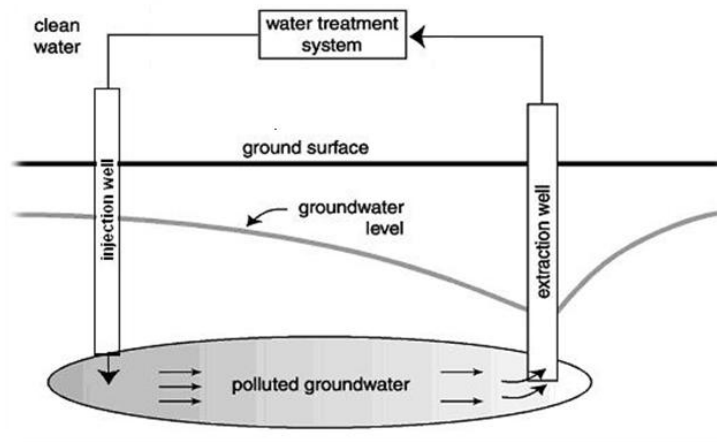


Figure 5: Pump-Treat-Inject Method

In the pump-treat-inject method, both injection and extraction wells are required. The number of both types may be varied. Figure 6 shows the use of several well configurations involving no injection or extraction wells to multiple injection and multiple extraction wells.

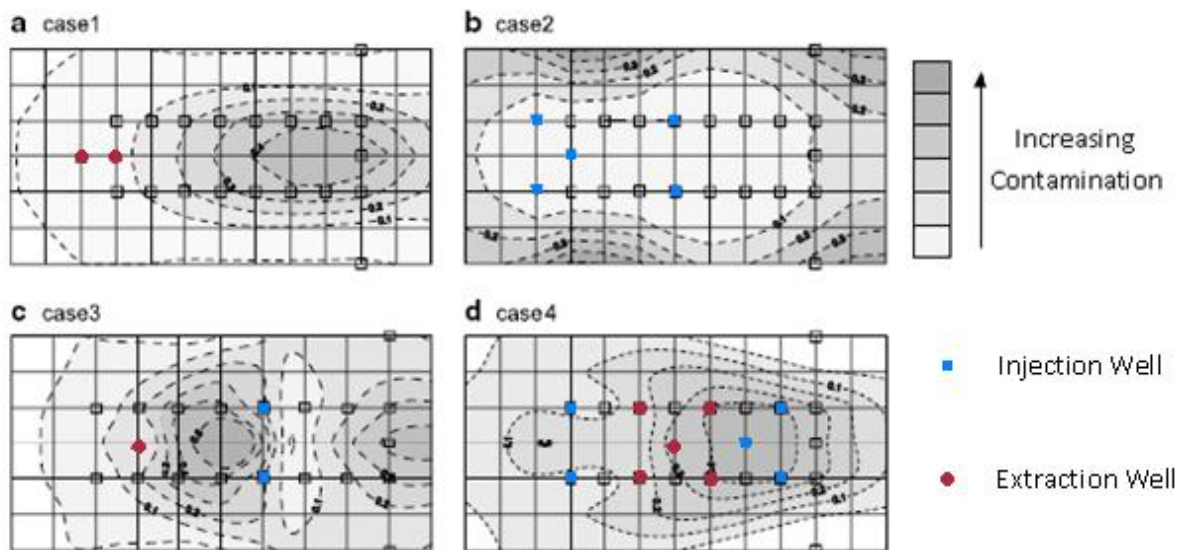


Figure 6: Depiction of PTI vs Dilution Only

In Figure 6, the darker gray represents higher contamination and the white represents the lowest contamination. From Figure 6, case 2, we can see the affects of dilution only. It is clear from the large white portion toward the center of the plume and the darker gray outer rings that the contamination is only being pushed and the problem is not being resolved. In case 1 only extraction is being used and it

can be observed that the aquifer is being cleaned near the well sites but remains highly contaminated away from the extraction. It is clear that a treatment method is necessary for resolving contamination issues.

Some methods for purifying groundwater are use of membranes, distillation, reverse osmosis, liquid-liquid extraction, ion exchange chromatography, and point of service treatments such as household filters. Koch has developed membrane bioreactors for the treatment of water. A chart of some possible water treatments and the contaminants they remove is given in Table 2.

Treatment Method	Contaminant																
	Iron bacteria	Bacteria	Giardia & Cryptosporidium Cysts	Hard Water, Calcium, Magnesium	Arsenic	Asbestos	Chlorine	Copper	Fluoride	Iron and Manganese	Mercury	Lead	Nitrates	Other Inorganics	Disinfection Byproducts	MTBE	Pesticides, Herbicides & Insecticides
Chlorination	x	x								x							
Water Softener				x				/	/	/				/*			
Ion Exchange Resin				/	/	/	/	/	/	/	/	/	/	/	/	/	/
Magnetic Conditioning																	
Whole House Sediment Filter										x							
Whole House GAC Filter							/								/	/	/
Ozonation Device		x	x							x							/
Manganese Greensand Oxidization Filter				/						x				x			
Distillation	x	x	x	x			x	x	x	x	x	x	x	x	/	/	/
Reverse Osmosis	x	x	x	x			x	x	x	x	x	x	x	x	/	/	/
KDF Filter					x		x	x		x		x		/			
Ceramic Filter	x	x								x							
GAC Filter							x			x		x			/	/	/
SBAC Filter	x	x					x			x	x	/			x	x	x
Activated Alumina Filter					x				x								
UV Disinfection	x																
Boiling	x	x					x								x		/

x = Removes Contaminant  
 / = Removes Some of the Contaminant  
 \* = May Add Other Contaminants

**Table 2: List of Treatments and Contaminants Removed**

It can be seen in this table that distillation and reverse osmosis are two of the methods with the widest range of applications for removing contamination. In the United States, the standards for the maximum allowable concentrations of such contaminants in groundwater are set by the Environmental Protection

Agency. The EPA standards for concentration in drinking water for some common groundwater contaminants are shown in the following table.

Compound	EPA Standard Maximum Concentration
Benzene	5 ppb
Vinyl Chloride	2 ppb
Arsenic	10 ppb
Copper	1.3 ppm
Lead	15 ppb
Mercury	2 ppb
Trihalomethanes	80 ppb
Nitrate	10 ppm

Table 3: Common Contaminants and EPA Standards

## Industrial Practices and Current Research

Separation processes, including those aimed at cleaning undesirable components out of water, are processes that exploit chemical and physical properties of the components in the mixture. Table 4 shows a list of some of the general treatment methods and the separation principles they use.

Treatment Method	Method / Principle of Treatment							
	Size	Solubility	Volatility	Chemical Reaction	Charge	Precipitation	Adsorption	Pressure
Chlorination				x				
Ion Exchange Resin					x		x	
Magnetic Conditioning						x		
Ozonation Device				x				
Distillation			x					
Reverse Osmosis								x
UV Disinfection				x				
Surfactants		x						
Membranes and/or Filters	x						x	x
Boiling			x		x			

Table 4: General Treatment Methods and Separation Principles

## Optimization

Because a pump-treat-inject approach is more expensive than simple dilution, these processes can be optimized to reduce the cost of treatment while keeping the concentration of contaminants at an acceptable level. The major factors contributing to the cost of groundwater remediation are as follows:

- Fixed Initial Costs
  - Permits, patents and royalties
  - Cost of drilling
  - Cost of equipment
    - Well and pumping equipment
    - Treatment equipment
- Fixed Continuous Costs
  - Depreciation
  - Fixed operating cost
- Variable Continuous Costs
  - Variable operating cost
    - Labor cost
    - Utilities
  - Treatment Cost

Parameters which may be used in order to minimize the cost of treatment are pumping rates, number of wells, well configurations and remediation time. All of these factors affect the concentration profiles of the plume, which affects the cost to clean the plume. For example, the pumping rates will affect the cost of electricity and the size of the pumps required. Overall remediation time will directly affect the cost of labor and the cost to purchase new equipment. The number of wells directly affects the cost of drilling. All of these variables must be taken into account in order to optimize the remediation process.

## Uncertainties and Problems with Remediation

Uncertainties and unknowns associated with the remediation parameters present many obstacles in the design of an optimized process. Table 5: Problems with Remediation Information and Associated Effects shows possible problems with the information for remediation of a contamination plume and the effects these problems have on the design of the process.

Unknown	Problems with				Effect on Design				
	Uncertainties in Measurement	Information Not Easily Obtained	Needs to be Monitored	Uncertainties in Accuracy	Affects Well Locations	Affects Number of Wells	Affects Total Remediation Time	Affects Pumping Rates	Affects Treatment Method
Flow Patterns	x	x	x	x	x	x		x	
Concentration Profiles	x		x	x	x	x	x	x	
Plume Position		x	x	x	x	x	x		
Plume Size		x		x	x	x	x	x	
Contaminants	x	x		x					x
Geological Profile	x	x		x	x			x	

**Table 5: Problems with Remediation Information and Associated Effects**

Table 5 shows that things such as flow patterns and concentration profiles need to be monitored but cannot necessarily be measured with any accuracy. Also, it may be difficult to determine the contaminants present and the initial amounts of these contaminants with good accuracy. The only parameter which affects the treatment process chosen is the types of contaminants present in the aquifer. All of the inadequacies of the information affect the ability to mathematically model the process.

## Previously Developed Models

Several mathematical models have already been developed to optimize the remediation process of a contamination plume. There are several advantages and drawbacks to each of these models. Table 6 shows some of the characteristics of some mathematical models that have been developed recently.

	Chang, Chu, Hsiao	Minsker, Shoemaker	Schaerlaekens, Carmeliet, Feyen	Rogers, Dowla, Johnson
Considers Fixed Cost	x			x
Considers Operating Cost	x	x	x	x
Determines Optimal # of Wells	x		x	
Optimizes Well Locations	x		x	x
Has Time-Varying Pumping Rates (not strictly on/off)	x	x		
Optimizes Pumping Rates	x	x	x	x
Is a 3D Model			x	
Avoids Local Minimum	x	x	x	x
Contains Contamination Plume	x	x		x
Considers Concentration of the Contaminant(s)	x	x	x	x
Uses Pump and Treat Method	x	x	x	x
Is Not Specific to Particular Compound	x	x		

**Table 6: Previously Developed Mathematical Models**

It can be seen that the Chang, Chu Hsiao method is the most thorough of the models examined. Although the Chang, Chu Hsiao model is fairly good, it does not model flow in three dimensions. While two of these models explore varying pumping rate with time, none investigate changing the well configuration with time. The aim of this project was to improve upon the current models and optimize the remediation process while including three dimensional fluid flow characteristics and dynamic optimization.

## Fluid Flow Analysis

In order to have a more accurate understanding of the behavior of the flow in the aquifer, fluid flow simulations were used. Fluent, a computational fluid dynamics program, was used in this analysis.

### Initial Fluid Flow Approach

#### Gambit

Before conducting the simulations in Fluent, the geometry of the aquifer must be drawn into Gambit, Fluent's geometry and mesh generation software. The aquifer was modeled as a rectangular prism or a hexahedron. The general shape of the aquifer is shown in Figure 7: 20 x 10 x 10 Hexahedron. Figure 7: 20 x 10 x 10 Hexahedron is a  $20 \times 10 \times 10$  hexahedron generated in Gambit.

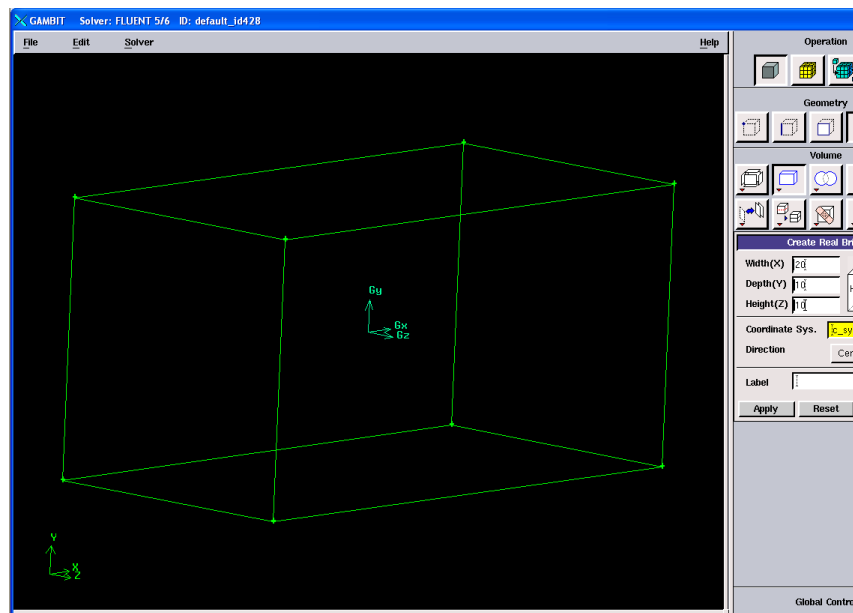


Figure 7: 20 x 10 x 10 Hexahedron

Gambit is also used to draw the placement of the injection and extraction wells. The injection and extraction wells are simulated as small volumes,  $1 \times 1 \times 0.01$  in the x y and z directions respectively, and were attached on the yz plane. To clearly depict this, a volume of  $1 \times 1 \times 0.5$  is shown in Figure 8 in the position of a possible injection well. The injection and extraction wells for the simulations were drawn this way except the volume of the injection and extraction sites were minimized by making the z dimension only 0.01. This was done in order to minimize effects of this volume on fluid flow so the simulations would only represent the flow patterns in the aquifer volume.

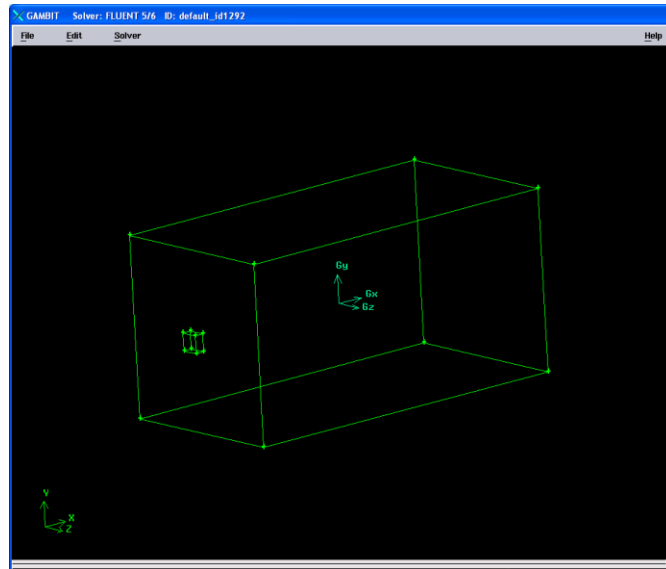


Figure 8: Gambit Geometry with  $1 \times 1 \times 0.5$  Cube Attached

Figure 9 shows a simple geometry drawn in Gambit. This is a geometry representing one injection and one extraction well. The  $1 \times 1 \times 0.01$  cube attached to the aquifer volume at  $x = -10$  represents the injection well and the  $1 \times 1 \times 0.01$  cube attached to the aquifer volume at  $x = 10$  represents the extraction well.

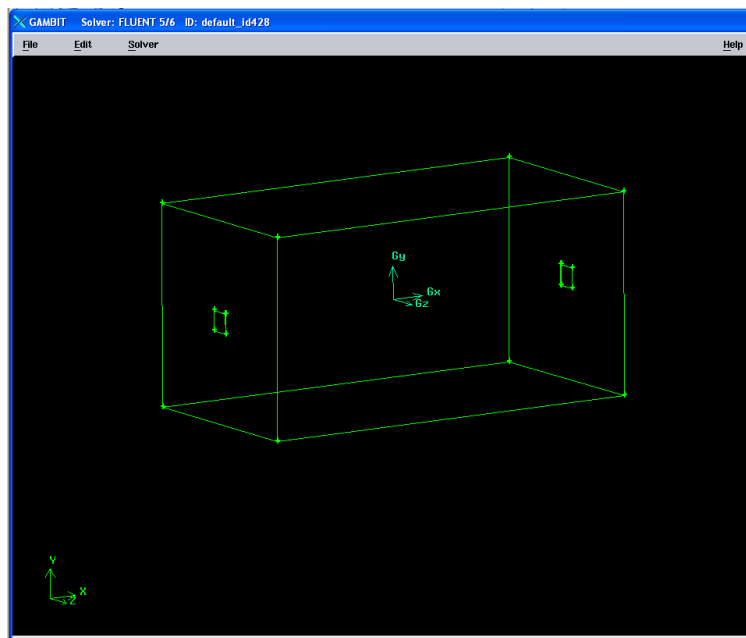


Figure 9: Gambit Geometry with 1 Injection Well and 1 Extraction Well

In Gambit, the specific faces are given boundary types or boundary conditions. The outer face of the injection volume is given the boundary condition of a mass flow inlet. The outer face of the extraction

site is given the boundary condition of an outlet. Gambit assumes all other faces to be walls. Figure 10 shows these boundary conditions specified in Gambit. It is important to clarify that the depth (z-distance) of the volumes representing injection and extraction volumes is increased to 0.5 for visualization purposes only.

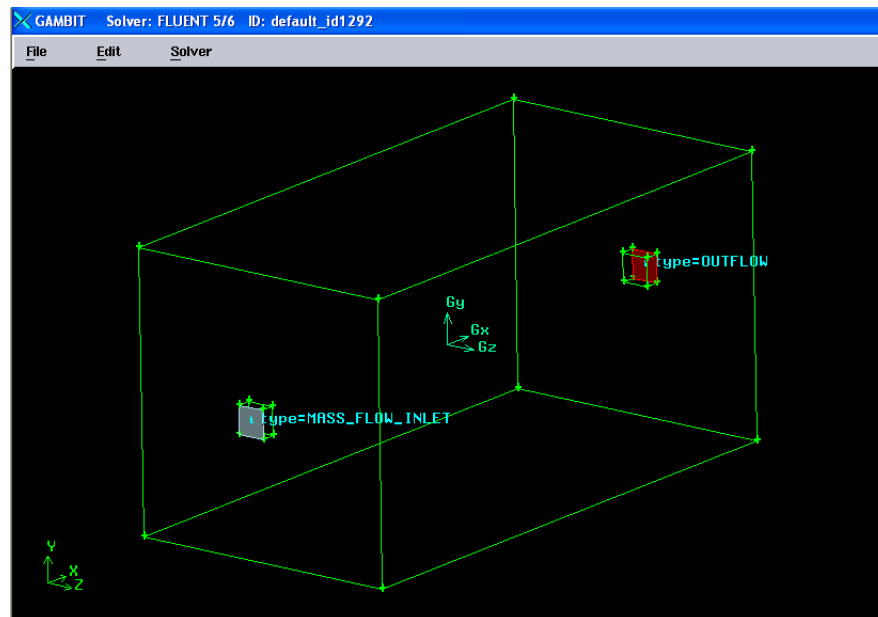


Figure 10: Gambit Geometry with Boundary Conditions Displayed

Several geometries were drawn into Gambit and exported into Fluent for fluid flow analysis. Finally, one generic geometry was created for convenience. The generic geometry consisted of the same aquifer volume with a grid of possible injection and extraction wells drawn on the injection and extraction faces of the aquifer. This drawing of a generic geometry lessened the time for analysis of different well configurations because the boundary conditions were varied each time rather than having to draw a new geometry each time. This means that the face located in the desired location for an injection well would be named a mass flow inlet and the faces in the desired extraction positions would be named outflows while all other faces would remain named as walls. This generic geometry is shown in Figure 11: Generic Geometry in Gambit is the generic geometry that was used.

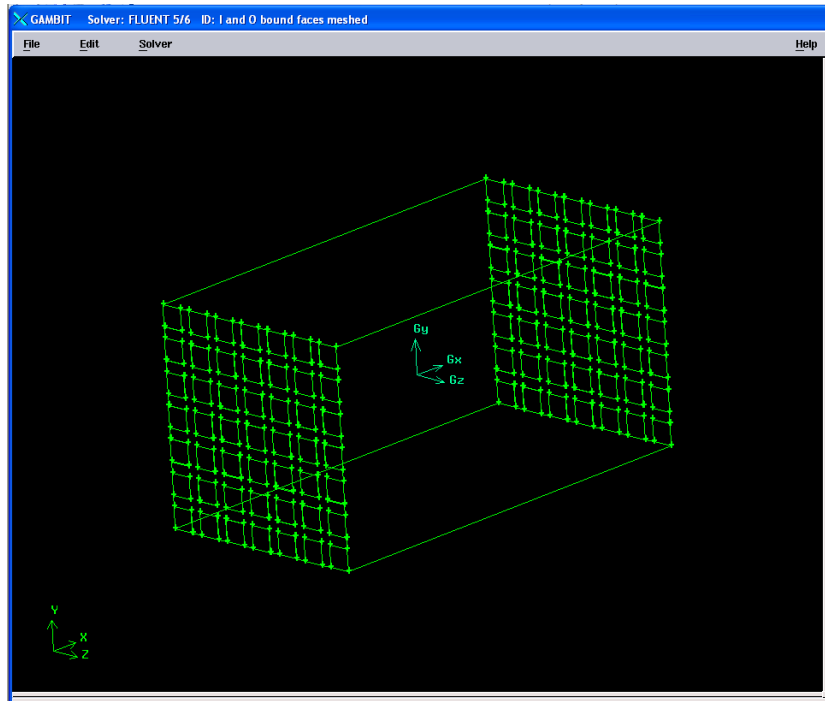


Figure 11: Generic Geometry in Gambit

To identify the individual planes, the following nomenclature was used:

- The first letter in the name of the planes indicated inlet or outlet (I for inlet, o for outlet)
- The second letter in the name of the plane represented the column
- The third letter indicated which row of the plane

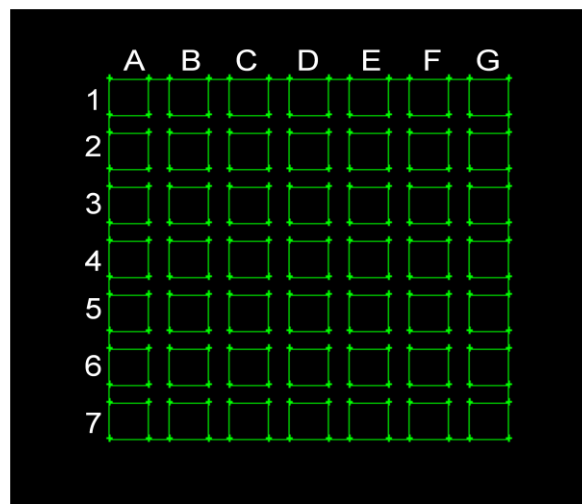


Figure 12: Nomenclature for Naming of Inlet and Outlet Planes

Figure 12 shows the naming of the rows and columns. Figure 13 shows an example of how an individual plane, C3, would be named. If it were located on the inlet side of the aquifer it would be “ic3” and on the outlet side it would be named “oc3.”

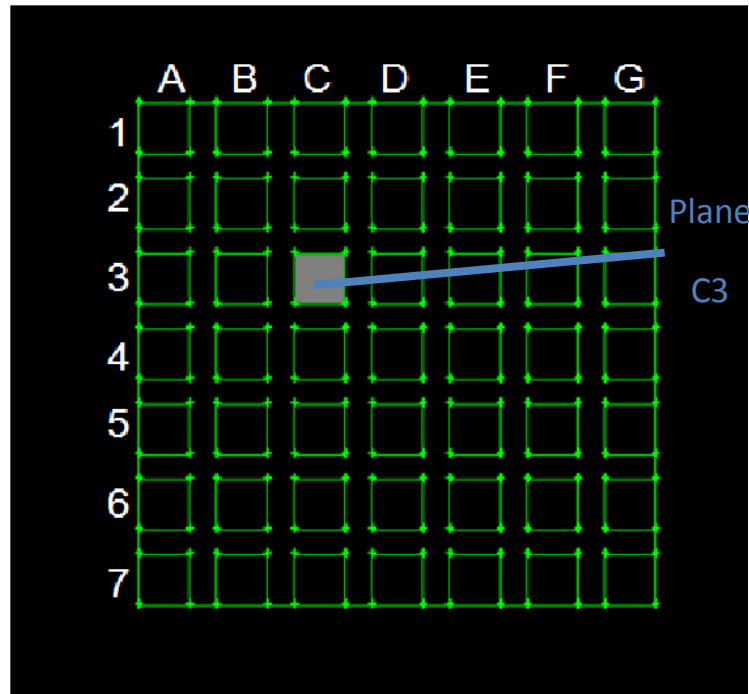


Figure 13: Example of Naming Planes

Once the planes were named, the different well configurations were created by naming the boundary conditions. Seven well configurations were analyzed. The following table outlines the different well locations for the different well configurations.

Well Configuration	Number of Inlets	Number of Outlets	Location of Inlets				Location of Outlets			
1	1	1	id4				od4			
2	1	2	id4				ob4		of4	
3	1	3	id4				ob6	od2	of6	
4	2	1	ib4		if4		od4			
5	2	2	ib4		if4		ob4		of4	
6	4	1	ib2	ib6	if2	if6	od4			
7	4	4	ib2	ib6	if2	if6	ob2	ob6	of2	of6

Table 7: Well Configurations

## Fluent

Once the geometry was set in Gambit, it was exported to Fluent. In Fluent the boundary conditions were again specified. The planes were specified as inlets or outflows, a mass flow rate in was specified as well as the porosity of the medium and the operating pressure. The operating pressure and the porosity of the medium were based off of data obtained from Dr. Jeffrey Harwell for the Newalla contamination site. The porosity of the medium is given from

$$porosity = \frac{V_p}{V_c}$$

Equation 1

where  $V_p$  is the static pore volume and  $V_c$  is the volume of the contamination site. The medium was estimated to be 25% porous.

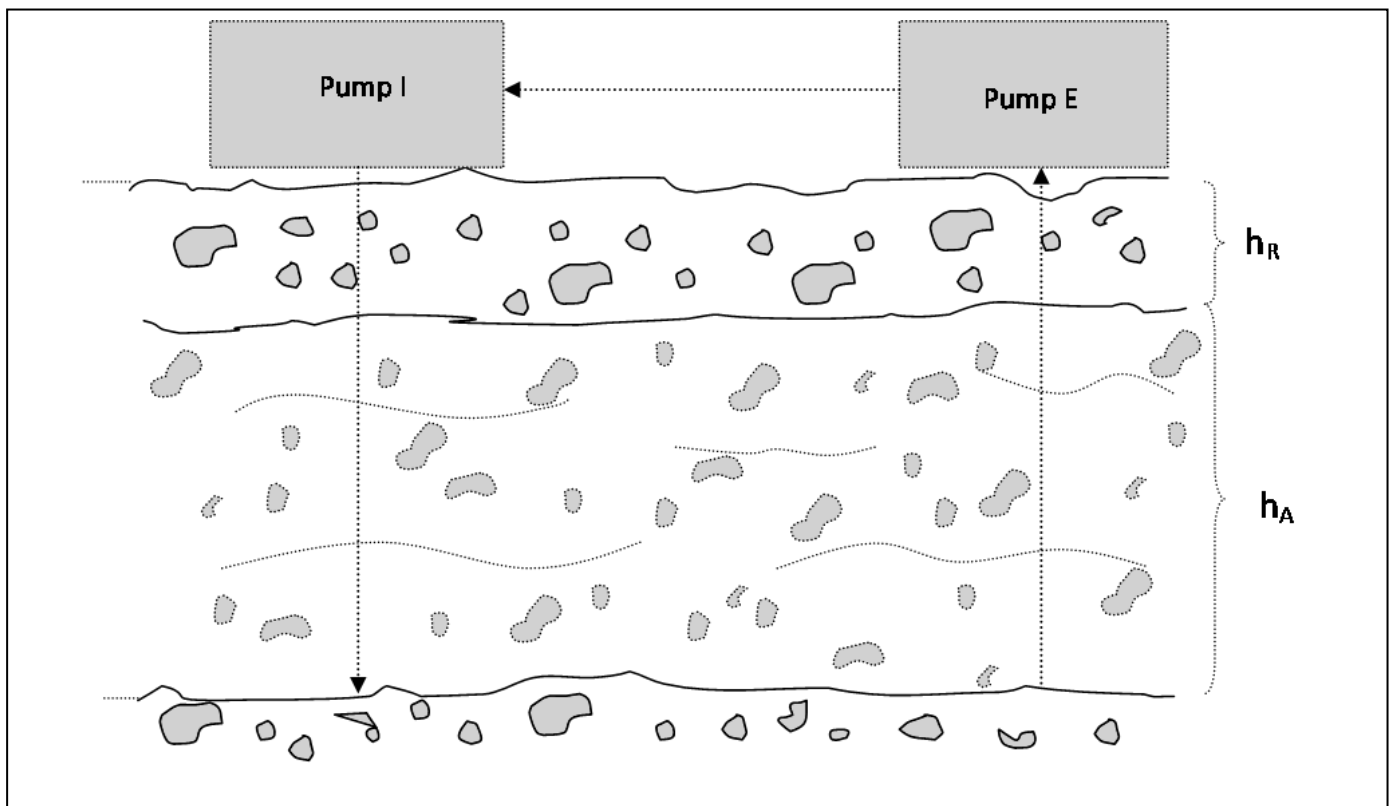


Figure 14 depicts (not to scale) the parameters used in the estimate of the operating pressure.

Figure 14: Depiction of Estimate of Operating Pressure

The operating pressure was estimated by  $P = \rho_{media}gh_M + P_{atm}$  Equation 2 and

$h_M = h_A + h_R$  Equation 3 where  $\rho_{media}$  is the density of the media, P is the operating pressure,  $P_{atm}$  is atmospheric pressure and g is gravity.

$$P = \rho_{media}gh_M + P_{atm} \quad \text{Equation 2}$$

$$h_M = h_A + h_R \quad \text{Equation 3}$$

This gave an operating pressure of 205.205 kPa. Also, the size of the aquifer was scaled by equating each unit in the Gambit mesh to 1 meter. In other words, the  $20 \times 10 \times 10$  geometry equated to a 2000 m<sup>3</sup> volume aquifer.

These parameters were input into Fluent for simulations. In order to analyze the flow through the aquifer, imaginary planes were drawn into the Fluent geometry.

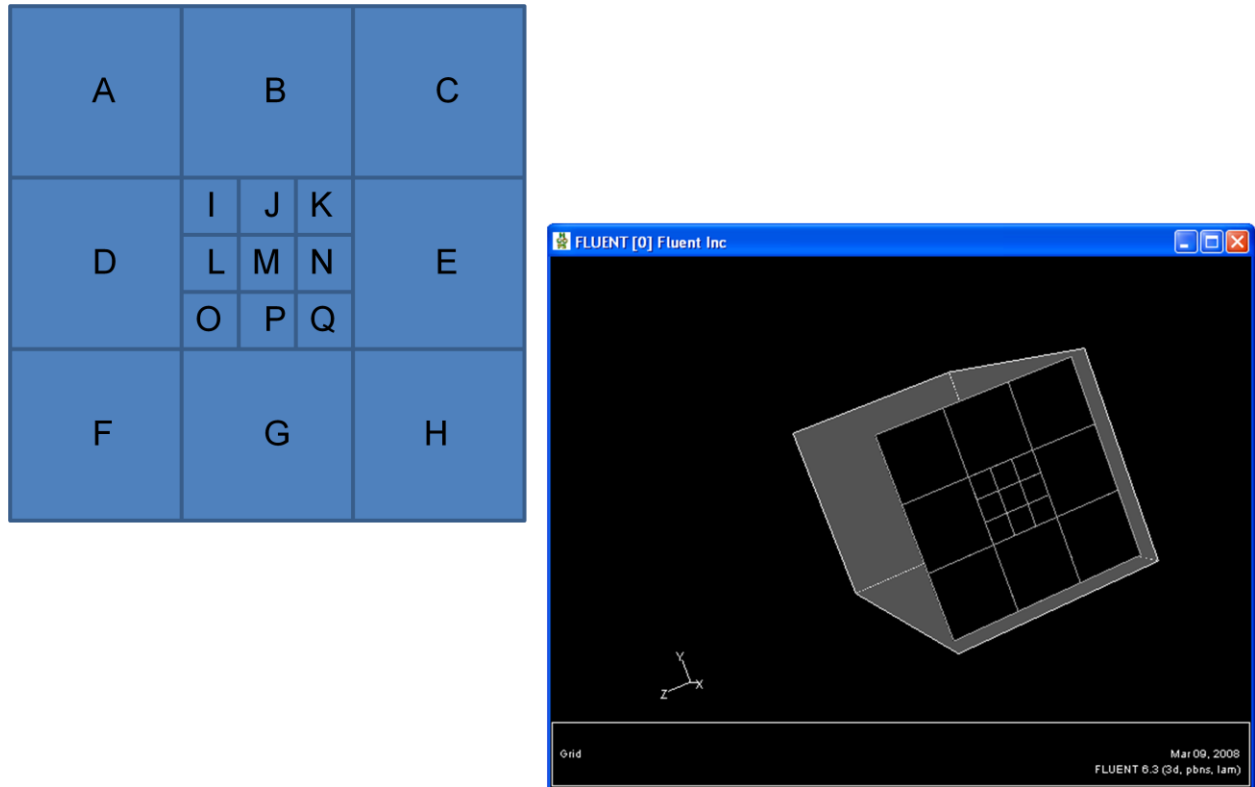


Figure 15: Imaginary Planes in Fluent and Nomenclature

After simulations were run, Fluent would output the mass flow rate through each plane. For this analysis, imaginary planes were drawn down the length (x-direction) of the aquifer volume. The imaginary planes through the aquifer are shown in Figure 16. The nomenclature for these imaginary planes are as follows:

- The first letter in the name indicates the location of the plane in the specific slice (Figure 15)
- The number in the name of the plane indicates the slice number in which the plane is located (Figure 16)

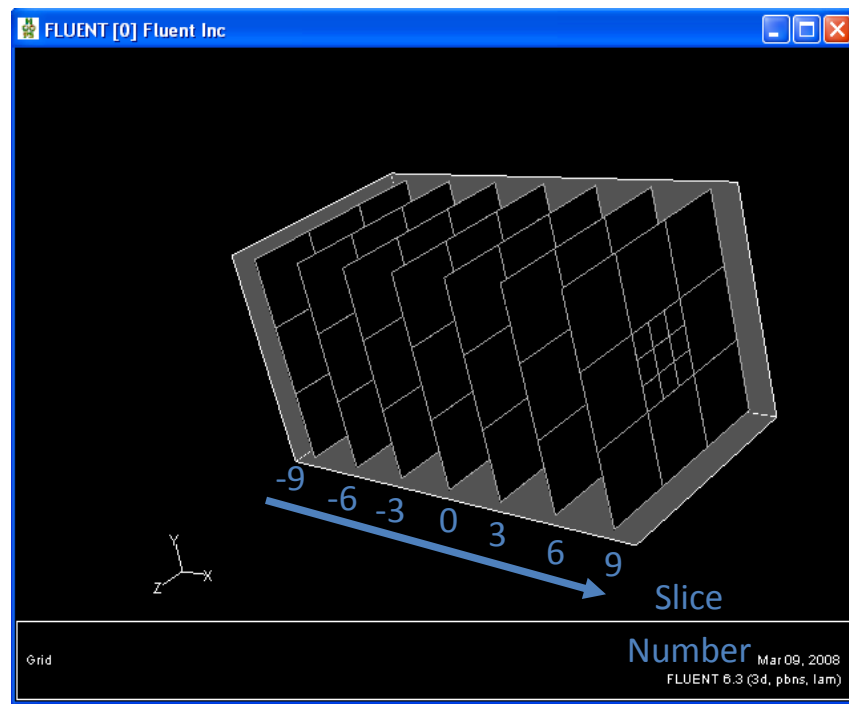


Figure 16: Planes Through the Length of the Aquifer

### Initial Fluid Flow Simulations

Simulations were run for each of the well configurations. Flow rate was varied for each well configuration. The flow rates tested were 100, 50, 10, 5, 1, 0.5 and 0.1 kg/s. A constant pumping rate over the entire remediation time was assumed. Also, to keep from creating accumulation or movement of the plume, it is required that the total mass flow in be equal to the total mass flow out of the aquifer.

In order to get an understanding of the behavior of the fluid flow in the aquifer with the various well configurations, the path lines were examined. An example of the behavior for the fluid flow in the aquifer with configuration 1 is shown in Figure 17. The color scale is given for the velocities along the

path lines. It is clear that the highest velocities in the aquifer are along the centerline. This is expected because the water is flowing directly from the inlet to the outlet. It can also be seen that because the amount of water being pumped into the aquifer, 1 kg/s, is so small compared to the volume of the aquifer, the velocity at any point in the aquifer is very small. The highest velocity in the aquifer with this flow rate and well configuration is about  $2.67 \times 10^{-4}$  m/s. Figure 18 through Figure 23 show the path lines for the fluid flow for several other configurations.

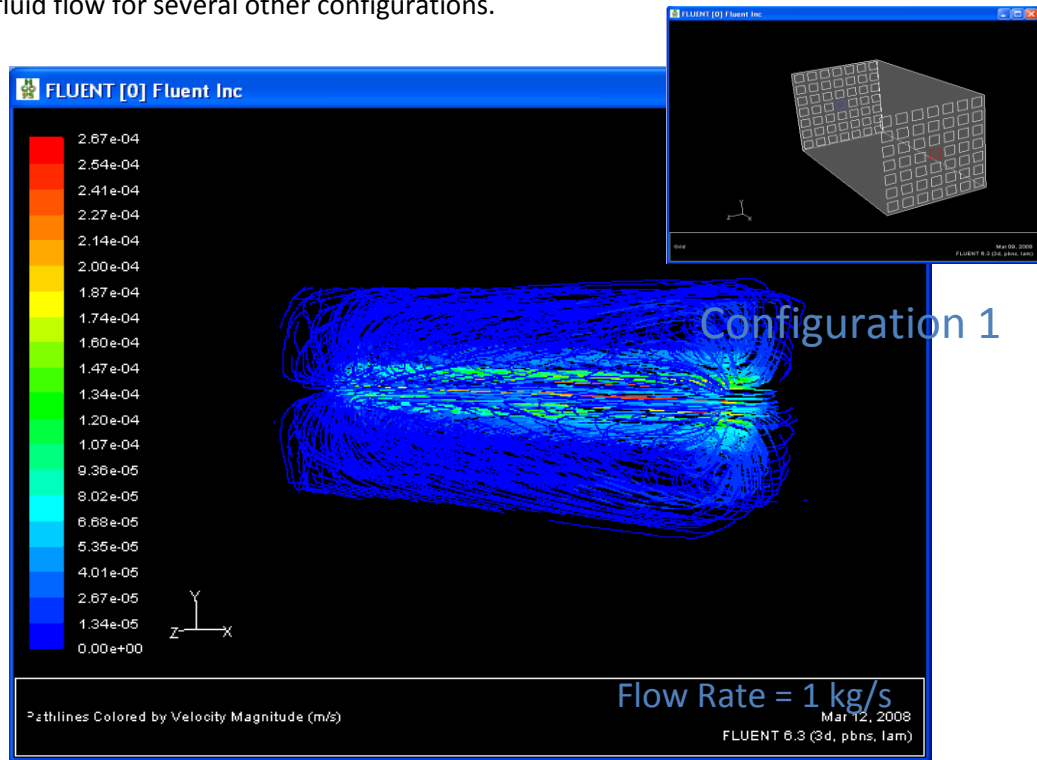
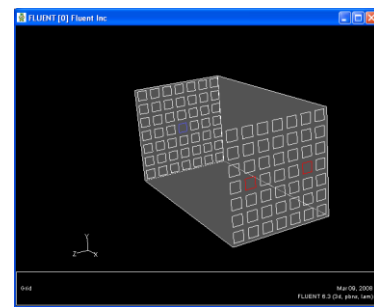


Figure 17: Path Lines for Configuration 1



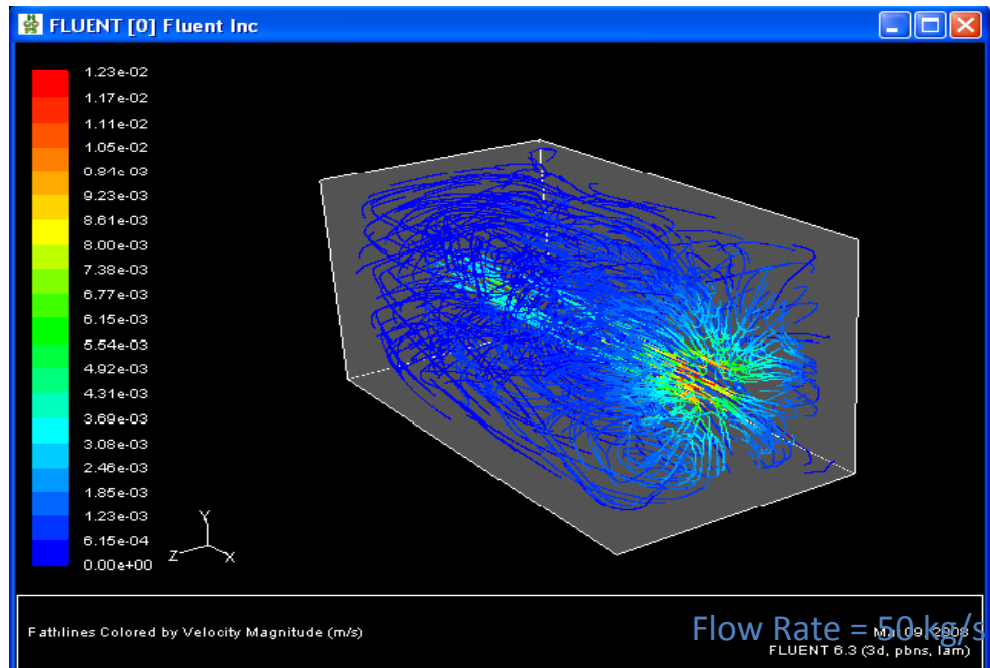
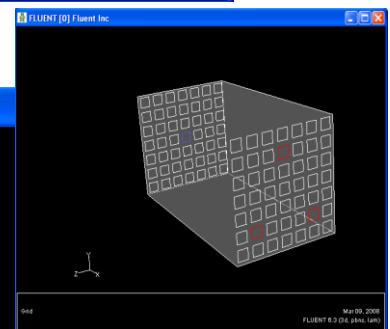
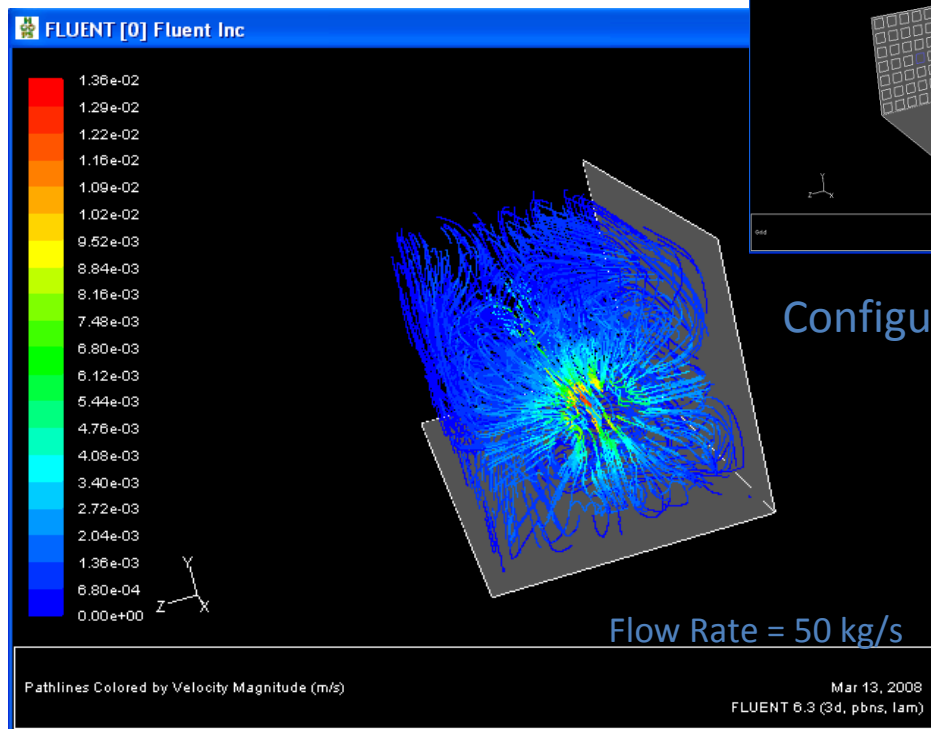
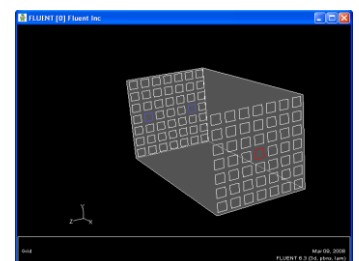


Figure 18: Path Lines for Configuration 2



Configuration 3

Figure 19: Path Lines for Configuration 3



Configuration 4

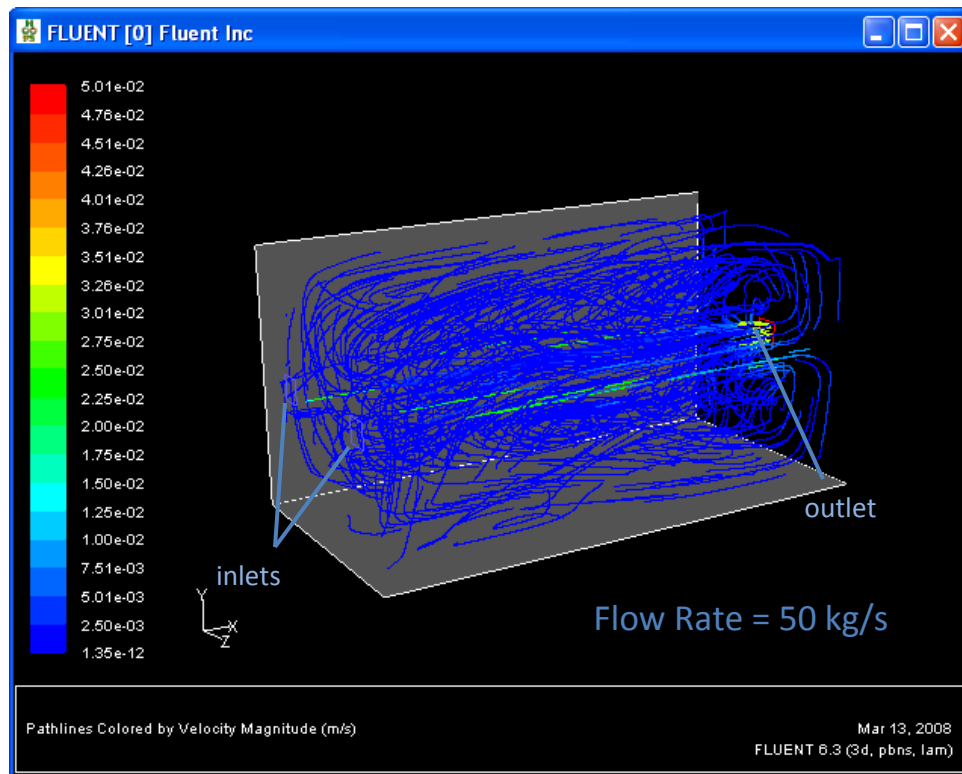
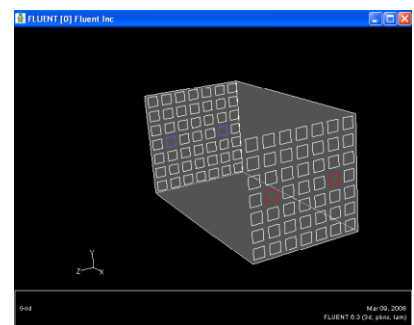


Figure 20: Path Lines for Configuration 4



Configuration 5

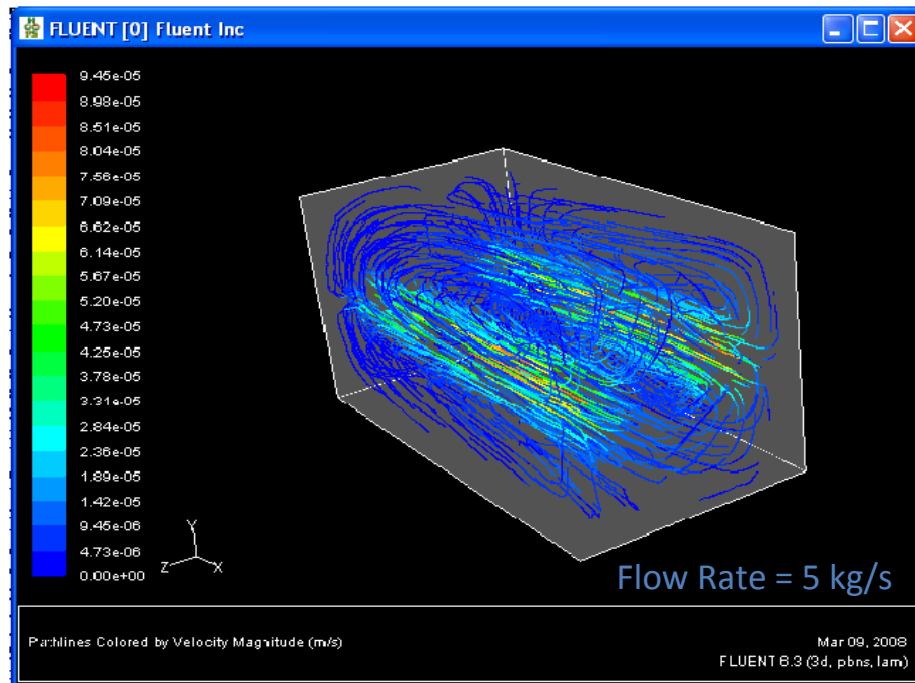


Figure 21: Path Lines for Configuration 5

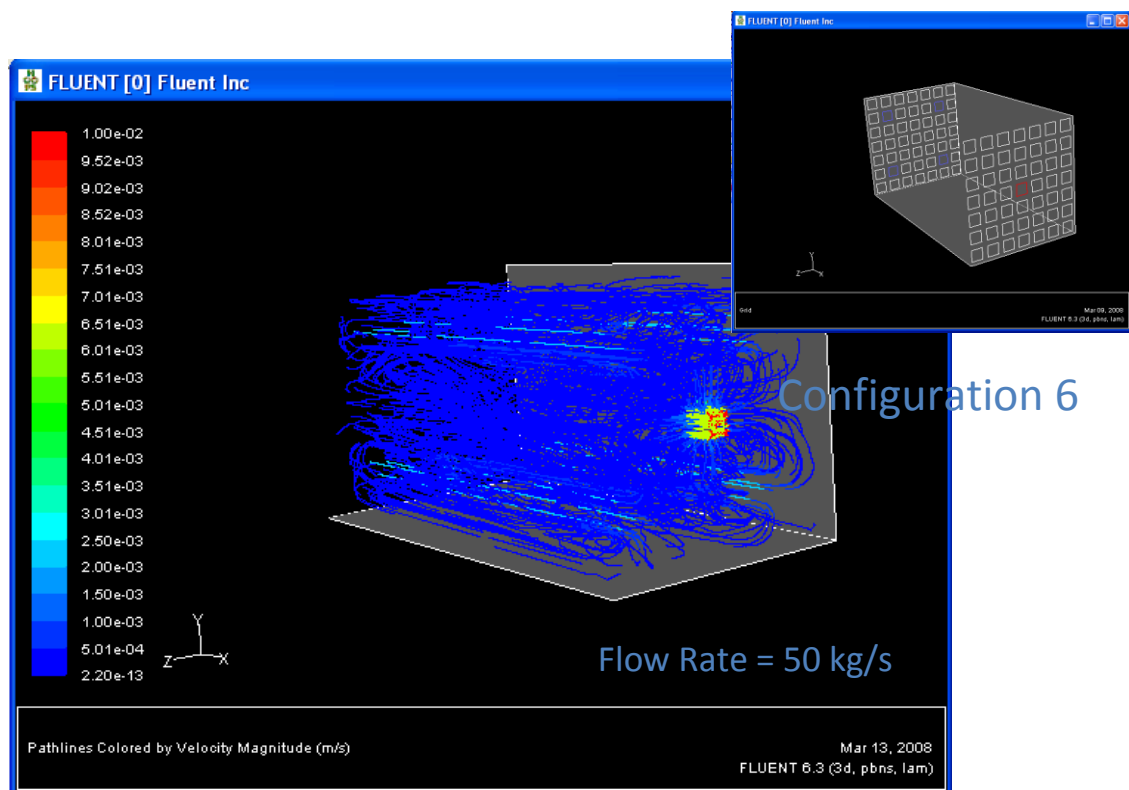


Figure 22: Path Lines for Configuration 6

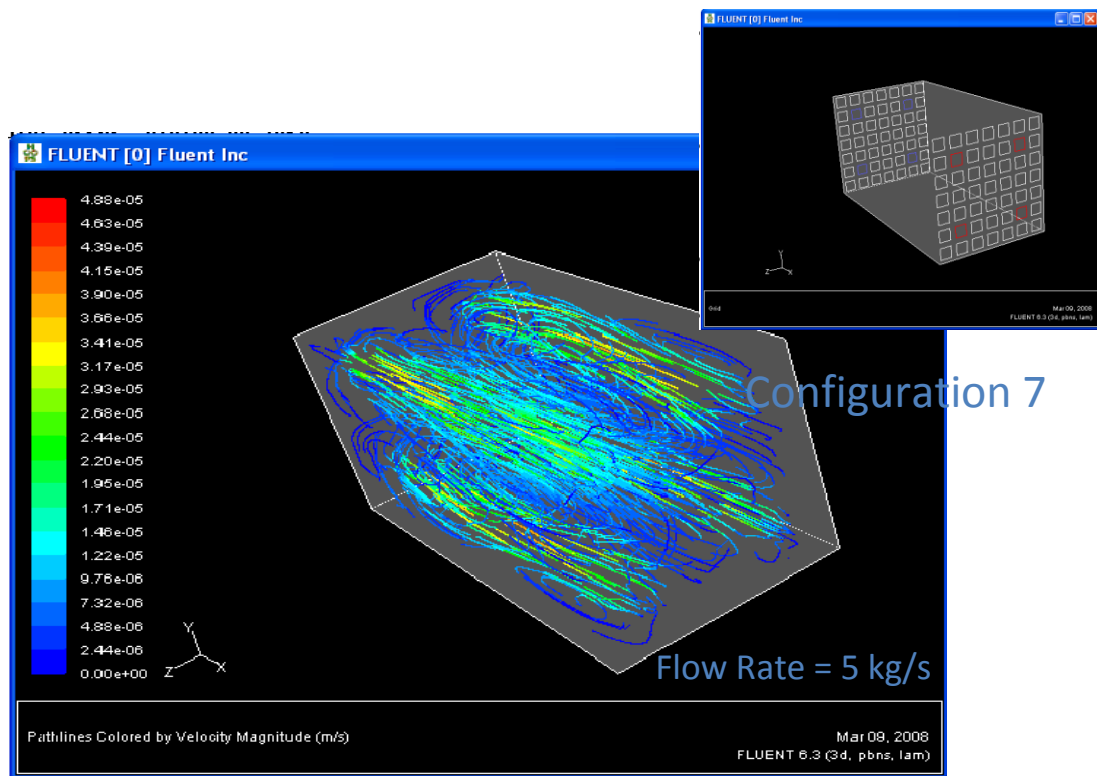


Figure 23: Path Lines for Configuration 7

Another way to visualize the behavior of the fluid flow within the aquifer is to display the velocity contours at a specific slice in the aquifer. Displaying imaginary planes a-q at slice -9 (closest to the inlet) and slice 9 (closest to the outlet) for configuration 7 is shown in Figure 24.

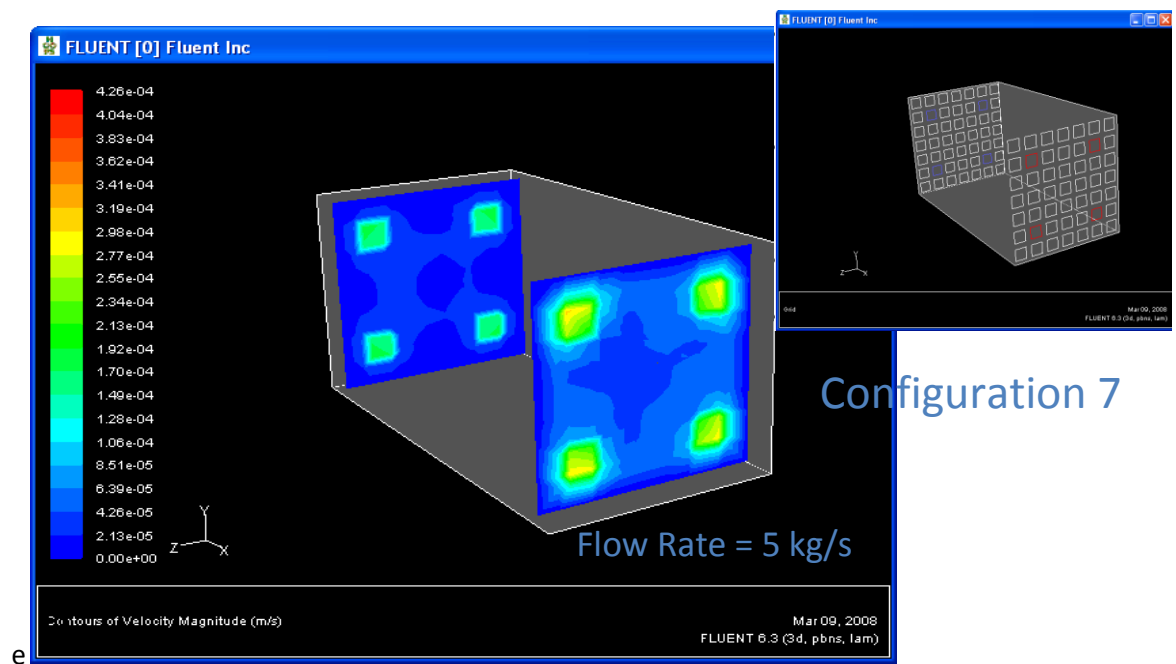


Figure 24: Velocity Contours for Configuration 7 Slices -9 and 9

It can be seen that the velocity is very high through each of the inlets. By the time the water reaches the outlets, some of the water drags the water in the middle of the aquifer and leads to some movement in the middle of the aquifer. It also leads to the spread of the velocity profile at each of the outlets.

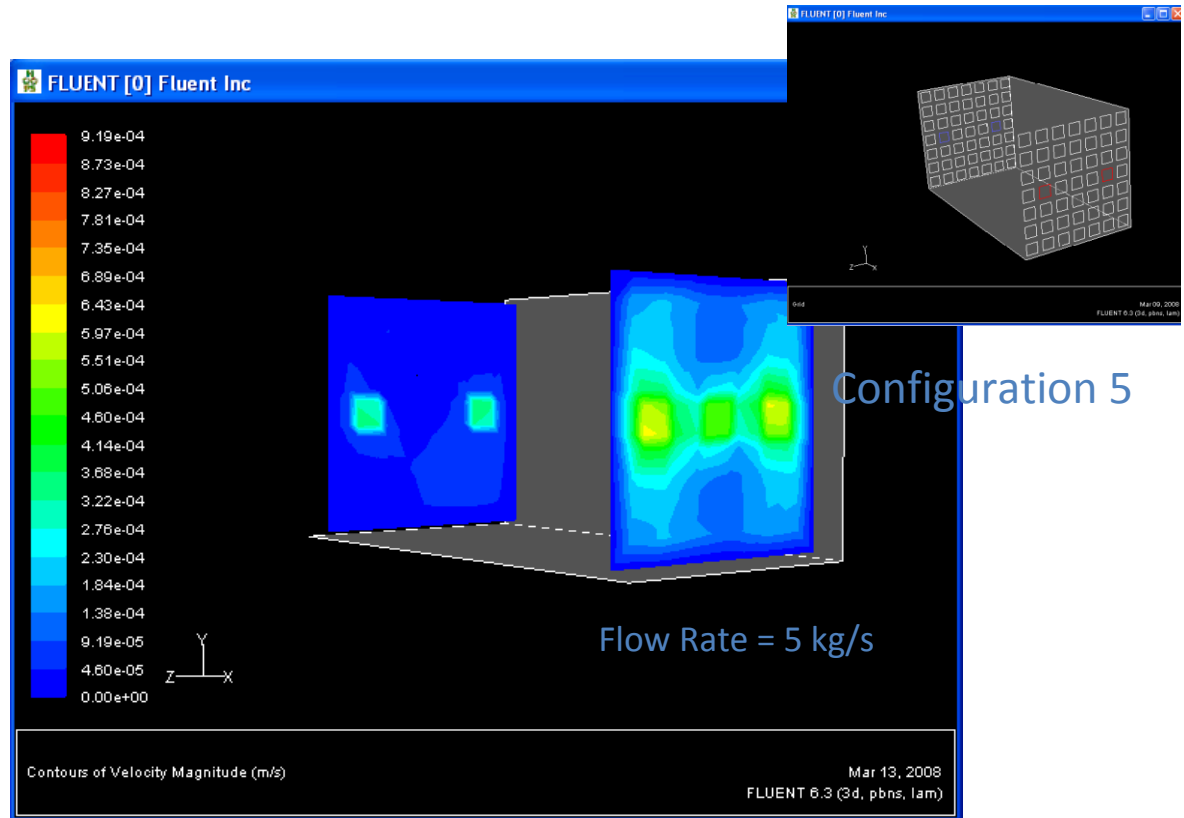


Figure 25: Velocity Contours for Configuration 5 Slices -9 and 9

Fluent was used to give the mass flow rate of water through each of the imaginary planes in the aquifer for each of the well configurations and flow rates.

### Concentration Profiles

The concentration profiles for the various well configurations and flow rates were calculated in Excel. The flow of water through the planes was treated as a “front” of water. It was seen that the water entering through the inlet is not causing large amounts of mixing in the aquifer but was more pushing the contaminated water toward the outlets. This phenomenon is depicted in Figure 26.

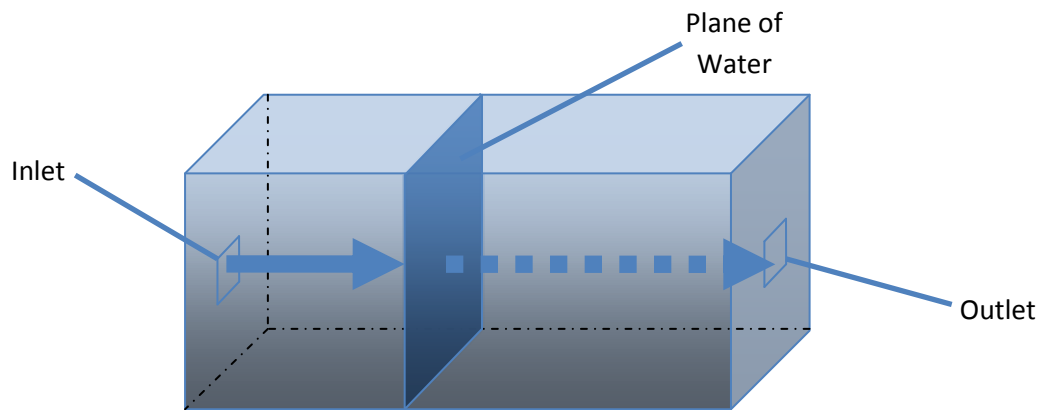


Figure 26: Front of Water Traveling Through the Aquifer

This depiction is not entirely accurate, however, since the velocity through the different planes will not be the same (i.e. the velocity through the center plane, M, will not be the same as one of the outer planes such as plane A for this configuration). A more accurate depiction of how the fronts of water would move through the aquifer in configuration 1 is shown in Figure 27.

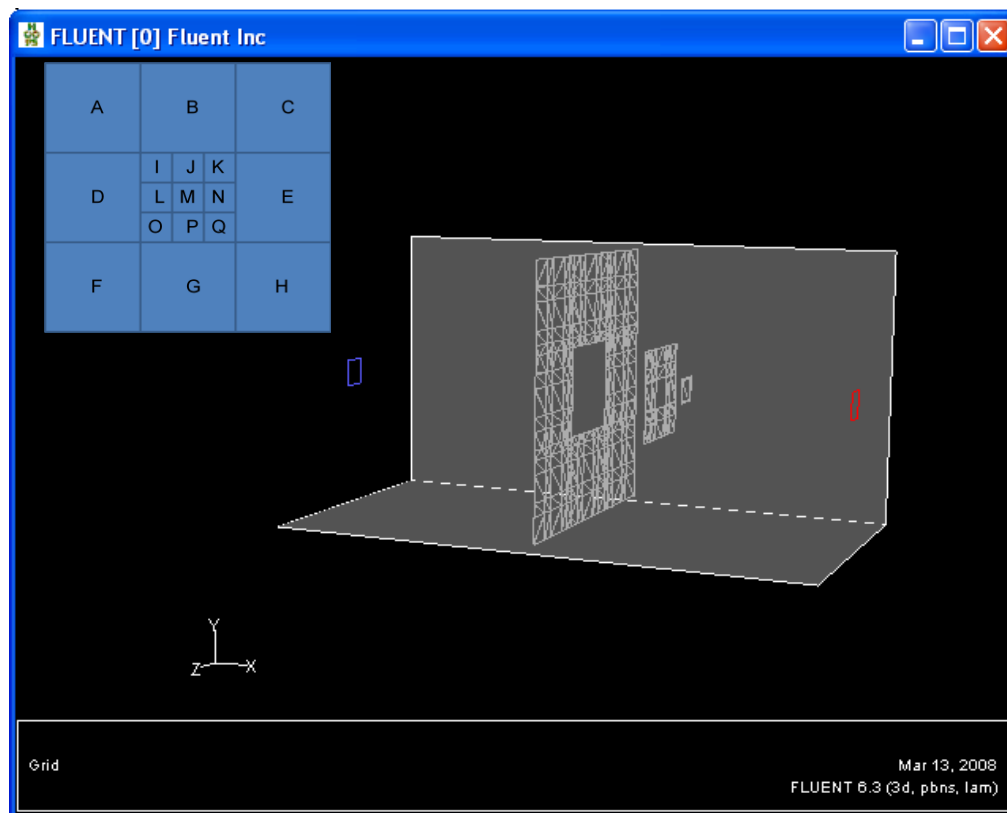


Figure 27: Fronts of Water Through the Aquifer for Configuration 1

An example of how this phenomenon might appear for configuration 5 is shown in Figure 28.

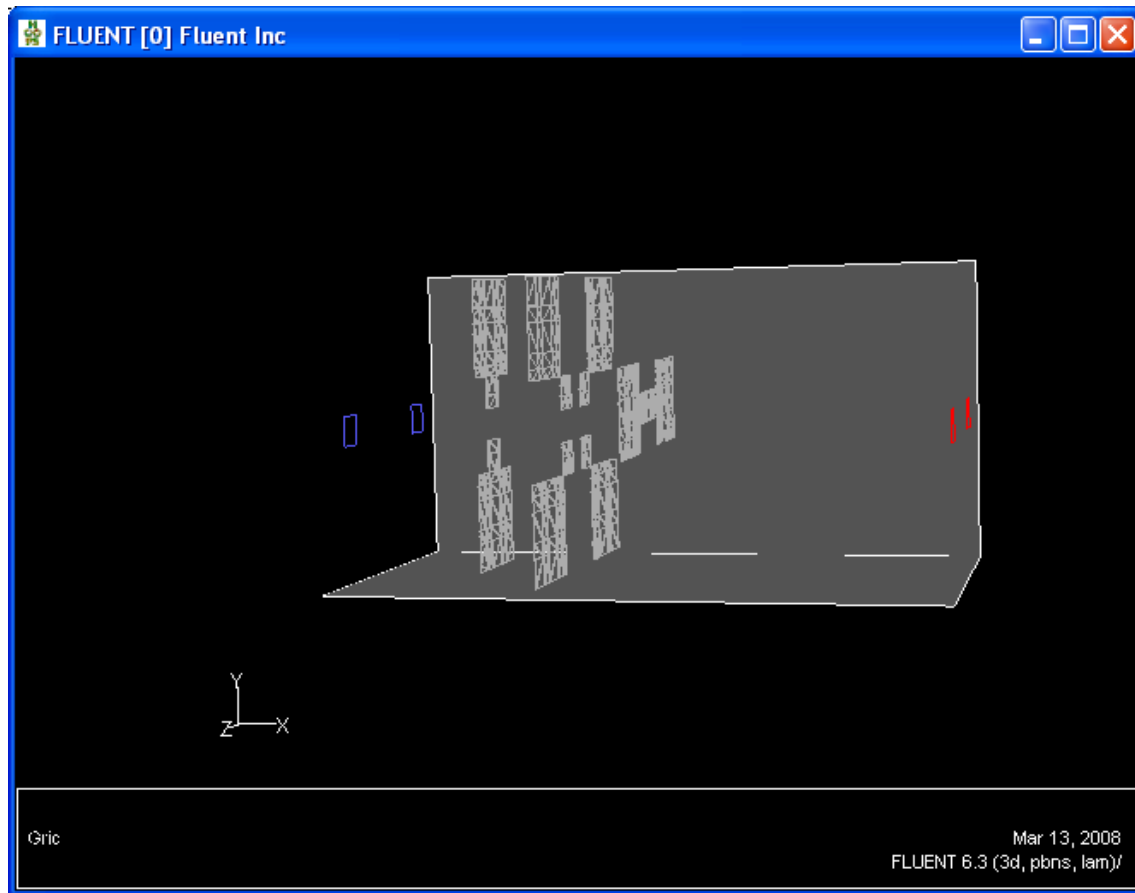


Figure 28: Fronts of Water Through the Aquifer for Configuration 5

The middle section of planes would be expected to move fastest through the aquifer based on the geometry and the fluid flow characteristics generated by Fluent for this configuration. Using these behaviors, the concentration profiles were analyzed.

### *Construction of Concentration Profiles from Fluent Data*

Fluent provides a mass flux through a given plane in the simulation volume. Since the flow is at steady state it is assumed that the flux will not change with time. The volume is broken up into the planes described previously in the Initial Fluid Flow Approach, Gambit section. At time  $t = 0$ , the aquifer was assumed to be well-mixed and was assumed to have a uniform initial concentration. The flux through each of the planes is averaged along the x-axis to get a constant flux through each of the planes. Next the volume between each of the planes is calculated using the size of and spacing between each of the planes. From this information and the following equation the concentration profile with time and position can be formulated for any given initial concentration.

$$C_f = \frac{V(C_o) - F(C_{out})\Delta t + F(C_{in})\Delta t}{V}$$

Equation 4

where  $c_f$  is final concentration,  $V$  is the volume between planes,  $c_o$  is initial concentration in the volume being calculated,  $c_{out}$  is the concentration leaving,  $c_{in}$  is the concentration entering,  $F$  is the flux through the given plane and  $\Delta t$  is the change in time. Flux not only provides the magnitude of the flux through the plane, but also the direction of that flux depending on whether the flux is specified to be in the positive or negative direction. This information complicates the execution of the above formula. The inlet and outlet concentrations are decided by the direction of the flux. If the flux passes in the forward direction, then the inlet concentration comes from the previous volume (the volume in the negative  $x$  direction), and the outlet concentration comes from the current volume. If, however, the flux is negative, then the inlet concentration comes from the following volume (the volume in the positive  $x$  direction) and the outlet concentration comes from the current volume. For clarification on these fluxes, directions, and concentrations, refer to Figure 29 below. If, for example, the flux through Plane A in Figure 29: Method for Determining Concentration In and Out of the Plane is positive then the flux will be moving into the volume between Planes A and B. The flux will be added (going in to the volume) and the concentration which will be entering through Plane A is  $c_{previous}$ . Conversely, if the flux through Plane A is negative, the flux will be moving in the negative  $x$  direction out of the volume and the concentration used will be  $c_o$ . If the flux through Plane B is positive, the flux will be leaving the volume between Plane A and Plane B, and the concentration which will be leaving is  $c_o$ . A negative flux through Plane B will result in concentration  $c_{next}$  entering the volume between Planes A and B.

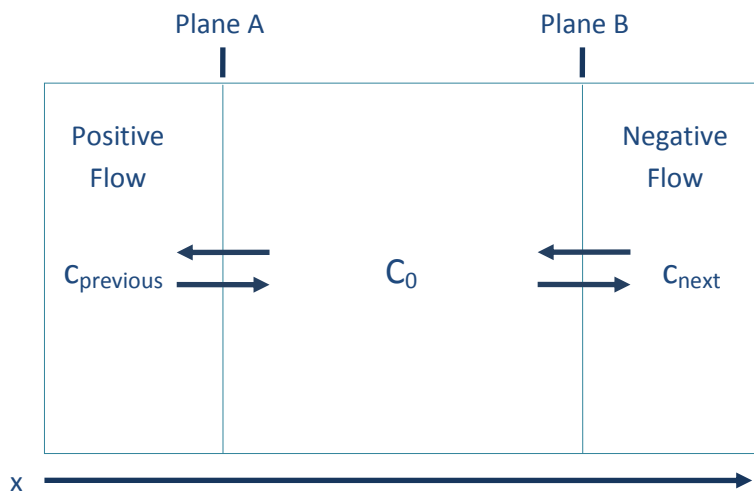


Figure 29: Method for Determining Concentration In and Out of the Plane

This calculation is performed sequentially with respect to both time and position. The result is a concentration profile that is a function of both position in the aquifer and time. The overall final concentration is found by taking the average of the concentrations in each of the planes. To achieve the desired concentration inside the aquifer, solver is used to set the final concentration to the proper EPA specification by changing delta t. This gives the overall remediation time and concentration profile. Once these are found, an economic analysis can be performed to find the optimum well configuration and flow rate.

## Results and Discussion

An example application was performed to test the model. Several case studies, including a groundwater remediation site in Newalla, Oklahoma (courtesy of Dr. Jeffrey Harwell) and an example by Chang et al., were referenced to find realistic aquifer properties. The characteristics chosen for the simulations are displayed in **Error! Reference source not found.** below.

Aquifer properties	
Media Bulk density	2.12 g/cm <sup>3</sup>
Porosity	0.25
Width	10 m
Length	20 m
Depth	10 m
Contaminant	Benzene
Initial Concentration	0.0001 kg/L
Injection Concentration	0.0000 kg/L
Desired Concentration	3.15 x 10 <sup>6</sup> kg/L

Table 8: Aquifer Properties

Each of the well configurations was run in Fluent at seven different flow rates: 0.1, 0.5, 1, 5, 10, 50, and 100 kg/s. The total flow rate was the same for each of the configurations, only the amount pumped at each well was changed with the configuration. Fluent provided the mass flux through all of the imaginary planes and these were then converted into volumetric flow rates using the density of water. Contaminant concentrations are too low to have an effect on the density, thus it is valid to assume a density of 1 kg/L. The volumetric flow rate was then multiplied by the concentration to find the mass flux of contaminant through the plane. The initial mass of contaminant between the planes is known.

$$C_f = \frac{V(C_o) - F(C_{out})\Delta t + F(C_{in})\Delta t}{V}$$

Thus, these values can be plugged into

Equation 4 to perform a mass balance between the planes and produce a concentration profile of the aquifer.

The data for several of the planes in each configuration is analyzed at a flow rate of 5 kg/s. This flow rate was chosen because it is a flow rate which is the median value for the flow rates to be investigated. The results for planes A, D, and M in Configuration 1 at a flow rate of 5 kg/s are displayed in Figure 30 through Figure 32 below. Planes A, D, and M were chosen to give a varied view of the flow behavior throughout the aquifer.

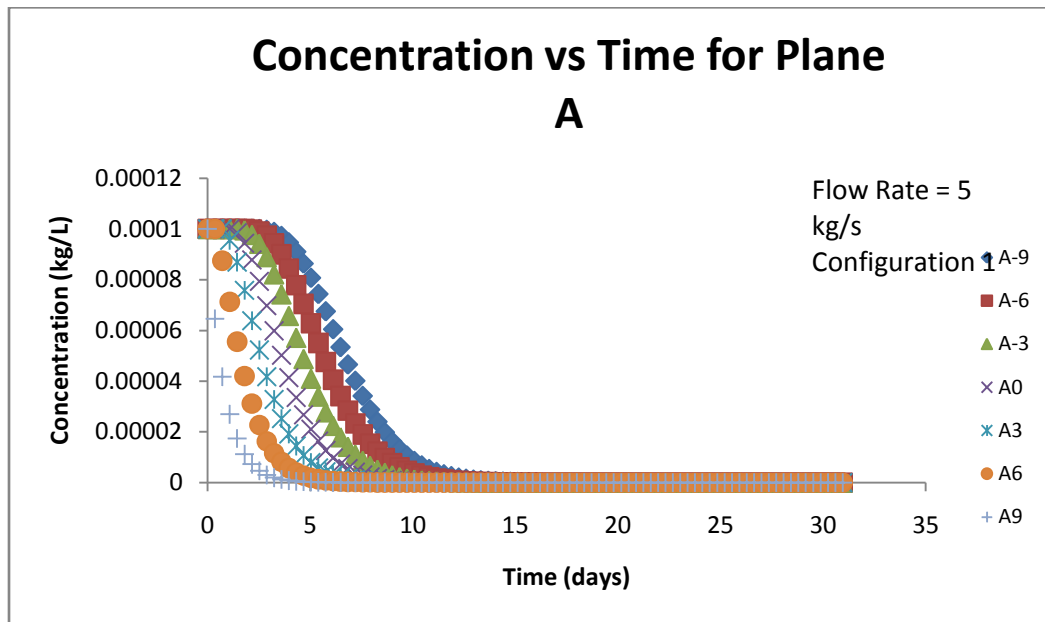


Figure 30: Concentration vs Time for Plane A, Configuration 1, 5 kg/s

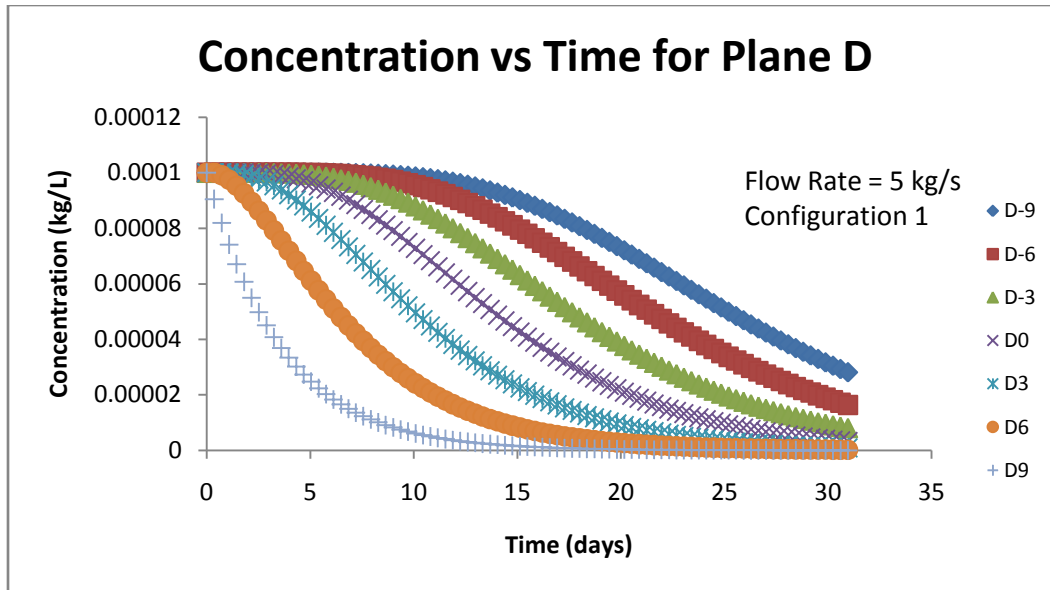


Figure 31: Concentration vs Time for Plane D, Configuration 1, 5 kg/s

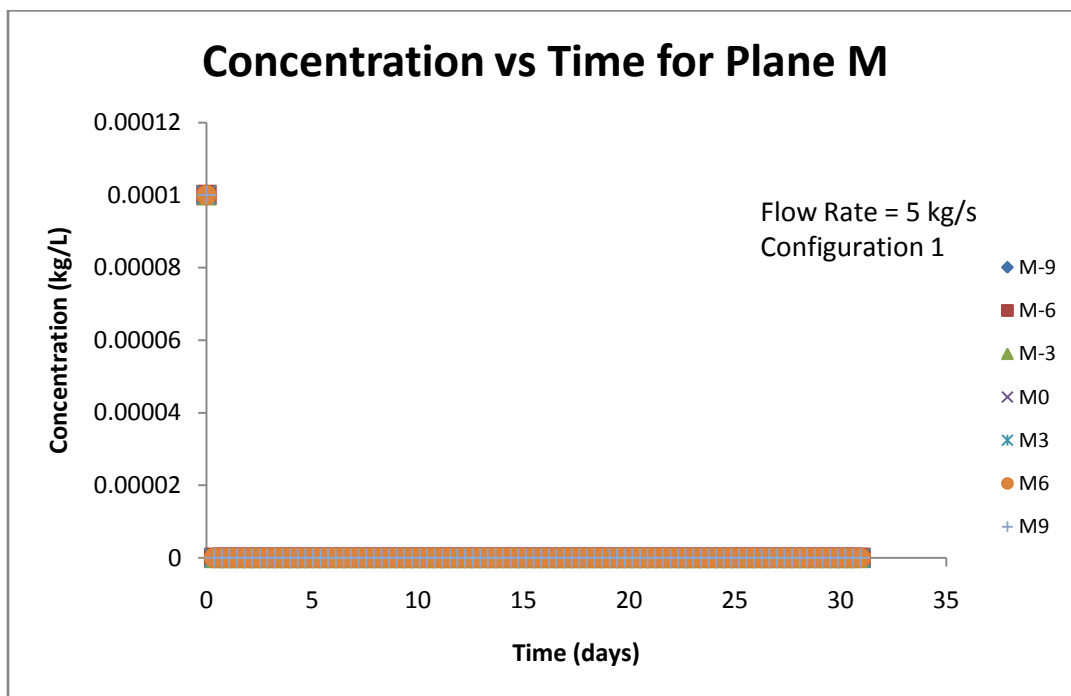


Figure 32: Concentration vs Time for Plane M, Configuration 1, 5 kg/s

In configuration 1 there is only 1 inlet and 1 outlet and both are positioned in the center of their respective faces on the simulation volume. This causes the fastest velocities to be in the center of the

aquifer. This is why Plane M (the very center plane) is immediately clean (See Figure 32). Planes A and D however, are along the edges of the volume where the velocity is much slower leading to a more subtle decrease in concentration as opposed to the step function seen in Plane M. This slower change also results in a longer remediation time for the entire aquifer.

The same planes and flow rate that are analyzed above are used in Configuration 2. These results are exhibited in Figure 33 through Figure 35.

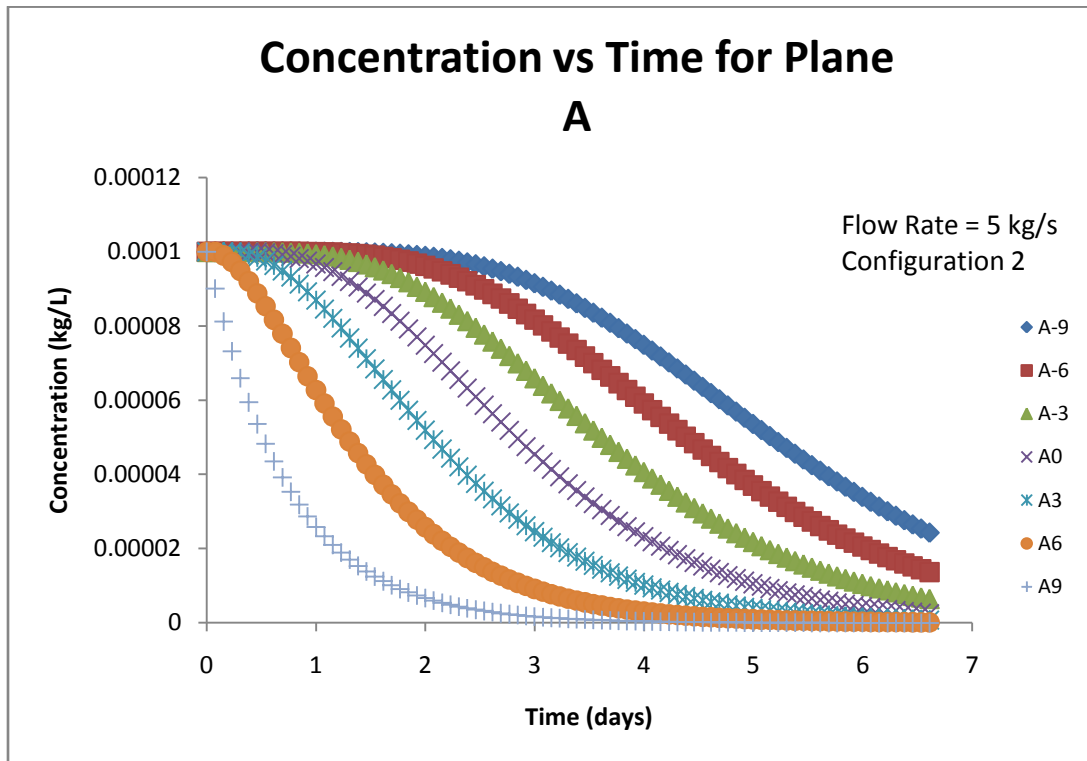


Figure 33: Concentration vs Time for Plane A, Configuration 2, 5 kg/s

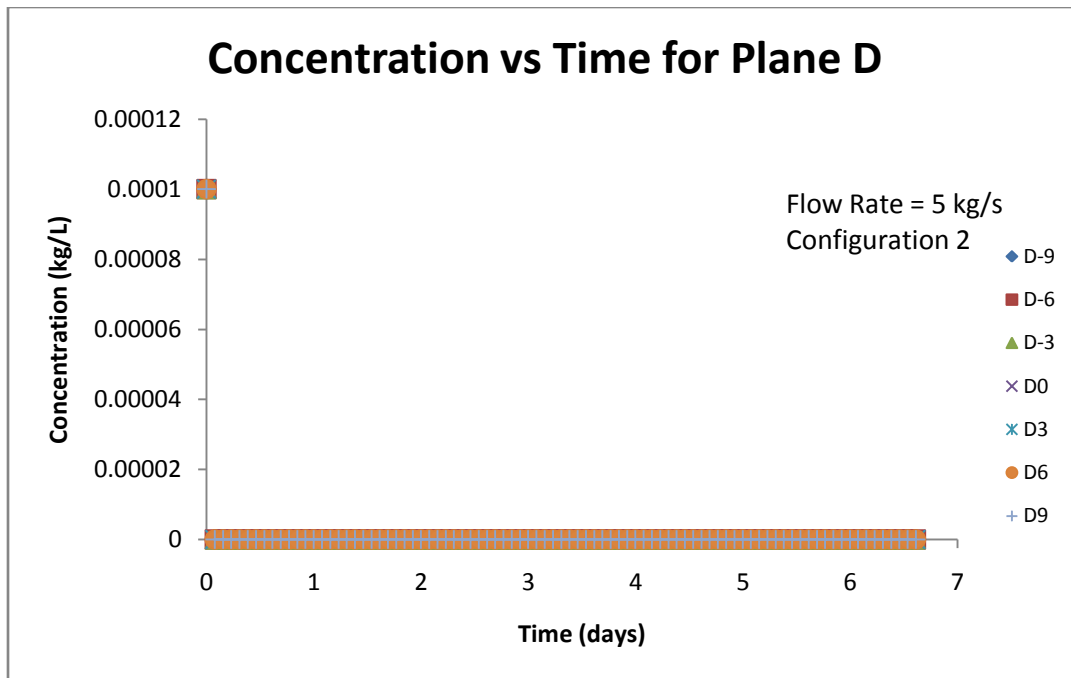


Figure 34: Concentration vs Time for Plane D, Configuration 2, 5 kg/s

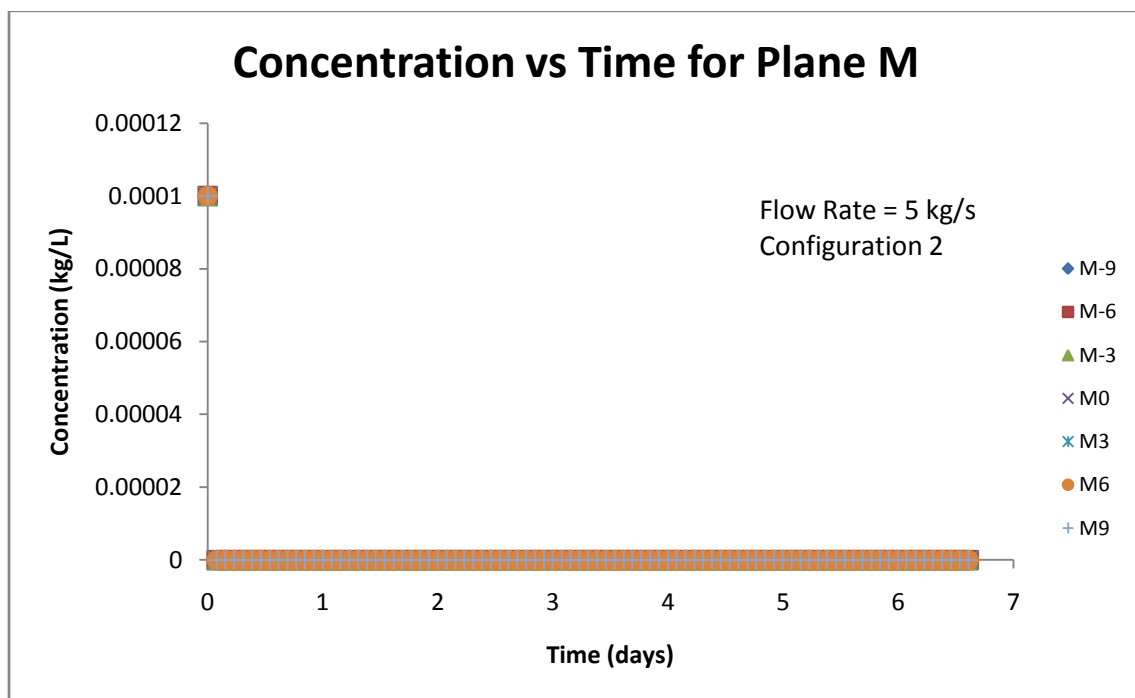


Figure 35: Concentration vs Time for Plane M, Configuration 2, 5 kg/s

Configuration 2 consists of 1 inlet and 2 outlets. This gives a very similar flow profile to the 1 inlet, 1 outlet configuration, except that the fast velocities are more widespread in the z-direction. This is illustrated by the step function displayed in Plane D as well as Plane M. The contaminant change in Plane A is more gradual because the flux through any given x-coordinate is always the same, and in this configuration there is increased flow in other planes taking flow away from Plane A.

The concentration plots of configuration 3 can be seen in Figure 36 through Figure 38 below.

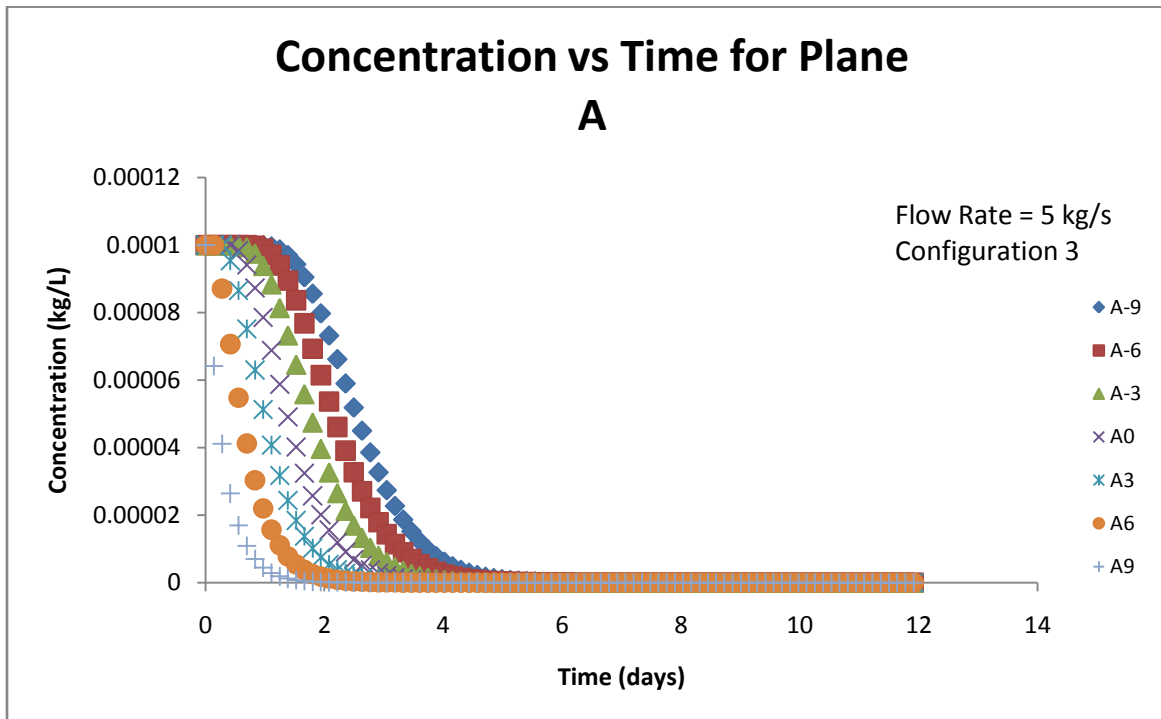


Figure 36: Concentration vs Time for Plane D, Configuration 3, 5 kg/s

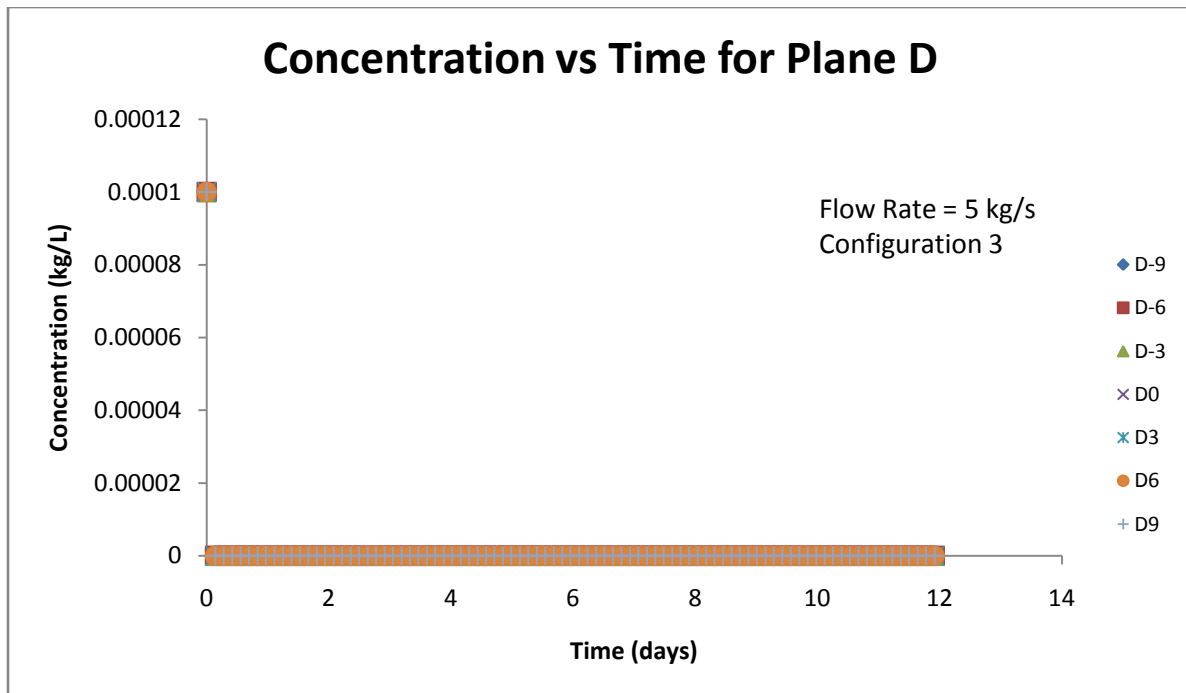


Figure 37: Concentration vs Time for Plane D, Configuration 3, 5 kg/s

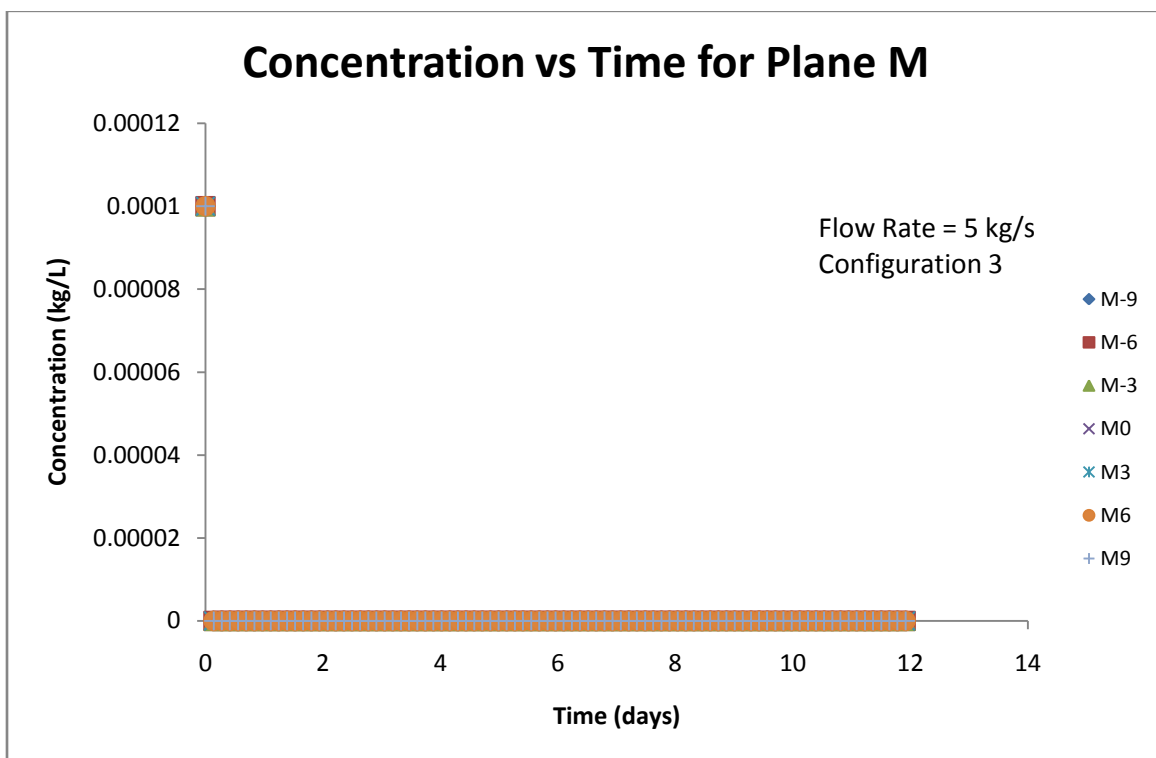


Figure 38: Concentration vs Time for Plane M, Configuration 3, 5 kg/s

Configuration 3 is made up of 1 inlet and 3 outlets. The outlets are arranged in a triangle with two near the bottom and one near the top of the aquifer. The flow is more widespread due to the multiple outlets and their more expansive positioning. This leads to the step functions observed in Planes D and M, and the steeper decrease seen in Plane A. The three outlets allow a more even distribution in the velocities which in turn cleans the entire aquifer more quickly.

In Figure 39 through Figure 44 below Configurations 4 and 5 are presented. Arrangement 4 consists of 2 inlets and 1 outlets, and arrangement 5 consists of 2 inlets and 2 outlets.

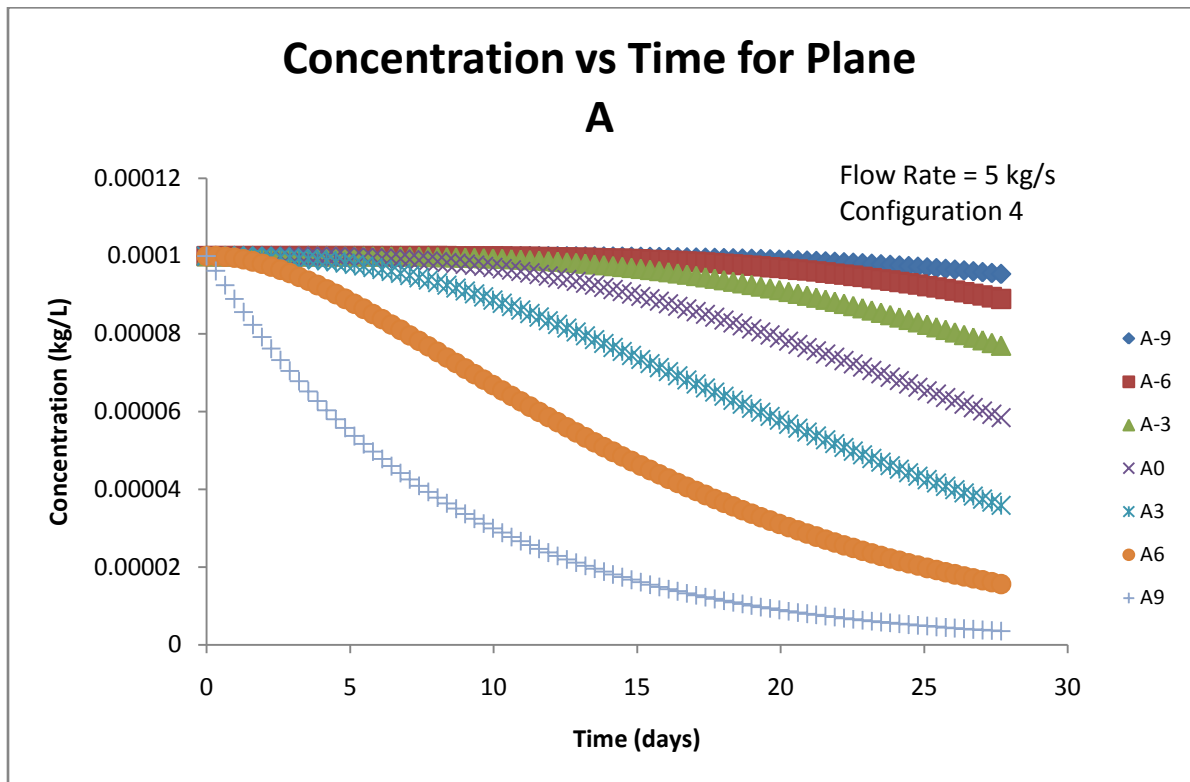


Figure 39: Concentration vs Time for Plane A, Configuration 4, 5 kg/s

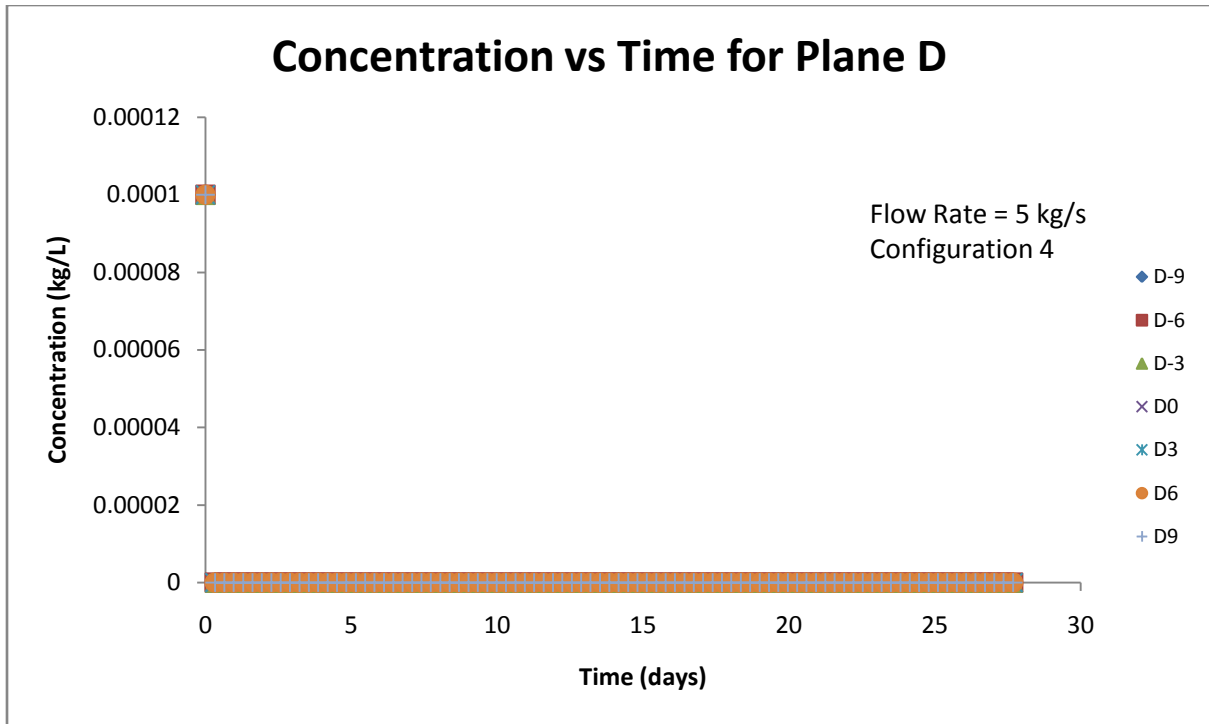


Figure 40: Concentration vs Time for Plane D, Configuration 4, 5 kg/s

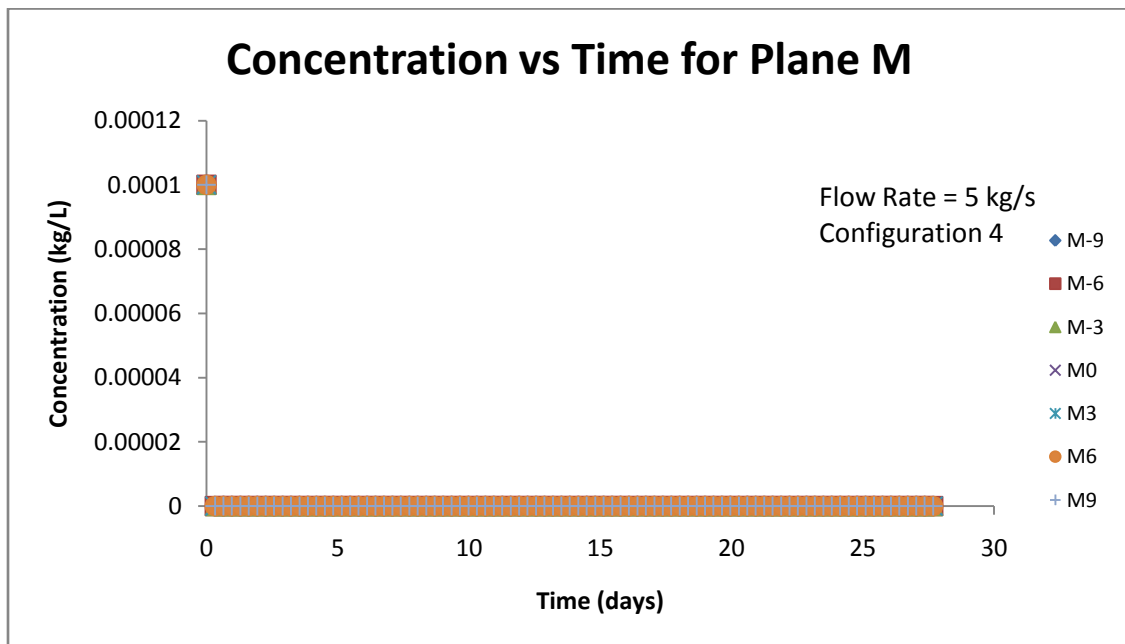


Figure 41: Concentration vs Time for Plane M, Configuration 4, 5 kg/s

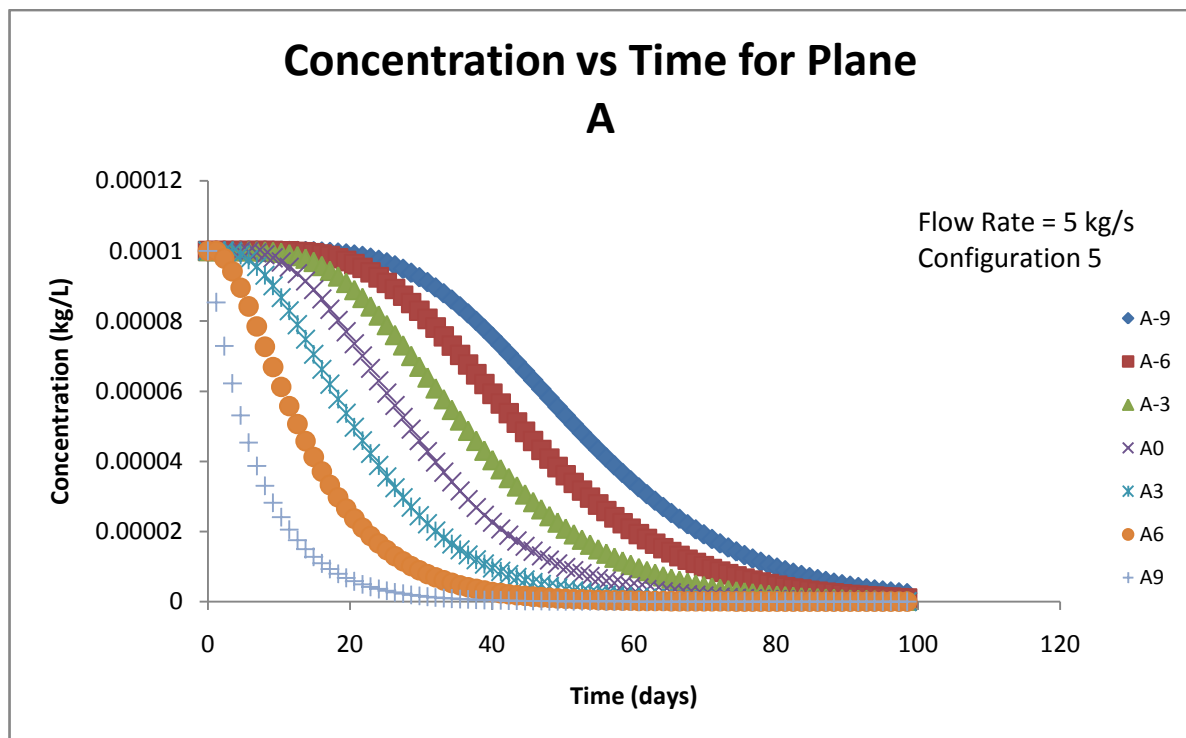


Figure 42: Concentration vs Time for Plane A, Configuration 5, 5 kg/s

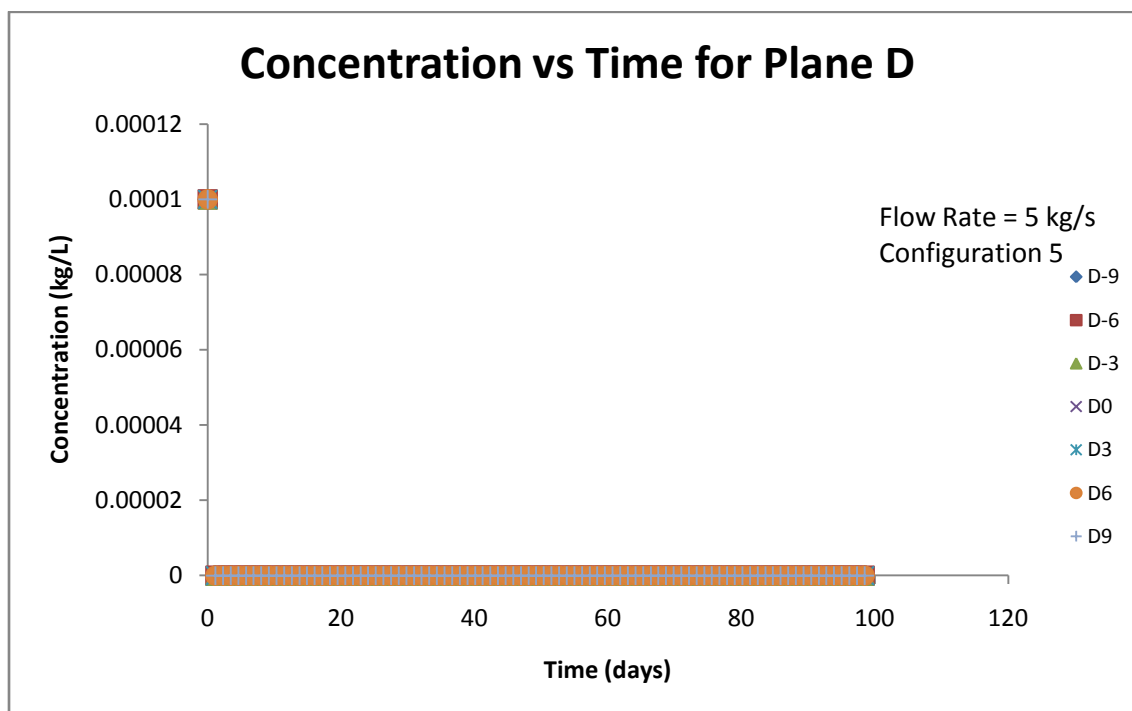


Figure 43: Concentration vs Time for Plane D, Configuration 5, 5 kg/s

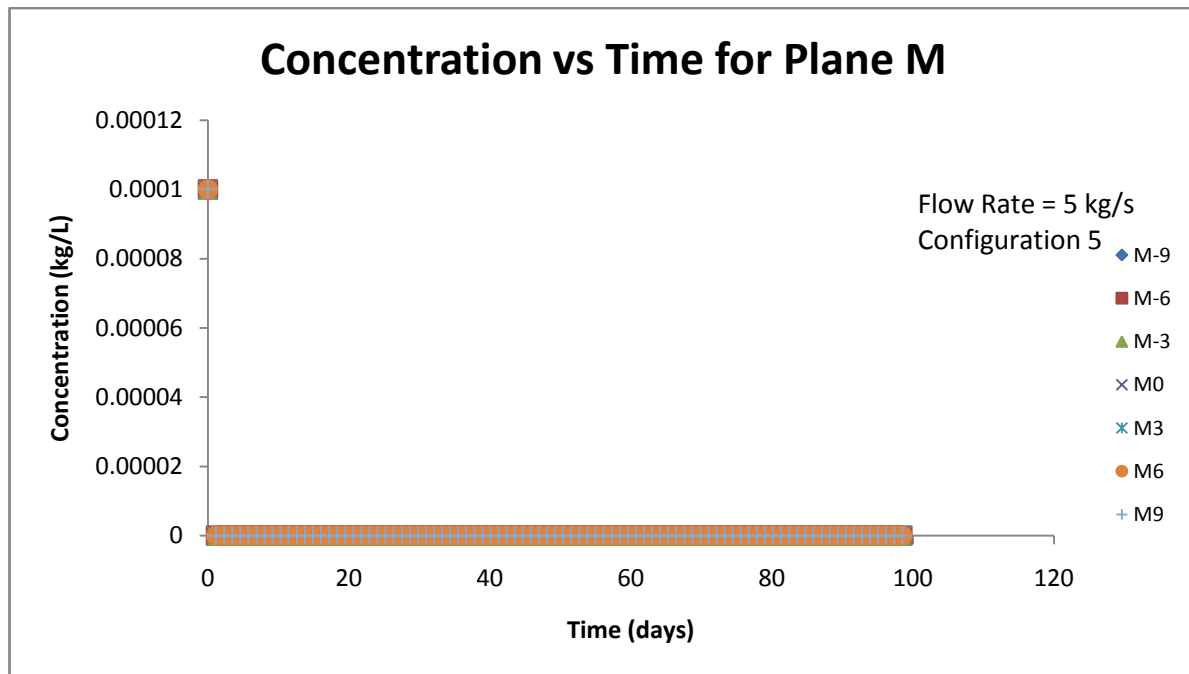


Figure 44: Concentration vs Time for Plane M, Configuration 5, 5 kg/s

These setups give results almost identical to Configuration number 2. Again The flow spreads out in the z-direction, but not the y-direction, resulting in a larger flux in Plane D, but a lower flux, and more gradual concentration profile in Plane A.

Configuration 6 is comprised of 4 inlets and 1 outlet, the resulting concentration profiles can be seen below in Figure 45 through Figure 47.

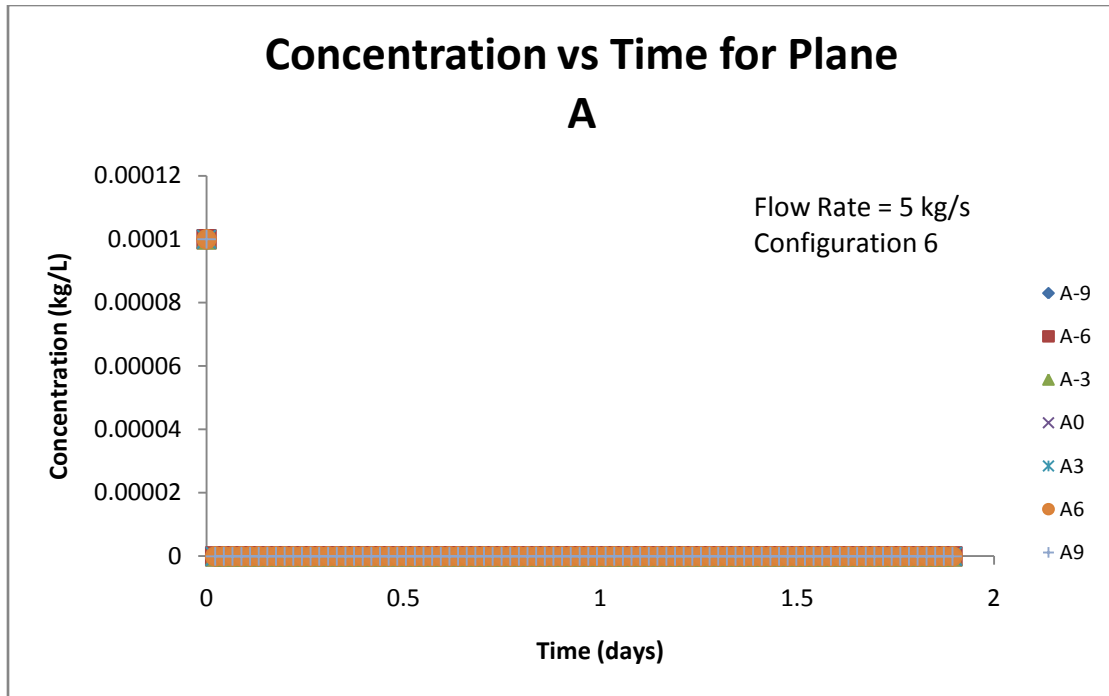


Figure 45: Concentration vs Time for Plane A, Configuration 6, 5 kg/s

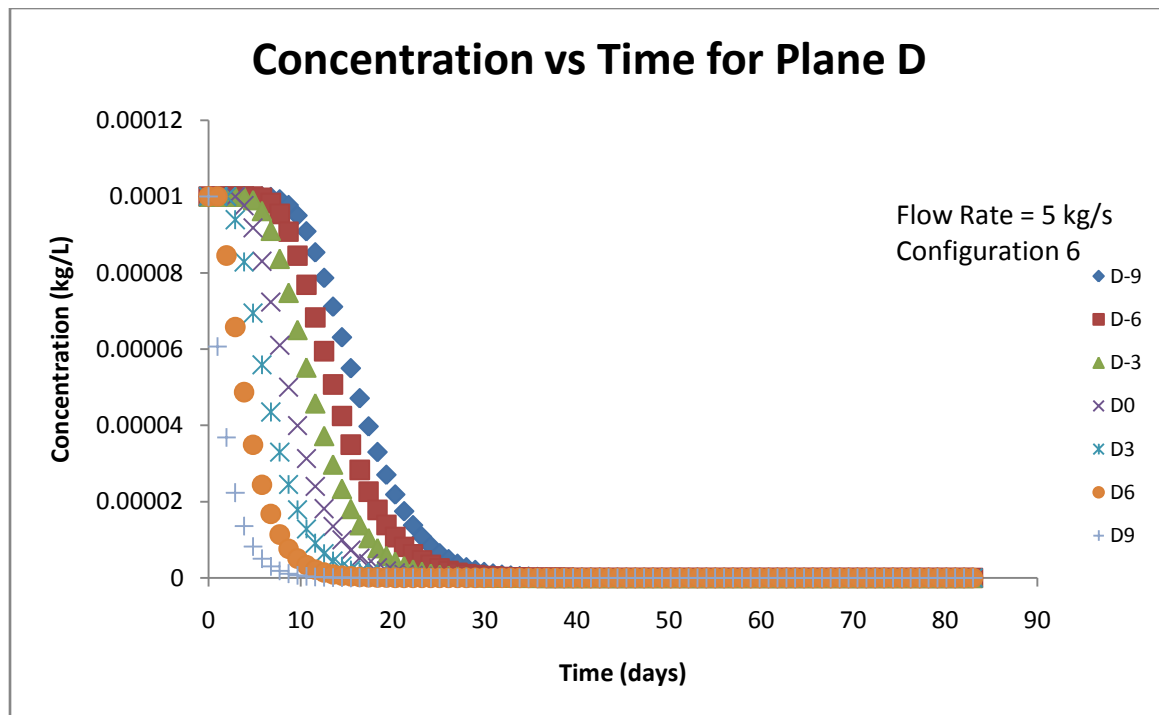


Figure 46: Concentration vs Time for Plane D, Configuration 6, 5 kg/s

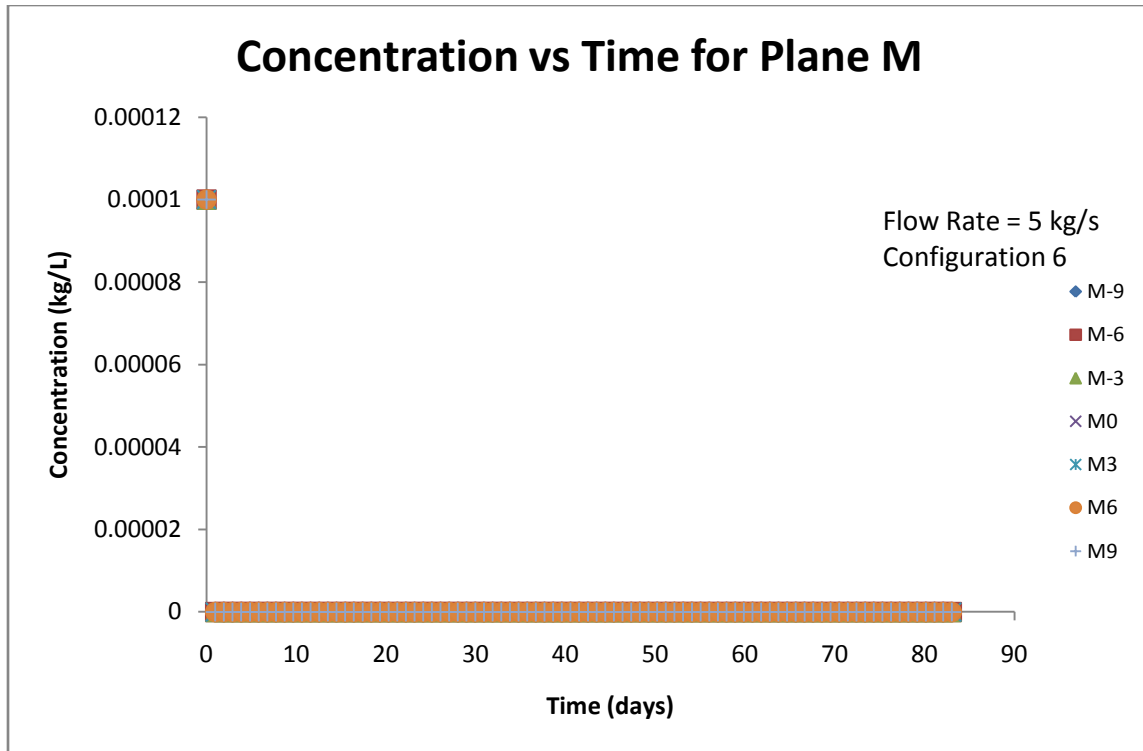


Figure 47: Concentration vs Time for Plane M, Configuration 6, 5 kg/s

The 4 inlets are placed near the corners, and the 1 outlet is in the center of the simulation volume. This causes the flow to travel mainly through the corners and the center with some dispersion to the sides producing an instant concentration decrease in Planes A and M, and a more gradual decrease in Plane D.

The outcome of the final arrangement simulated, Configuration 7, can be seen in Figure 48 through Figure 50 below.

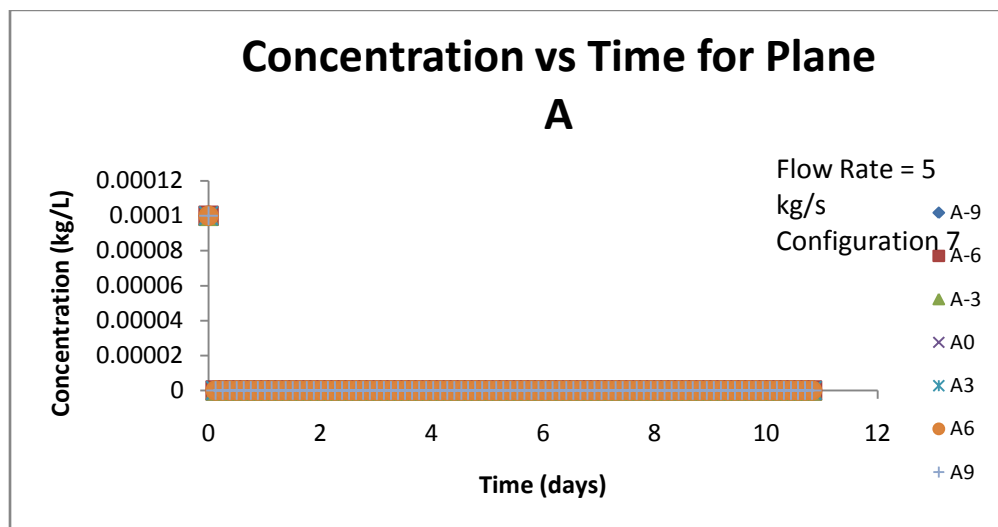


Figure 48: Concentration vs Time for Plane A, Configuration 7, 5 kg/s

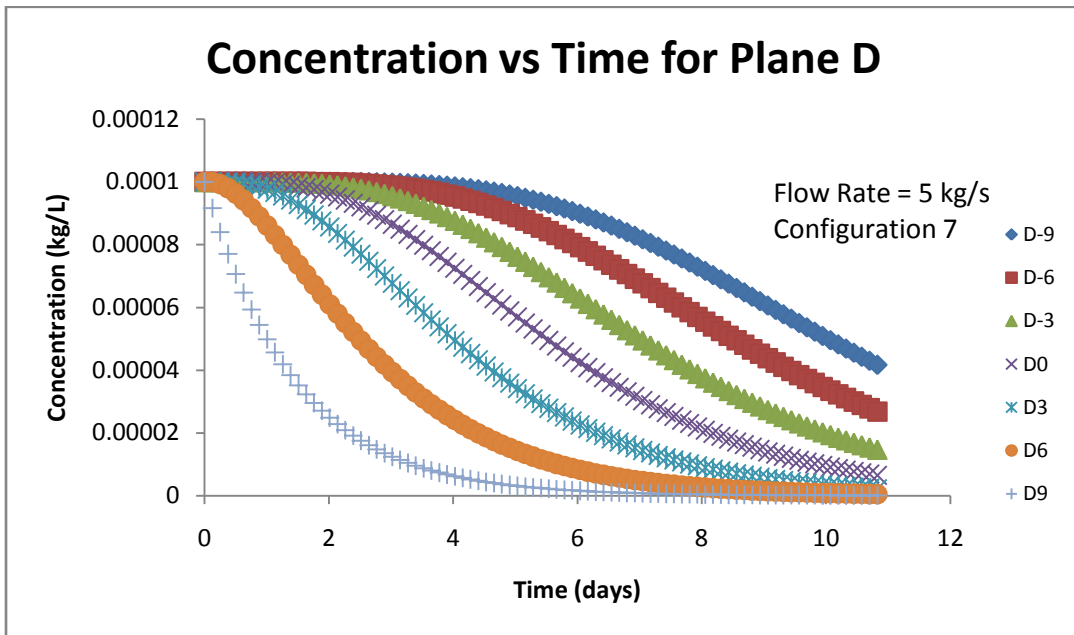


Figure 49: Concentration vs Time for Plane D, Configuration 7, 5 kg/s

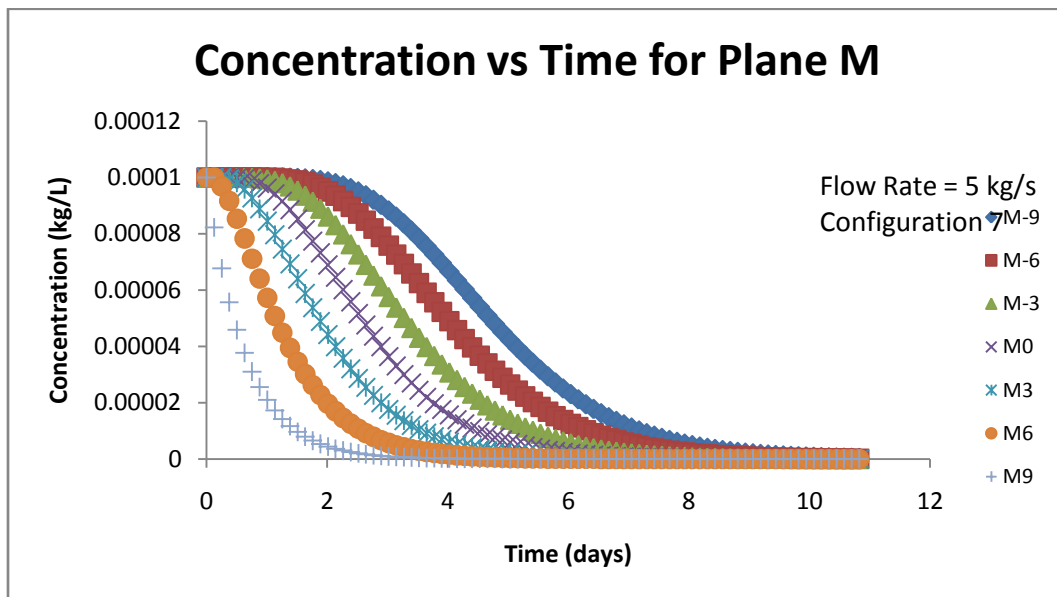


Figure 50: Concentration vs Time for Plane M, Configuration 7, 5 kg/s

This design includes 4 inlets and 4 outlets all placed near the corners of the aquifer. In this simulation the flow remained primarily in the corners consequently giving an instant concentration drop in Plane A, and a gentle decrease through the center planes.

Below in Figure 51 is a graph of the overall aquifer concentration vs time with configuration as a parameter.

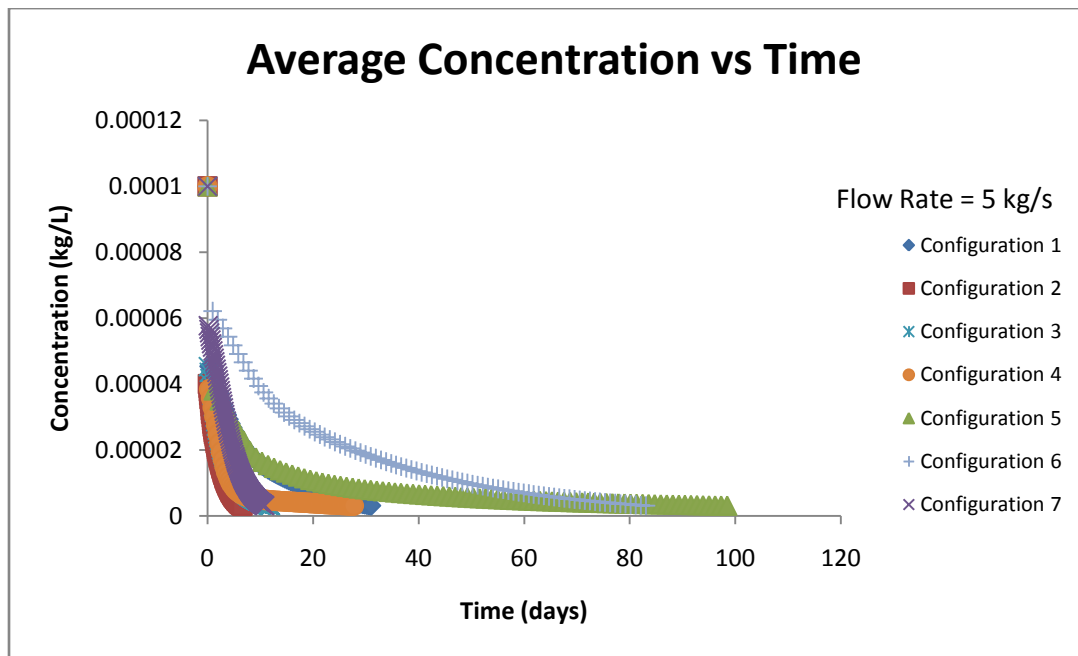


Figure 51: Average Concentration vs Time with 5 kg/s and Configuration as a Parameter

The well configuration has a highly pronounced effect on the remediation time. This is due to the distribution of the clean injected water. The designs with fewer number of extraction wells than number of inlet wells were observed to perform the slowest. This is because when the streams are narrowed to only one outlet they are unable to flow through all areas and, as a result, the arrangement cannot effectively clean the entire aquifer. Along the same lines, arrangements with the same number of inlets and outlets being positioned in the same z and y coordinates are not highly effective. This is because flow is forced directly from the inlet to outlet and does not radiate in the z or y directions. This leaves many essentially stagnant regions in the aquifer. Conversely, the formations that possess one inlet and several outlets are able to rid the aquifer of contaminants more efficiently because the flow can disperse more uniformly in all three dimensions.

Displayed below in Figure 52 is a comparison between remediation time and flow rates with configuration as a parameter.

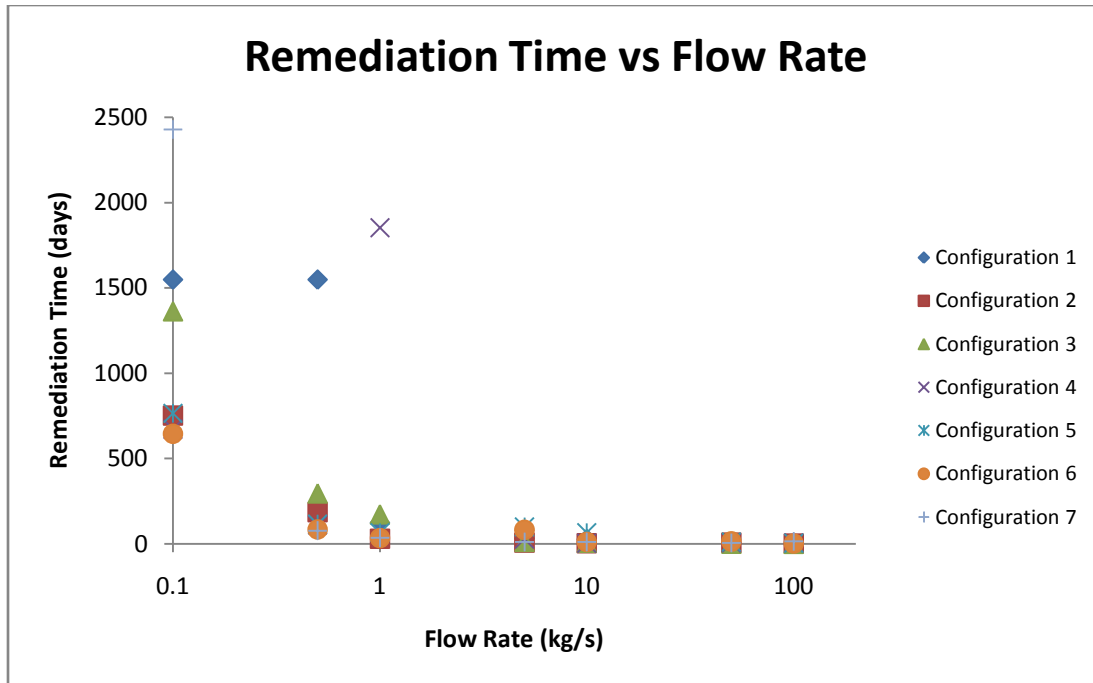


Figure 52: Remediation Time vs Flow Rate with Configuration as a Parameter

For most configurations, as flow rate increases the total remediation time decreases exponentially. The configurations that do not comply with this trend are configurations 1 and 4. These have 1 and 2 inlets respectively and both have only 1 outlet. These arrangements force the majority of the flow to remain on a limited path resulting in a longer remediation time, particularly at lower flow rates. At higher flow rates the injection fluid is able to replace dirty water very rapidly, reducing the contaminant concentration in the areas it can pass through to zero. These zeroes quickly overpower the concentrations remaining in other sections of the aquifer and bring the average down to the desired concentration, possibly before the aquifer is entirely clean. Although this is the case the general trends between remediation time and well configuration remain true. The more efficient configurations can only be refined a limited amount with higher flow rates, while the less efficient ones have much room for improvement. As a result all configurations have similar remediation times at higher flow rates.

## Economics

The economic model used makes simplifications and assumptions. For the fixed initial costs an overestimate of \$50,000 per well is used to cover permits, patents, royalties, and any hidden fees. It is also assumed that the water treatment equipment is already owned and the cost associated with it will not vary with well configuration and flow rate. Pumps were sized and priced using

$$g(z_2 - z_1) + \left( \frac{P_2 - P_1}{\rho} \right) + \left( \frac{V_2^2 - V_1^2}{2} \right) + \Sigma F$$

Equation 6 , the Bernoulli

equation, and Peters & Timmerhaus. It is also assumed that fixed continuous costs will remain constant regardless of arrangement and pumping rate. Within the variable continuous costs, water treatment is considered on a price per liter basis, labor costs were extracted from the U.S. department of Labor, and utilities were calculated using Peters & Timmerhaus.

These parameters were combined in

$$Cost = Labor + Drilling + Watertreatment + Pump + Electricity$$

Equation 5

$$Cost = Labor + Drilling + Watertreatment + Pump + Electricity$$

Equation 5

Labor costs are comprised of:

- Management
- Engineers
- Scientists
- Construction/Maintenance

The national average of wages for these positions in the watertreatment industry were found and then multiplied by the number of employees in each position and then by the number of hours necessary for the project. The drilling costs were calculated by multiplying the number of wells by the standard \$50,000 per well. Watertreatment costs were strictly based on a \$0.053 per liter treatment price. The

$$g(z_2 - z_1) + \left( \frac{P_2 - P_1}{\rho} \right) + \left( \frac{V_2^2 - V_1^2}{2} \right) + \Sigma F$$

Pump was sized using

Equation 6.

$$g(z_2 - z_1) + \left( \frac{P_2 - P_1}{\rho} \right) + \left( \frac{V_2^2 - V_1^2}{2} \right) + \Sigma F$$

Equation 6

g = gravity

z<sub>2</sub> = final height

z<sub>1</sub> = initial height

P<sub>2</sub> = final pressure

P<sub>1</sub> = initial pressure

ρ = density

V<sub>2</sub> = final velocity

V<sub>1</sub> = initial velocity

ΣF = frictional losses

The frictional losses were calculated by combining  $Re = \frac{D\rho v}{\nu}$  Equation 7 through Equation 9.

$$h_L = 2f_f \frac{L}{D} \frac{v^2}{g}$$

$$Re = \frac{D\rho v}{\nu} \quad \text{Equation 7}$$

Re = Reynold's Number

D = diameter

$\rho$  = density

v = velocity

$\nu$  = viscosity

$$f_f = \frac{16}{Re} \quad \text{Equation 8}$$

$f_f$  = fanning friction factor

$$h_L = 2f_f \frac{L}{D} \frac{v^2}{g} \quad \text{Equation 9}$$

$h_L$  = head loss

L = Length

D = Diameter

v = velocity

g = gravity

Once the head of the pump is calculated using the Bernoulli equation, figure 12-19 in Peters and Timmerhaus is used to price the pump and find the power required by the pump. This pump price is then multiplied by the number of pumps necessary. Due to the pressure gradient between the outlet of the extraction well (at the surface) and the inlet of the extraction well (in the aquifer), natural flow was assumed and pumping for extraction wells was neglected. Electricity cost is then calculated by multiplying the power required by the pump by the number of pumps, then by the number of hours, and finally by \$0.0969 per kWh.

This economic analysis was performed on each of the simulations run, and the results were compared to find the most economic configuration and flow rate. The least expensive flow rates for each arrangement were compared to determine the optimal remediation design. These results are displayed in Table 9.

Minimum Cost of each Configuration	
	Total Cost (\$M)
Configuration 1	0.14
Configuration 2	0.19
Configuration 3	0.27
Configuration 4	0.22
Configuration 5	0.28
Configuration 6	0.31
Configuration 7	0.51

**Table 9: Table of Minimum Costs for Each Configuration**

The drilling of the wells is the dominating cost in optimizing this process. It makes up more than 70% of the costs associated with Configuration 1. This fact will cause this optimization to select the 1 inlet 1 outlet arrangement in most cases. The next deciding factor is labor cost, which is dictated by the time necessary for the remediation. Thus higher pumping rates will be favorable. A plot of remediation cost vs flow rate is shown in Figure 53 to illustrate this point.

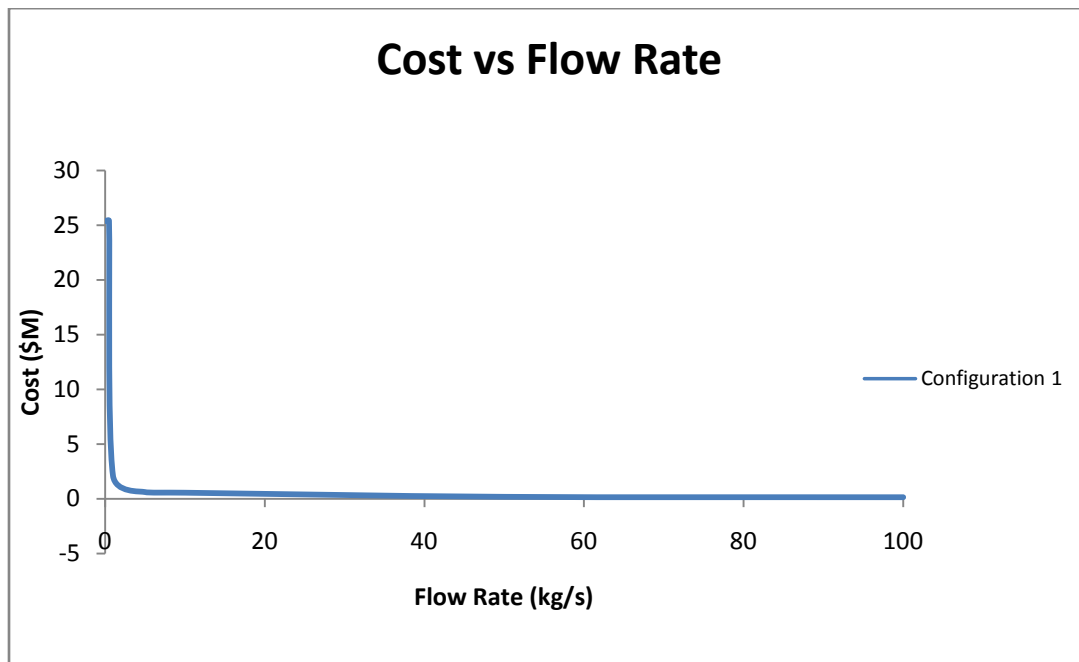


**Figure 53: Cost (in Millions of Dollars) vs Flow Rate for Configuration 1**

Taking these into consideration it is no surprise that in this example application Configuration 1 at a flow rate of 100 kg/s is the ideal design. The specific cost break down of this scenario is presented in Table 10.

Configuration 1 (100 kg/s)	
(1.55 days)	Cost
Pump	\$8,100.00
Drilling	\$100,000.00
Water Treatment	\$7,000.00
Pumping Electricity	\$27.00
Labor	\$25,000.00
Total	\$140,000.00

Table 10: Cost Breakdown for Configuration 1 with 100 kg/s

## Secondary Fluid Flow Approach

The aim of the secondary fluid flow simulations was to build upon the accuracy and complexity of the previous simulations and modeling. The path in which this was accomplished was by analyzing the cleaning of an aquifer, which had a non-uniform initial concentration profile, and by creating a more realistic aquifer geometry. Total pumping rate through the aquifer was chosen to have a value closer to flow rates that would be used in industrial practices for cleaning of this type of aquifer. This adjustment was made because the flow rates analyzed in the previous model were somewhat unrealistic for use in actual application. New approaches were taken to minimize remediation time and contamination in the plumes because an economic optimum can be met by minimizing remediation time while achieving highest possible purification. In this secondary approach, well location was also reformed to parallel industrial practice. Specifically, wells were positioned along the top of the aquifer in order to allow for placement of adjacent inlets and outlets. This is a practice that is standard in many concrete applications, as is seen in the Newalla site. Lastly, because many contamination distributions are generally non-uniform, three separate shapes of plumes with unique initial concentration profiles were created for remediation analysis. Pumping strategies for the cleaning of the plumes were designed for each scheme. The first step of this method was to create a new geometry in Gambit.

## Gambit

The geometry of the aquifer and pumping arrangement were redesigned in order to create simulations that are more realistic to characteristics seen in industry. One of the first important changes was to create a geometry where the wells have inlets and outlets in the middle of the aquifer. This geometry was created to simulate pipes drilled into the center of the well from the top of the aquifer. Another

change from the previous model is that the new geometry uses a  $40 \times 20 \times 10$  volume. This yields a volume of  $8000 \text{ m}^3$ . The flow rate used in the aquifer was then scaled according to the flow rate relative to the total volume, using the Newalla site as the reference values. In other words, since the total volume of the Newalla plume is  $2150 \text{ m}^3$  and the Newalla site uses a total flow rate through all the inlets of approximately  $0.4 \text{ kg/s}$ , scaling this up to clean an  $8000 \text{ m}^3$  aquifer, the total flow rate through the aquifer should be approximately  $1.5 \text{ kg/s}$ . For each configuration used, this value is divided by the total number of inlets to find the flow rate through each inlet. It is key to clarify that for any configuration, the pumping rate through a given well does not change with time. Also, the total mass being injected, which is the sum of the flow rate through each injection, is always constant. It is only the injection and extraction points that change at a point in time. The new generic geometry drawn for these simulations is shown in Figure 54.

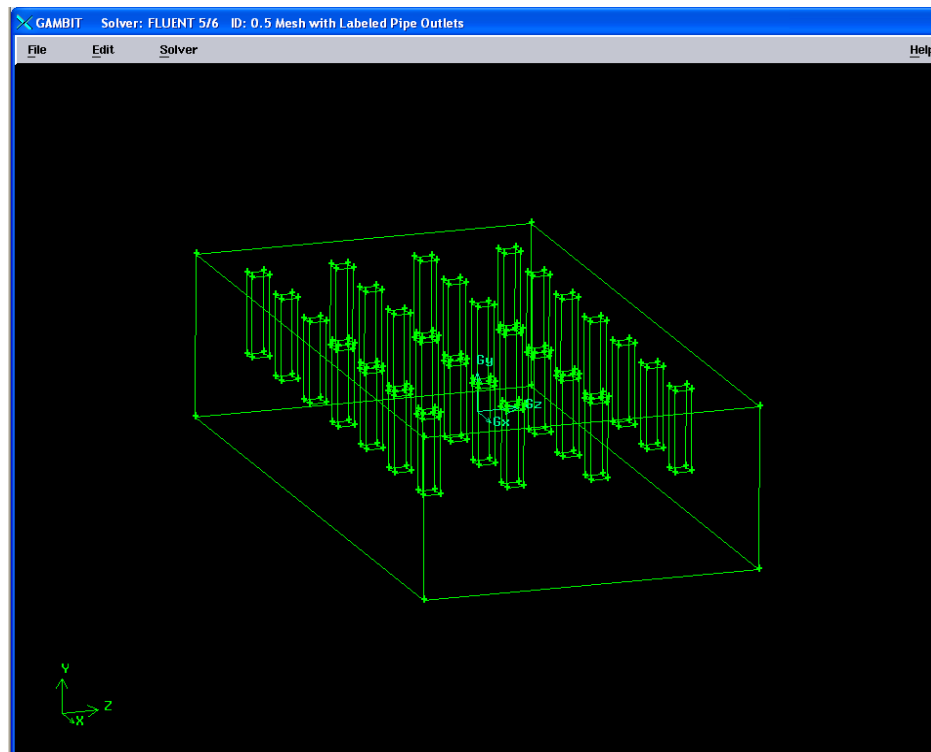


Figure 54: Refined Generic Geometry

The nomenclature for the naming of these wells is shown in Figure 55.

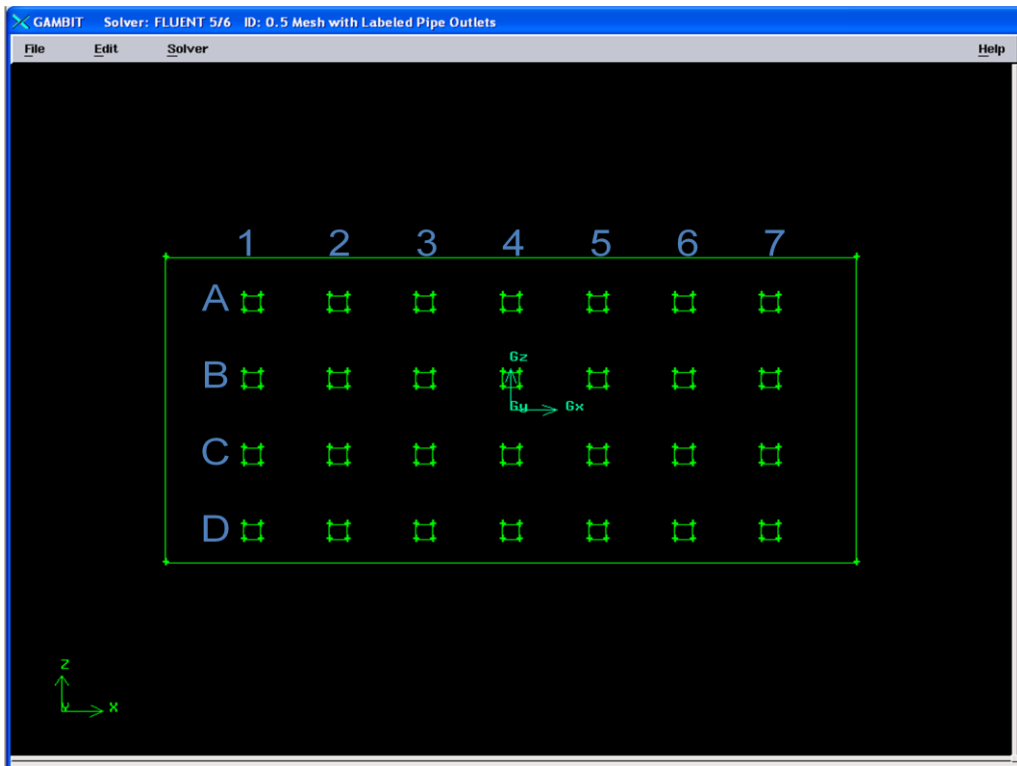


Figure 55: Nomenclature for Naming of Faces for Wells

Again, the faces may be designated as “on” or “off” depending on whether their boundary condition is specified to be a mass-flow inlet, outflow, or wall.

### Initial Plume Profiles

The three initial plume profiles that were created are as follows

- Plume 1: A “rectangular” shaped plume
- Plume 2: A “figure 8” shaped plume
- Plume 3: A “moon shaped” plume

The general shapes of the plumes, colored by contamination concentration, are shown in Figure 56.

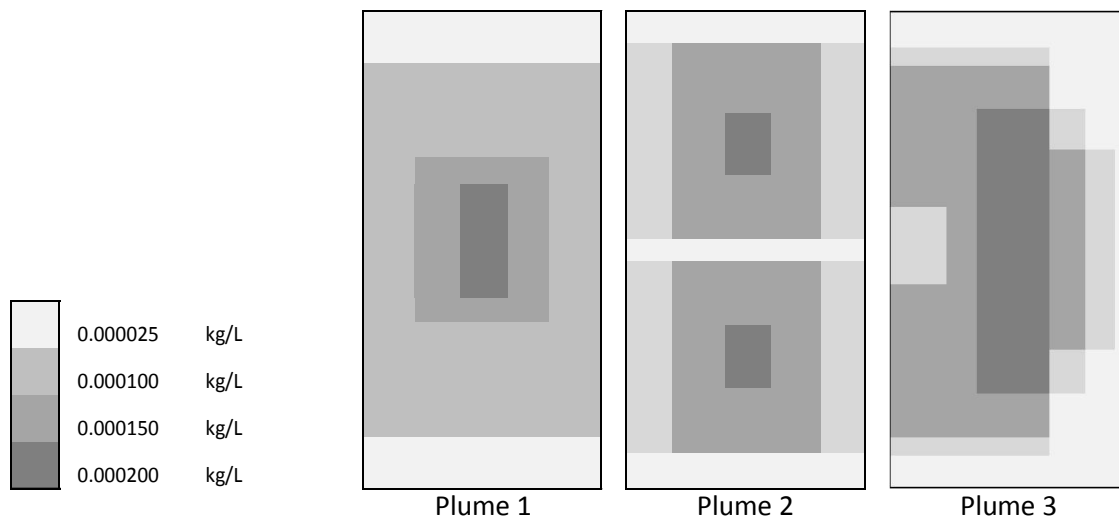


Figure 56: Non-Uniform Initial Concentration Profiles

It can be seen in Figure 56 that the highest concentrations are located toward the inner part of the aquifer in each plume profile, with the highest concentration being represented by the darkest gray and the smallest concentration being shown in the lightest gray.

### Pumping Strategies

To remediate the contamination problems in the three plumes, a unique pumping strategy was designed for each. The initial plume profile and its corresponding pumping strategy is shown in

Figure 57 through Figure 59 below. In the pumping strategies, the blue faces will be designated mass flow inlets and the red faces will be designated as outflows. The white faces will be “off,” or will be treated as walls.

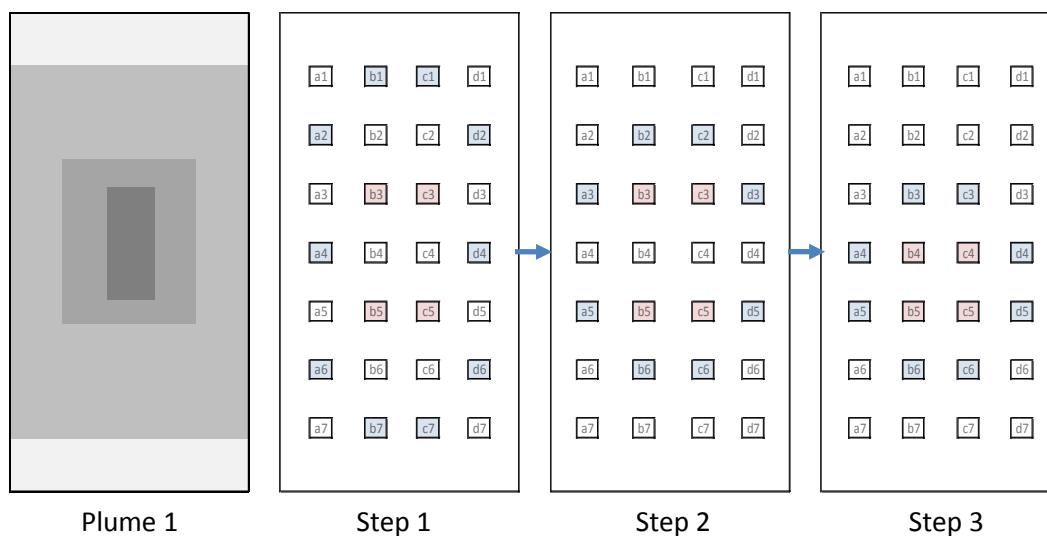


Figure 57: Pumping Strategy for Plume 1

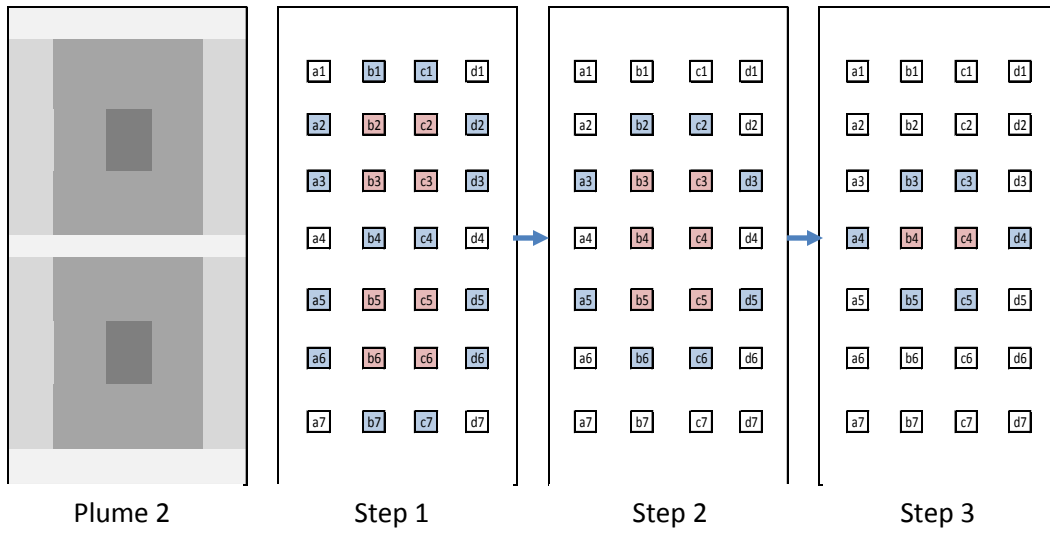


Figure 58: Pumping Strategy for Plume 2

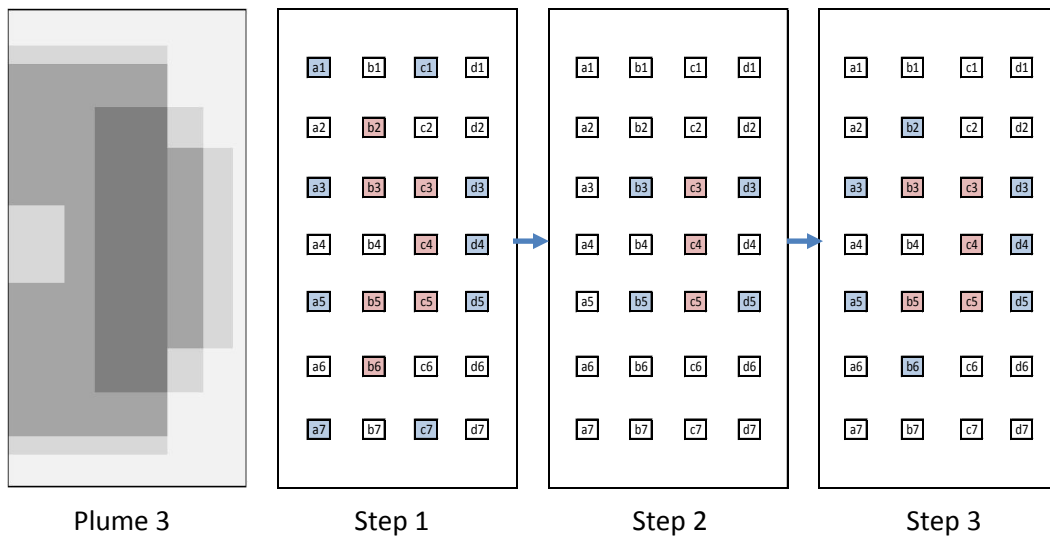


Figure 59: Pumping Strategy for Plume 3

The idea behind these pumping strategies is to attempt to push all of the contaminants, by pumping in clean water, toward the outflow locations where the contaminant-rich water will be removed from the aquifer.

## Secondary Fluid Flow Simulations

### Fluent

The geometry drawn in Gambit was imported into Fluent. Vertical planes were drawn in Fluent. Secondary simulations utilized more vertical planes than were in the initial fluid flow simulations in order to increase order to increase accuracy in the measurement of flux through the aquifer. The nomenclature for naming the vertical planes is shown in f

Figure 60 below.

pa1	pb1	pc1	pd1	pe1
pa2	pb2	pc2	pd2	pe2
pa3	pb3	pc3	pd3	pe3
pa4	pb4	pc4	pd4	pe4
pa5	pb5	pc5	pd5	pe5
pa6	pb6	pc6	pd6	pe6
pa7	pb7	pc7	pd7	pe7
pa8	pb8	pc8	pd8	pe8
pa9	pb9	pc9	pd9	pe9
pa10	pb10	pc10	pd10	pe10

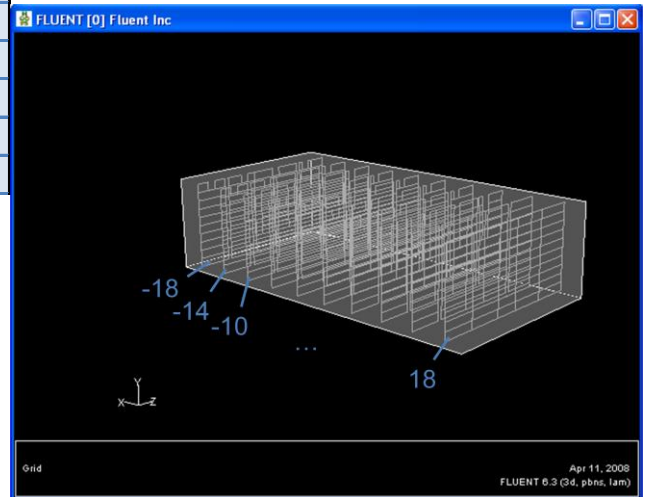


Figure 60: Vertical Planes in Fluent

The total number of vertical planes drawn for secondary simulations was 500. These planes were, again, drawn and named individually. Since the well configuration in these secondary trials creates more flow in the y direction, horizontal planes were also drawn below the bottom of the pipes in the aquifer. The nomenclature for naming the horizontal planes and some depictions of their locations in the aquifer is given in

Figure 61.

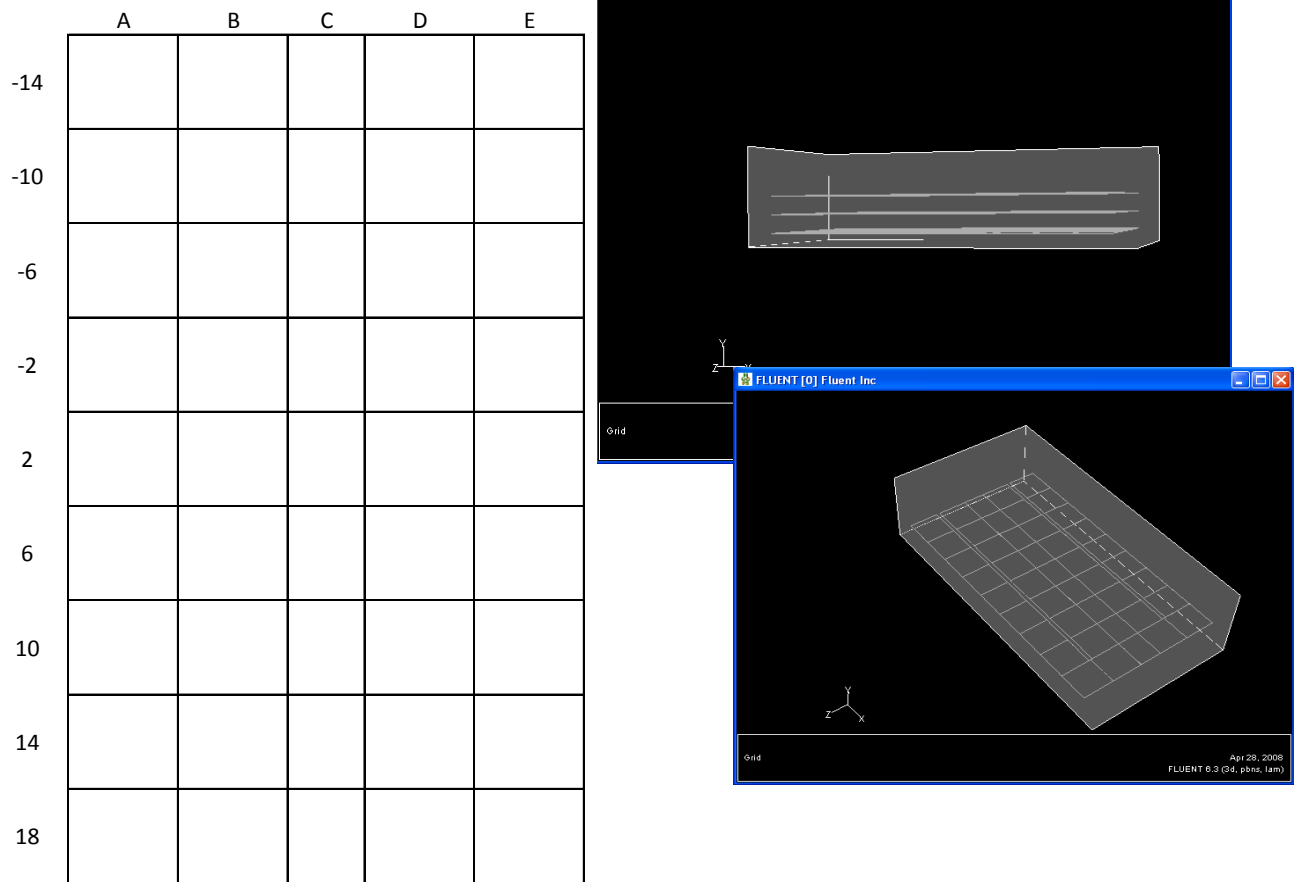
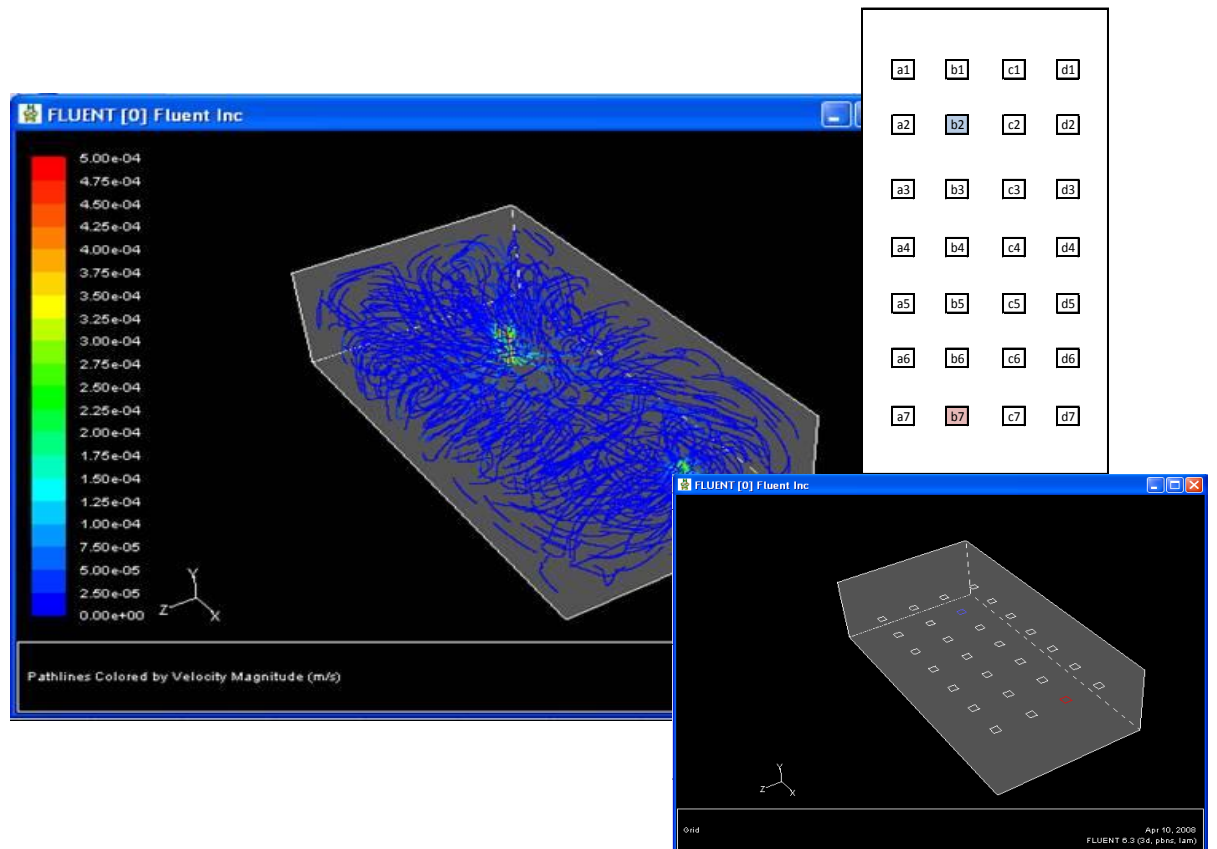
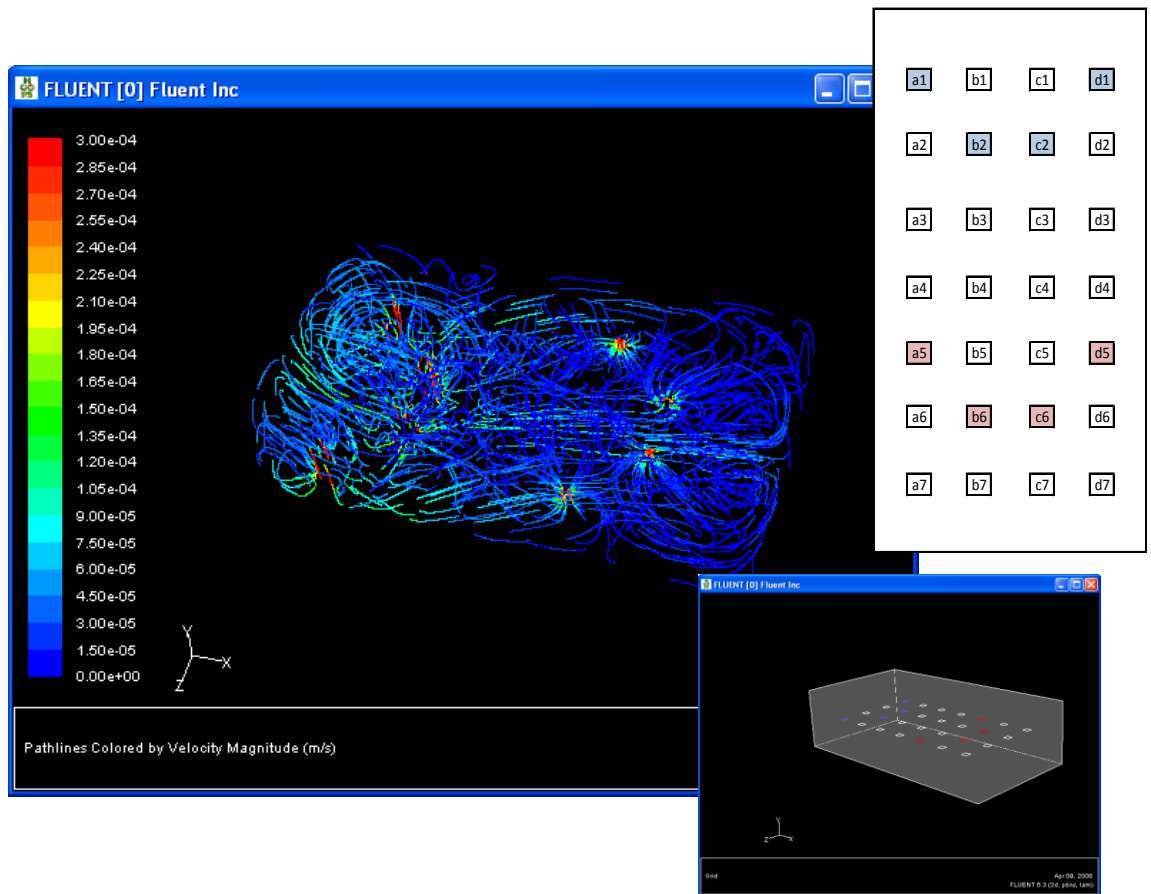
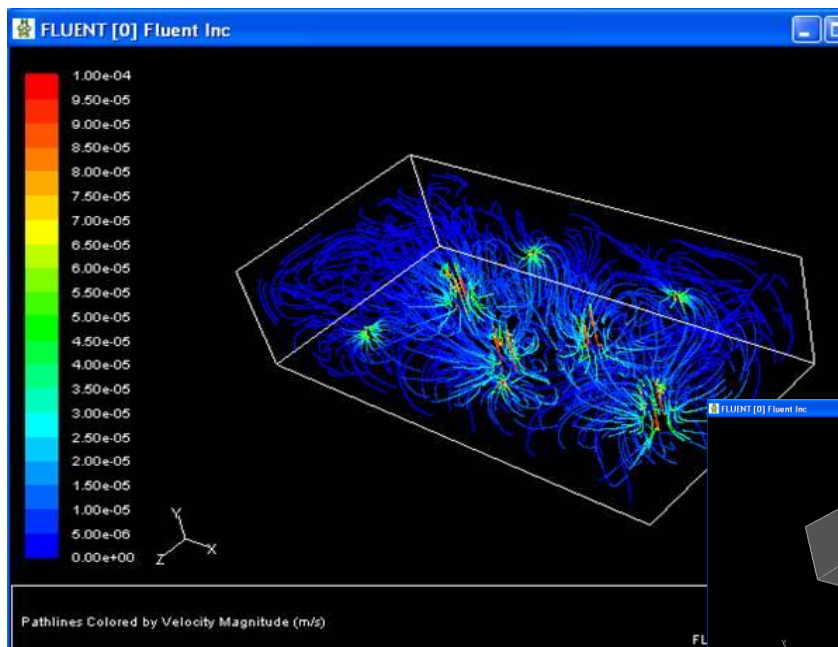


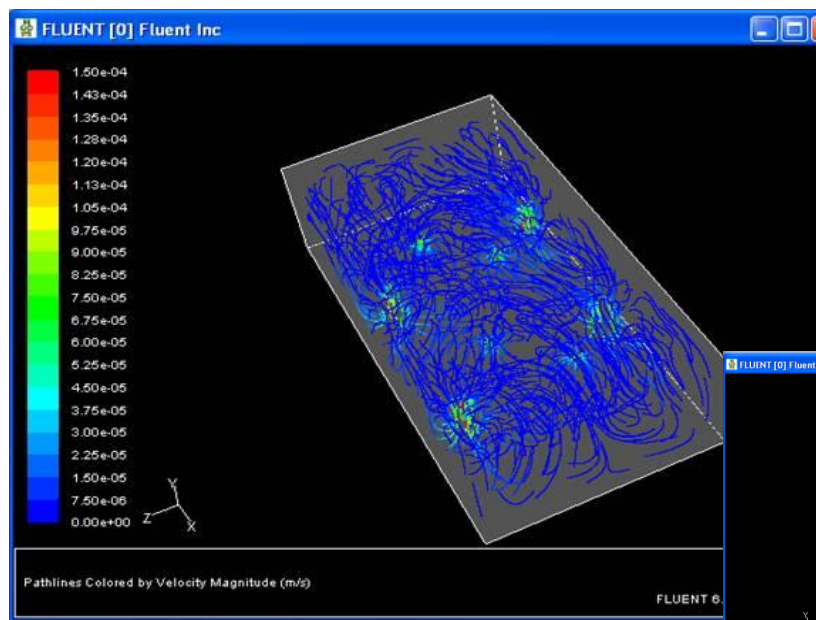
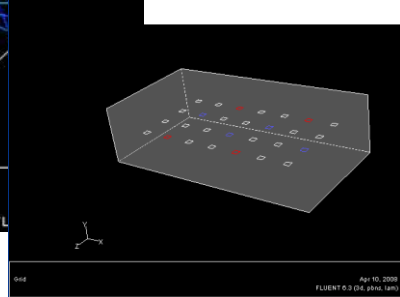
Figure 61: Layout and Nomenclature for Naming Horizontal Planes

Once the planes were drawn and named, several initial trials were run with different well configurations in order to examine the behavior of the flow with the new pipe and aquifer arrangement. Figures showing the arrangement of the wells and the resulting profiles are shown below. These profiles are, as in the primary fluid flow approach, path lines colored by velocity.

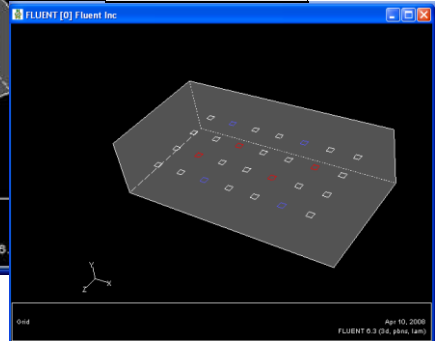




a1	b1	c1	d1
a2	b2	c2	d2
a3	b3	c3	d3
a4	b4	c4	d4
a5	b5	c5	d5
a6	b6	c6	d6
a7	b7	c7	d7



a1	b1	c1	d1
a2	b2	c2	d2
a3	b3	c3	d3
a4	b4	c4	d4
a5	b5	c5	d5
a6	b6	c6	d6
a7	b7	c7	d7



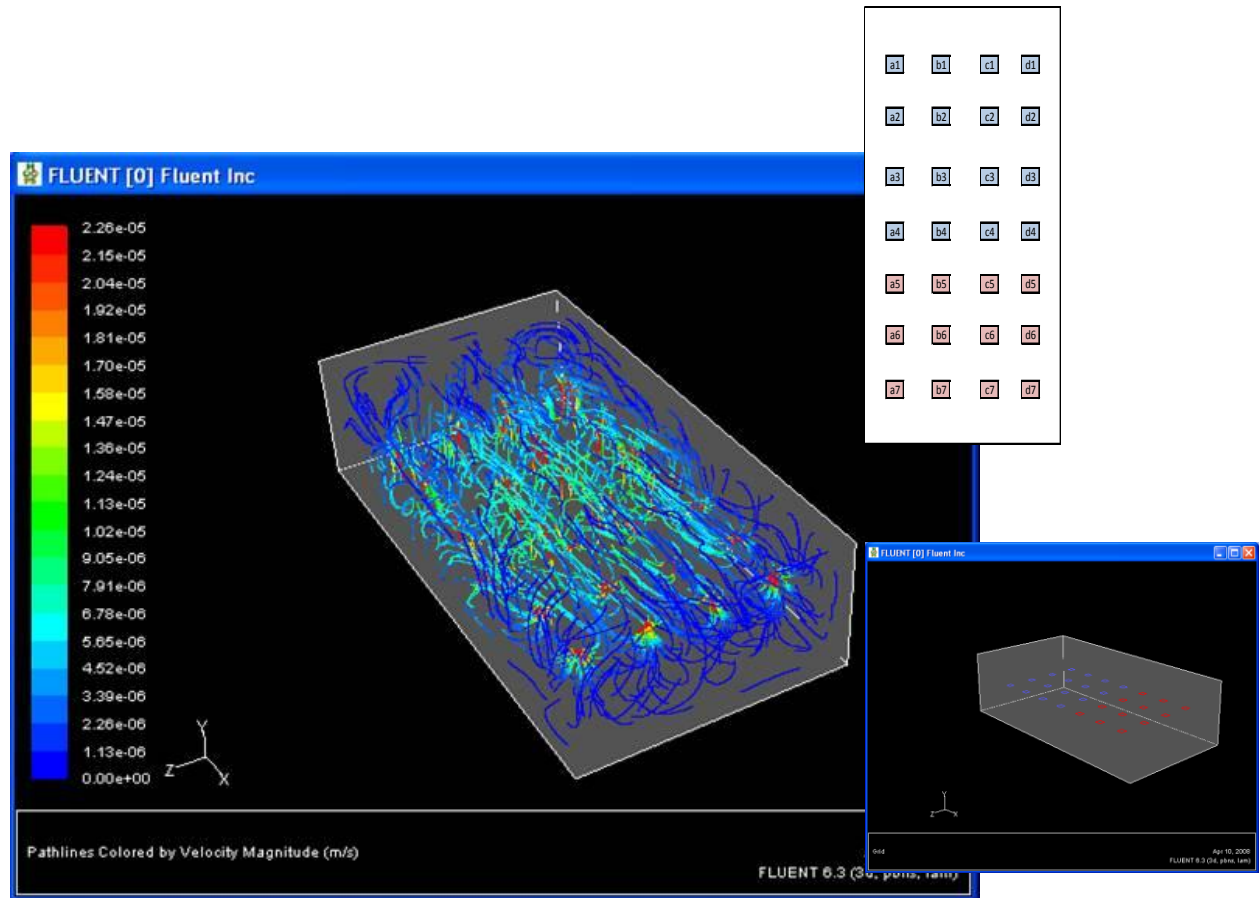
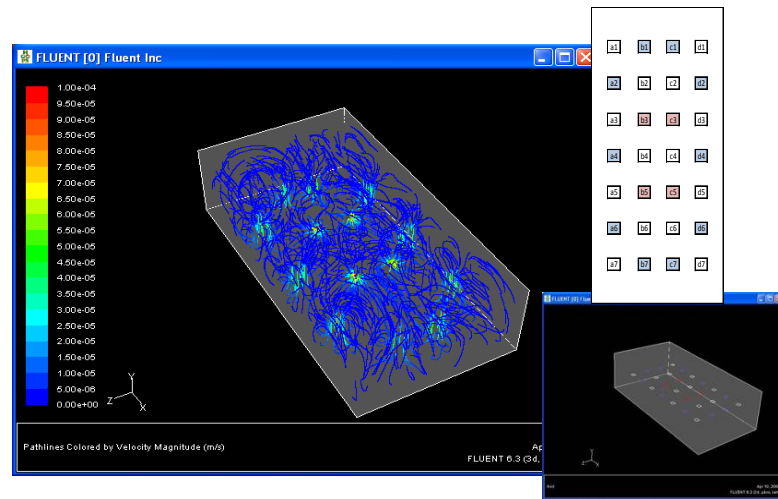


Figure 62: Examples of Several Well Configurations Simulated

The testing of these well configurations showed expected flow patterns. This gave validity to the new geometry and allowed for the pursuit of the new plume treatment and pumping strategy method.

Simulations were next run for the three steps in the pumping strategy for the three different initial plume profiles. The results for plume profile 1 are shown below in Figure 63.



The flow results and configurations depictions for plume 2 are shown in Figure 64.

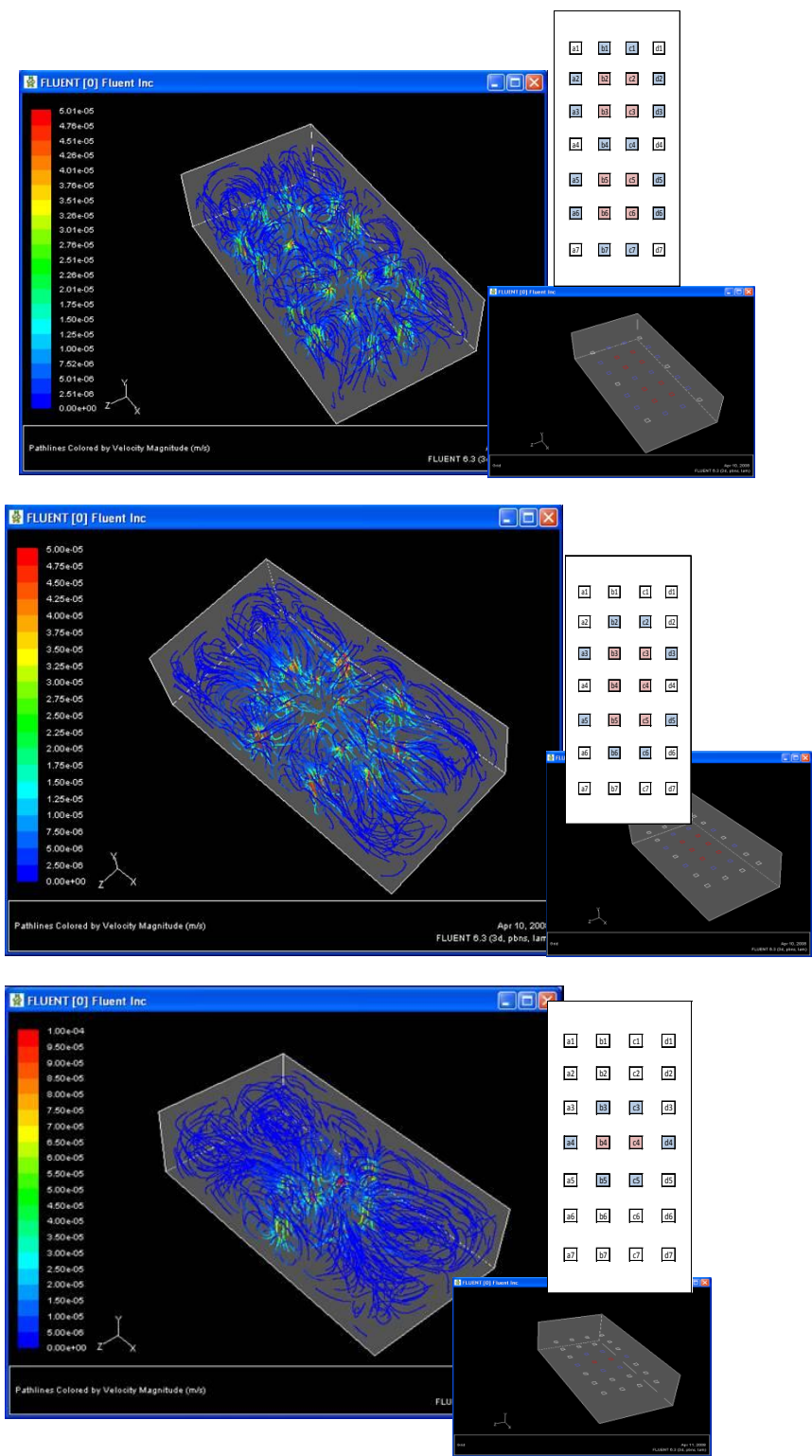


Figure 64: Plume 2 Steps 1 Through 3

The profiles for steps 1 though 3 of the pumping strategy for plume 3 are shown below.

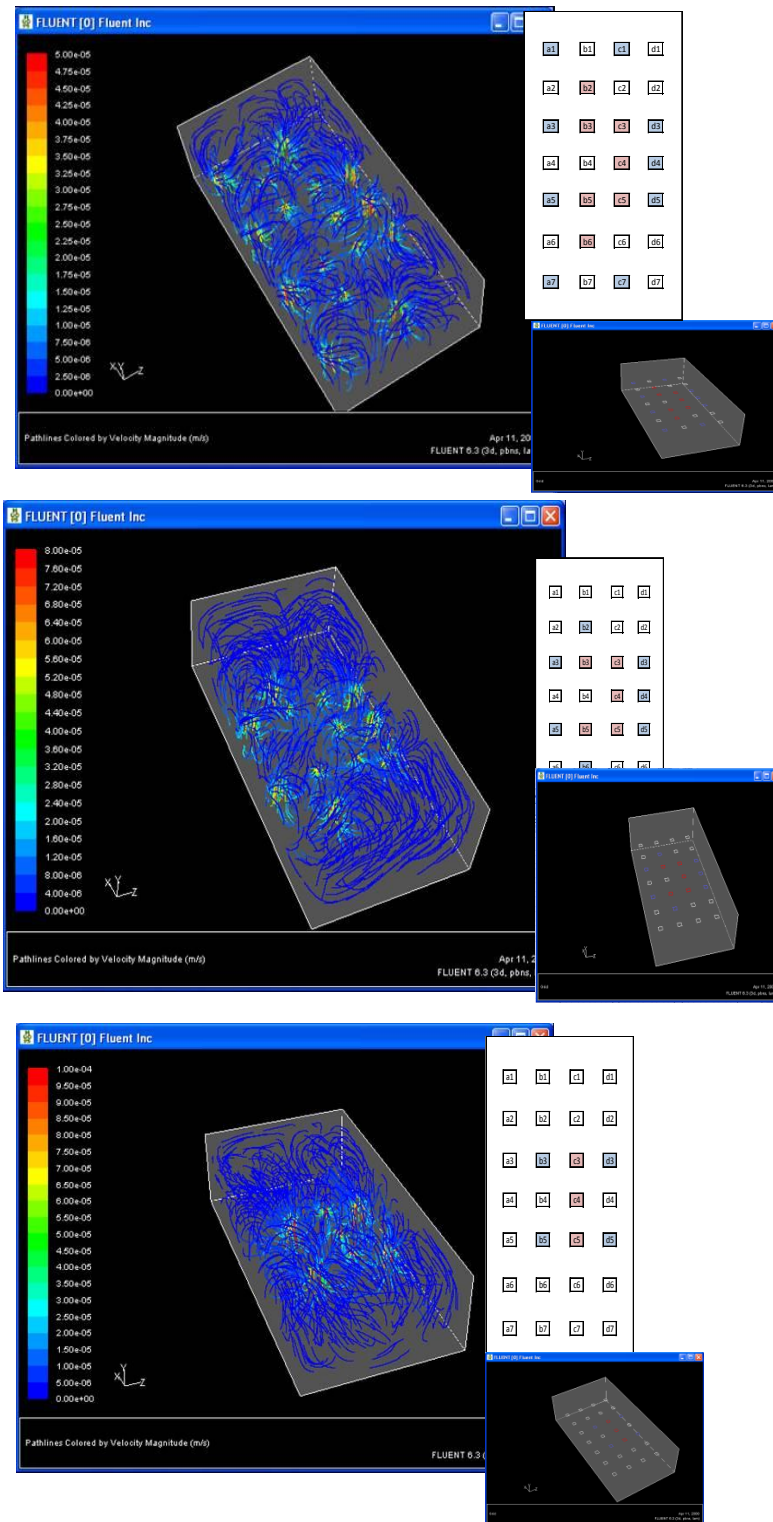


Figure 65: Plume 3 Steps 1 Thorough 3

In order to more easily visualize where the wells are located in the aquifer, filled contours may be displayed and colored by velocity. Two examples of these contours are shown in Figure 66 and Figure 67. Figure 66 is step 2 in the cleaning of plume 3 and Figure 67 is step 3 in the cleaning of plume 3.

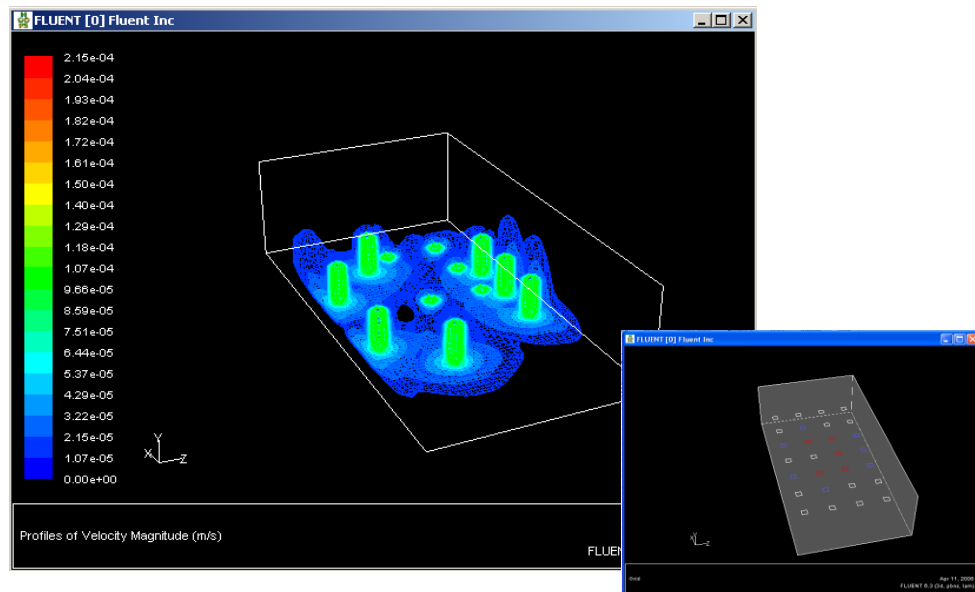


Figure 66: Velocity Contour for Step 2 of Plume 3

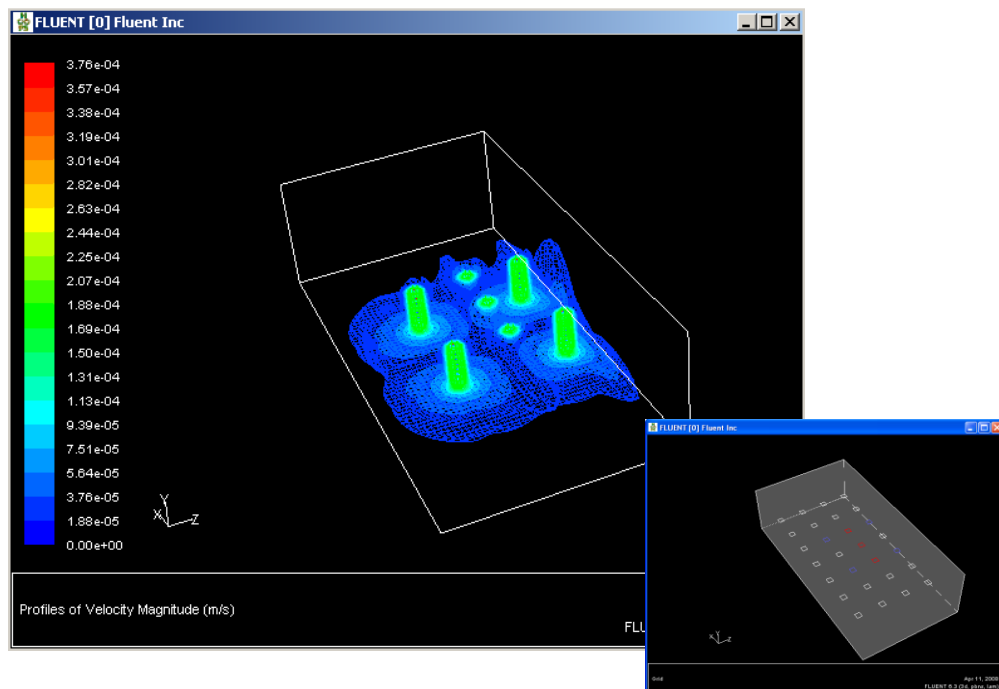


Figure 67: Velocity Contour for Step 3 of Plume 3

### Construction of Concentration Profiles from Fluent Data

As discussed earlier, 3 levels of horizontal planes were drawn. These three levels are all below the mouths of the wells. Because of this, the top half of the aquifer is treated as 9 large boxes. The fluxes through the sides of the 5 small planes located above the bottom of the pipes (positive y direction) are added together to create one large flux for the given plane. Visualization of this method is provided in Figure 68. For these boxes in the top of the aquifer, the mass balance includes the fluxes through the vertical planes and flux from a bottom horizontal plane. In the bottom half of the aquifer, there are 5 vertical planes that lie in the yz plane for each lettered segment. For the space between the drawn horizontal planes, an average is taken of the flux through the horizontal planes above and below that coordinate. The measured fluxes and the average fluxes are then used to calculate the flux into and out of the boxes in the y direction. This information is then used to calculate concentration profiles as shown in Figure 69: Schematic for Determining Fluxes for Mass Balance below.

pa1	pb1	pc1	pd1	pe1
pa2	pb2	pc2	pd2	pe2
pa3	pb3	pc3	pd3	pe3
pa4	pb4	pc4	pd4	pe4
pa5	pb5	pc5	pd5	pe5
pa6	pb6	pc6	pd6	pe6
pa7	pb7	pc7	pd7	pe7
pa8	pb8	pc8	pd8	pe8
pa9	pb9	pc9	pd9	pe9
pa10	pb10	pc10	pd10	pe10

pa1-5	pb1-5	pc1-5	pd1-5	pe1-5
pa2-5	pb2-5	pc2-5	pd2-5	pe2-5
pa3-5	pb3-5	pc3-5	pd3-5	pe3-5
pa4-5	pb4-5	pc4-5	pd4-5	pe4-5
pa5-5	pb5-5	pc5-5	pd5-5	pe5-5
pa6	pb6	pc6	pd6	pe6
pa7	pb7	pc7	pd7	pe7
pa8	pb8	pc8	pd8	pe8
pa9	pb9	pc9	pd9	pe9
pa10	pb10	pc10	pd10	pe10

Figure 68: Combining Planes to Make Large Planes in Top of Aquifer

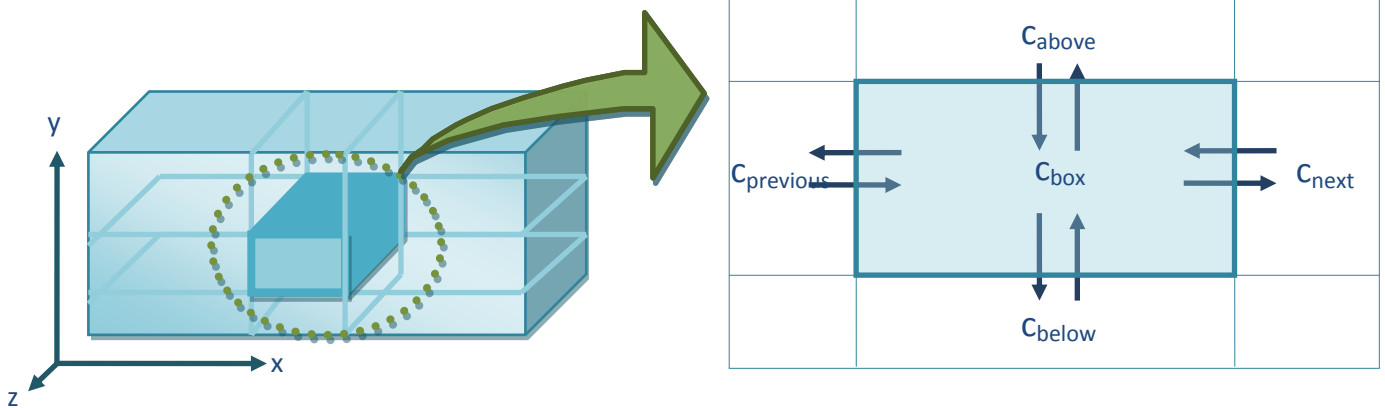


Figure 69: Schematic for Determining Fluxes for Mass Balance

The same strategy for calculating the concentration profiles with time using the magnitude and direction of mass flux through the planes is applied to the refined model with the addition of the flux through the horizontal planes. Different pumping strategies are examined over a period of approximately 60 days, and the ending concentrations are compared to determine the configuration which is most efficient in cleaning.

## Results and Discussion

Flow data for the three well configurations were obtained for plume 1. These flow profiles were used to determine the change in concentration with time for the three configurations individually and with changing configuration with time. In the dynamic model, configuration was changed when the decrease in concentration for the previous well arrangement began to plateau. The results of these runs are displayed in Figure 70 below.

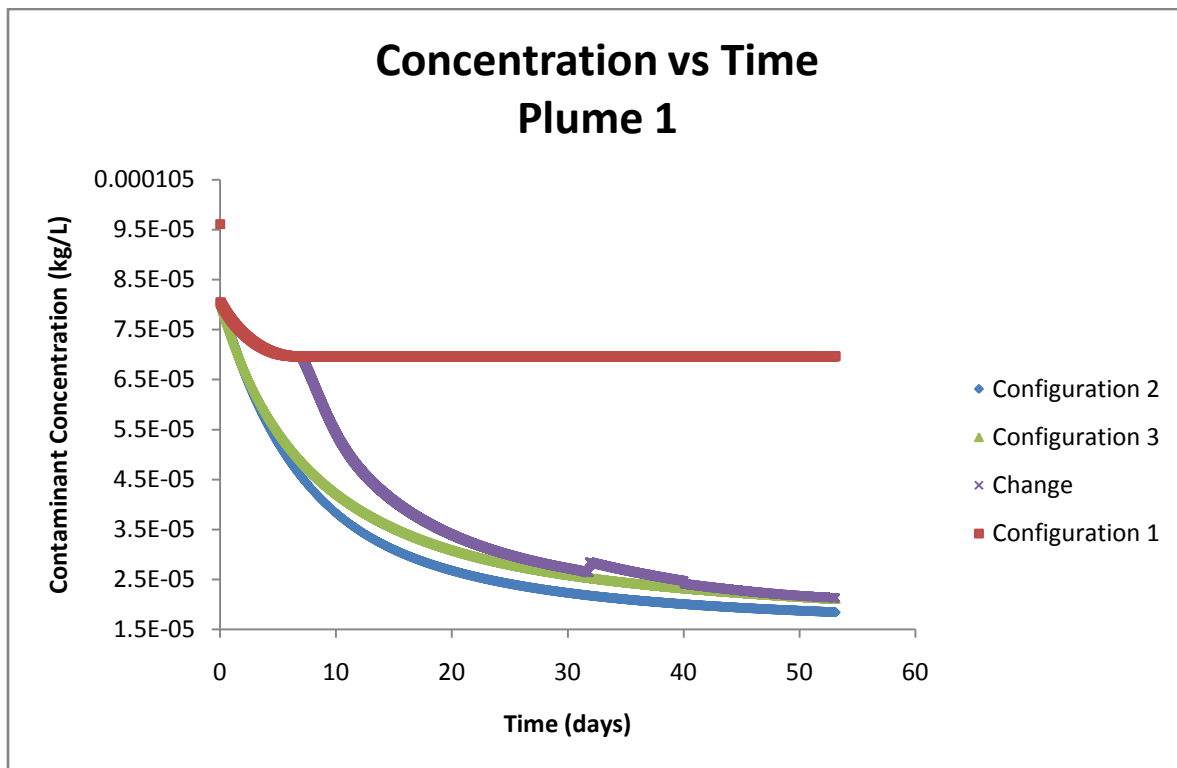


Figure 70: Concentration vs Time for Plume 1

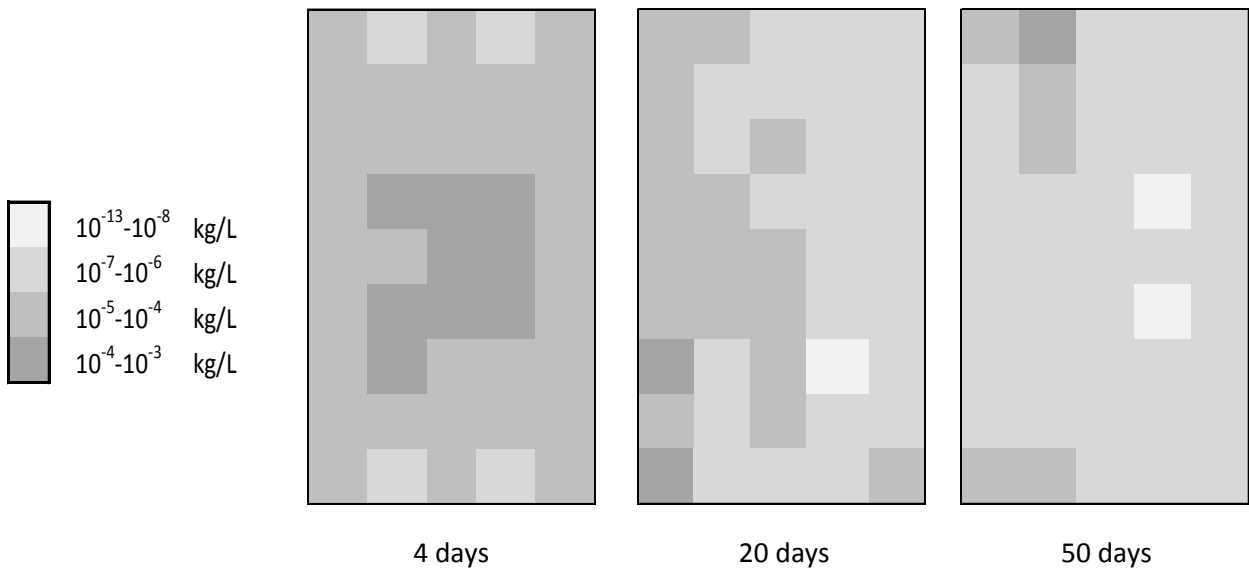


Figure 71: Plume 1 Profile Colored by Contamination Concentration with Dynamic Optimization

Configuration 1 is the least efficient; it is able to lower the contaminant concentration to  $7 \times 10^{-5}$  kg/L and then it levels off after 7 days. Configuration 2 is the most effective; it reaches lower concentrations faster and is still decreasing when the 53 day mark is reached. Configuration 3 behaves very similarly to configuration 2 but is not quite as successful. When the three configurations are combined the aquifer is cleaned roughly to the same degree as when only configuration 3 is used. However it is initially slower than configurations 2 and 3. This is because it begins with configuration 1 which is shown to be an unproductive arrangement. This slower beginning puts this strategy behind initially; in this particular case, configurations 2 and 3 could be explored for their efficacy in minimizing contaminant concentration.

The results from the dynamic strategy are used to make concentration profile contours as shown above in

in

Figure 71. After 4 days there is not much noticeable change in the concentration profile, but by day 20 there is a significant difference from the original plume. By day 50 the aquifer is almost completely clean.

Three new well configurations and the dynamic pumping strategy were applied to the second plume. The results of these simulations can be seen in Figure 72 below.

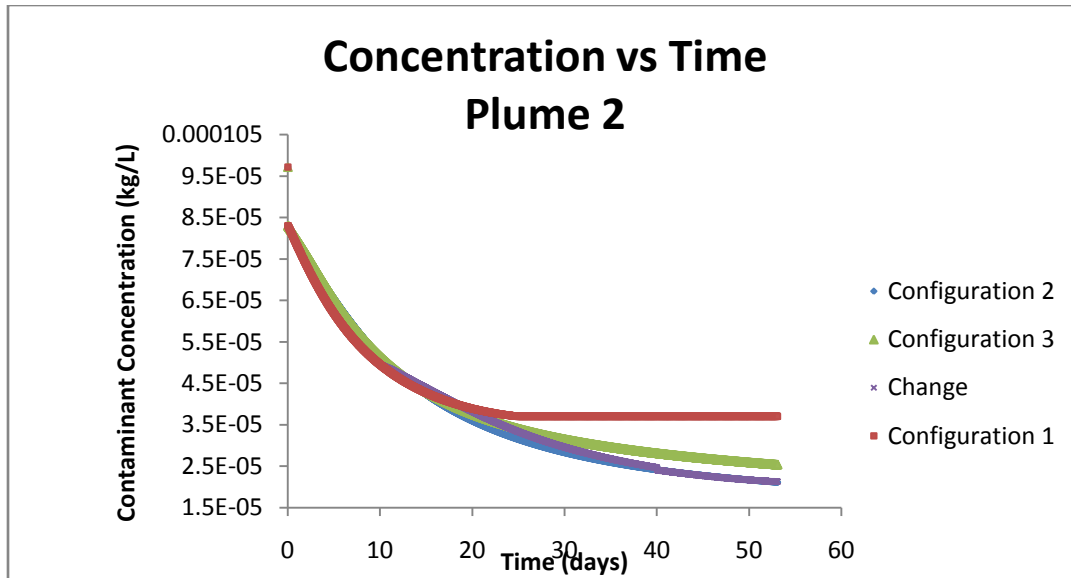


Figure 72: Concentration vs Time for Plume 2

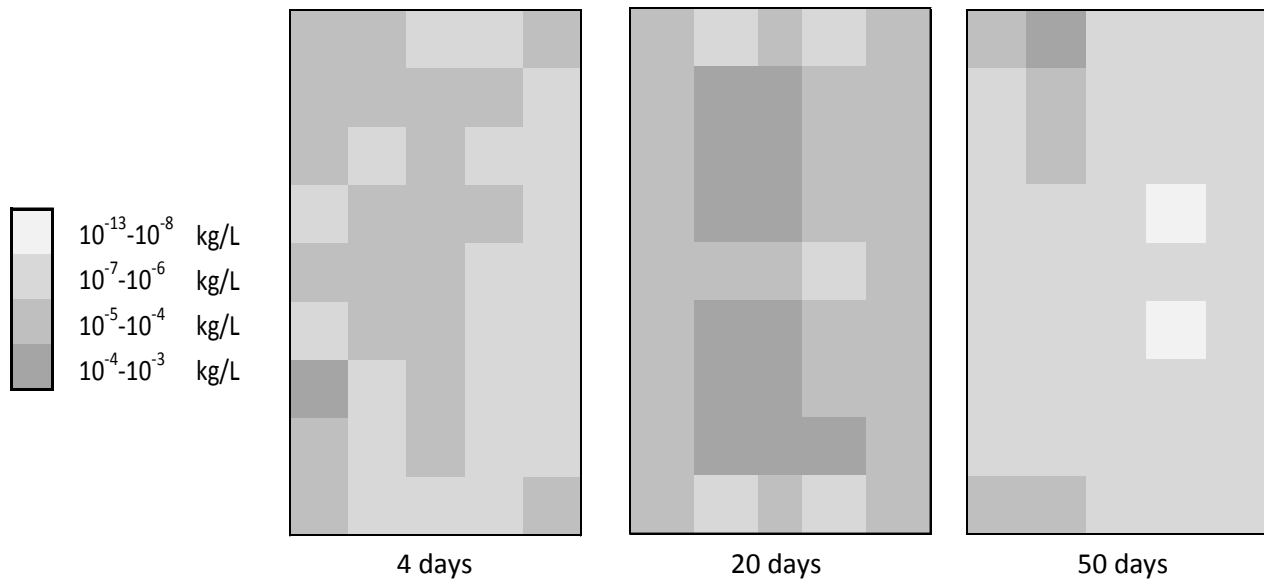


Figure 73: Plume 2 Profiles Colored by Contamination Concentration for Dynamic Optimization

In this plume all four pumping strategies behave very similarly until day 25. At this point configuration 1 reaches its limit and levels out. Configuration 3 also begins to level out and separate from configurations 2 and the dynamic arrangement.

Contours of concentration profiles are produced from the dynamic pumping simulation. These are exhibited in Figure 73 above. Just as in the first configuration there is little improvement in 4 days, but

when the pumps have been running for 20 days much progress has been made, and by the time 50 days is reached most of the contaminants have been removed from the aquifer.

The behavior of the third and final plume is presented in Figure 74 below.

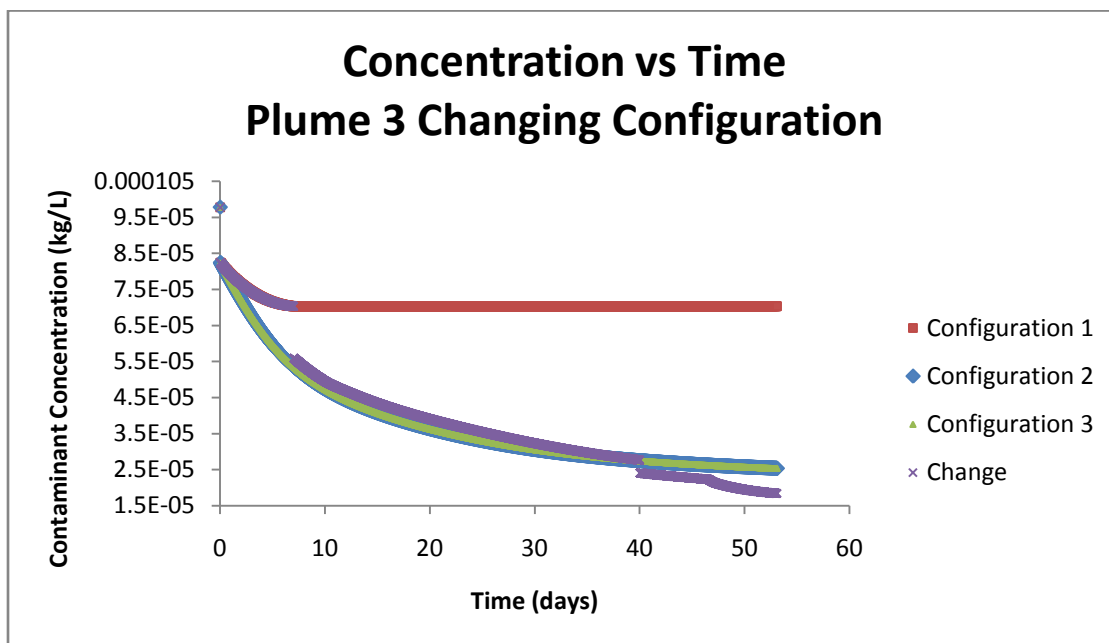


Figure 74: Concentration vs Time for Plume 3

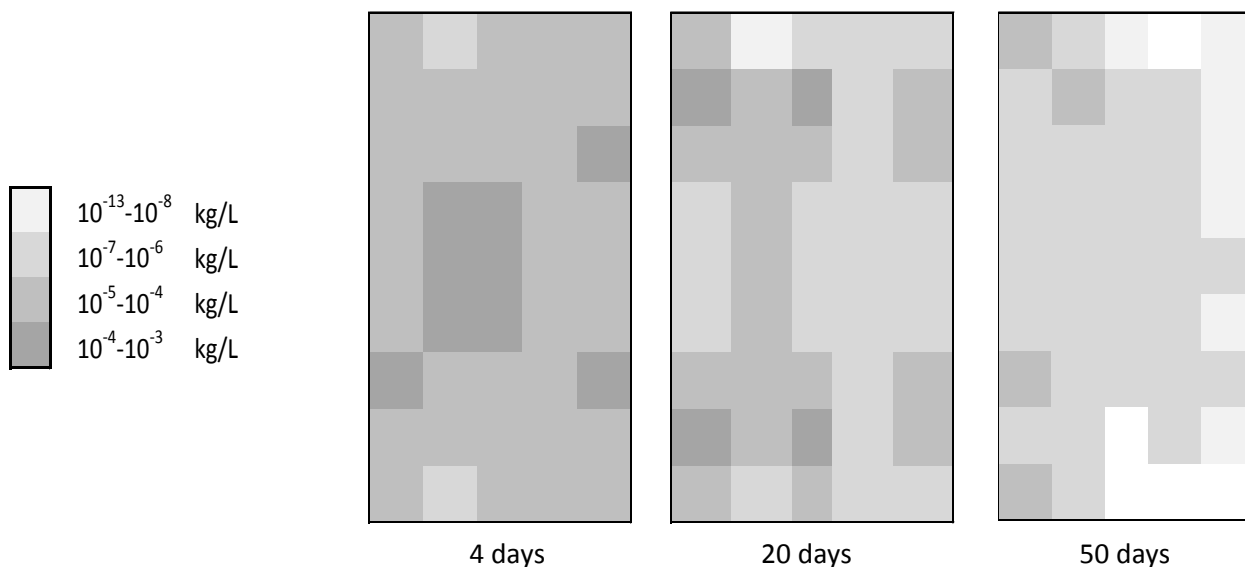


Figure 75: Plume 3 Profiles Colored by Contamination Concentration for Dynamic Optimization

In this contamination plume configuration one becomes ineffective at 7 days and levels off. Configurations 2 and 3 are almost identical. However, the dynamic design behaves very differently from the first two scenarios. It behaves like a step function at each of the configuration changes. At 40 days the dynamic system drops below all other configurations becoming the most efficient.

The contamination contours for plume 3 can be found in Figure 75 above. These contours follow the same pattern as the previous two for  $t = 4, 20$ , and 50 days. At the 4 day and 20 day periods it is still obvious which original contamination profile each contour began with, however, after 50 days, the overall contamination profile for the three different plumes do not show vast differences between the cases. In general, all three arrangements show both generally uniform and low contamination profiles.

## Further Studies and Future Work

Because of some key assumptions in the formulation of this model, several suggestions can be made for future studies and continued research. Some areas for improvement upon this model are as follows:

- Vary pumping rates for injection and extraction wells with time
- Analyze the possibility of injection concentrations greater than zero
- Create imaginary planes that lie in the xy plane
- Analyze more well configurations
- Analyze new plume profiles
- Incorporate more geological properties
- Account for natural degradation
- Incorporate natural flow
- Examine more economics
- Produce more accurate results for profile near injection and extraction

## Conclusions

The initial fluid flow model for the analysis of a pump-treat-inject method remediation of a contaminated aquifer plume provides a good idea of the time-based concentration profiles in the aquifer. A wider spread of extraction wells was found to result in a more efficient purification process. Well configuration was found have a high effect on the flow patterns in the plume. Two adjacent injection wells, for example, cause high flow directly from the well inlet and cause some drag in the remaining aquifer volume. Remediation time is inversely related to flow rate. Initial fixed costs, primarily costs of drilling, dominate the overall cost of remediation. Cleaning time is the next largest factor in overall cost. The overall time leads to the well number and configuration as well as flow rate being deciding factors in optimization. The most economical design was found to be using configuration 1 with a flow rate of 100 kg/s. This yields a cost of \$140,000.

The secondary fluid flow analysis is more realistic and more accurate. This model may be used to simulate plumes having different shapes and initial concentration profiles. The secondary fluid flow analysis technique may be applied as a unique and effective dynamic optimization model. It is shown that this strategy yields generally good cleaning of contaminants from the plume. The specific efficiency of the cleaning of a particular aquifer is seen to be highly dependent on the initial shape and profile of the contamination plume. This dynamic technique can also give more efficient cleaning than a static optimization model. A plateau is often seen in the cleaning profiles and, often, step changes are also seen in the contamination concentration. This dynamic optimization has been proven effective independent of initial plume profile.

## Works Cited

Agency, T. E. (n.d.). *EPA Superfund*. Retrieved March 12, 2008, from <http://www.epa.gov/safewater/contaminants/index.html#listmcl>

*Hanford site*. (n.d.). Retrieved February 20, 2008, from Hanford Site Groundwater Remediation Project: <http://www.hanford.gov/cp/gpp/>

*The Environmental Protection Agency*. (n.d.). Retrieved February 19, 2008, from Waterscience: <http://www.epa.gov/waterscience/criteria/drinking/dwstandards.pdf>

*The Groundwater Foundation*. (n.d.). Retrieved February 22, 2008, from National Water-Quality Assessment Program: <http://pubs.usgs.gov/circ/circ1292/pdf/circular1292.pdf>

Chang, L.-C., Chu, H.-J., & Hsiao, C. T. (2007). Optimal planning of a dynamic pump-treat-inject groundwater remediation system. *Journal of Hydrology*, 295-304.

EPA. (2008). Retrieved 2008, from <http://www.epa.gov/safewater/contaminants/index.html#listmcl>

Jewell, G. (2008). *Hanford site Groundwater remediation project*. Retrieved from <http://www.hanford.gov/cp/gpp/>

Peters, M. S., Timmerhaus, K. D., & West, R. E. (2003). *Plant Design and Economics for Chemical Engineers*. New York: McGraw-Hill.

Tenney, C., & Lastoskie, C. (2007). Pulsed pumping process optimization using a potential flow model. *Journal of Contaminant Hydrology*, 111-121.

Welty, J. R., Wicks, C. E., Wilson, R. E., & Rorrer, G. (2001). *Fundamentals of Momentum, Heat, and Mass Transfer*. New York: John Wiley & Sons, Inc.